

Copyright  
by  
Nada Kittikunakorn  
2020

**The Dissertation Committee for Nada Kittikunakorn Certifies that this  
is the approved version of the following Dissertation:**

**Continuous Twin-screw Melt Granulation of Poorly Compressible and  
Thermal Labile Drug**

**Committee:**

Feng Zhang, Supervisor

Robert O. Williams III

Hugh D. C. Smyth

James DiNunzio

Changquan Calvin Sun

**Continuous Twin-screw Melt Granulation of Poorly Compressible and  
Thermal Labile Drug**

**by**

**Nada Kittikunakorn**

**Dissertation**

Presented to the Faculty of the Graduate School of

The University of Texas at Austin

in Partial Fulfillment

of the Requirements

for the Degree of

**Doctor of Philosophy**

**The University of Texas at Austin**

**August, 2020**

## Acknowledgements

First of all, I would like to thank my supervisor, Dr. Feng Zhang, for providing me an opportunity to spend the enjoyable four years at the University of Texas at Austin to pursue my Ph.D. degree. He always encouraged and convincingly guided me to be a good scientist and person. He has taught me many things more than I could ever give him credit for here. Without his persistent help throughout my Ph.D. study, I would not have been so far and this project would not have been possible.

I would like to thank all my committee members, Dr .Robert O .Williams III, Dr . Hugh D .C .Smyth, Dr. James DiNunzio, and Dr. Changquan Calvin Sun for serving as members of my dissertation committee. I am grateful for their critical review of my dissertation and all their suggestion regarding my graduate research.

I would like to specifically thank Dr. James DiNunzio for a Co-op opportunity at Merck for six months which was a valuable time that allowed me to gain knowledge, skills, and experiences in the pharmaceutical company. I would also like to thank my mentor, Dr. Abbe Haser, for her mentorship throughout my Co-op at Merck. Thank you to Dr. Sutthilug Sotthivirat, Dr. Chris Pridgen, Dr. Erin Dippold, Dr. Sebastian Escotet, Blincoe William, Dr. Nazia Khawaja, Dr. Matthew Lamm, and all other great scientists I met at Merck for all their suggestions and scientific discussions. I appreciate so much the help I received from them.

Many thanks and appreciation to my student worker, Joseph Koleng, for all his assistance throughout my Ph.D. study. He is a very hardworking and smart person. His help and dedication were crucial to the completion of my research. I would also like to thank all my fellows in the college of pharmacy, especially Dr. Zhang's current and former lab members; Tongzhou Liu, Dr. Fan Meng, Dr. Xu Liu, Dr. Shahab Kashani Rahimi, Jamie E Spahn, and Yi Zhang for all their assistance, suggestions, and scientific discussion. In addition, I would like to acknowledge my other fellow graduate students for their assistance, support, and friendship including Xiangyu ma, Sawittree

sahakijpijarn, Tuangrat Praphawatvet, Yajie Zhang, Dr. Zachary Warnken, Dr. Chaeho Moon, Ashlee Brunaugh, Dr. Clara Dominguez, Patricia Martins, Li Ding, and Rashmi Mohanty. You were all great people to work with .

I would like to acknowledge my funding sources; Government Pharmaceutical Organization (Thailand) and College of Pharmacy Endowed Graduate Scholarships.

Additionally, I would like to thank our collaborators for the suggestion and technical resources of the instrument, material, and analytical technique including Charlie Martin, Augie Machado, and Dr. Brian Haight from Leistritz; Tony Listro from Foster, Dr. James DiNunzio from Merck; Vivian Bi from Ashland; Dr. Changquan Calvin Sun and Dr. Shubhajit Paul from University of Minnesota; Dr. Aditya Kumar and Rachel Cook from Missouri University of Science and Technology.

Most important, I would like to thank my parents, Tanant and Viyada Kittikunakorn, my sister and my brother for their love and support. They always pushed me and believed in me. I could not have finished my Ph.D. without the motivation and encouragement they provided.

## **Abstract**

# **Continuous Twin-screw Melt Granulation of Poorly Compressible and Thermal Labile Drug**

Nada Kittikunakorn, Ph.D.

The University of Texas at Austin, 2020

Supervisor: Feng Zhang

Continuous twin-screw melt granulation (TSMG) has been widely used for the last 50 years in various industrial processes. For pharmaceutical manufacturing, TSMG offers many advantages over continuous twin-screw wet granulation and roller compaction. However, TSMG is still limited since there is still a lack of understanding and familiarity by pharmaceutical scientists for the continuous manufacturing of tablets. Therefore, this dissertation aims to facilitate the broader adoption of TSMG by mechanistic understanding of the granulation behavior and the challenges that need to be concerned during the process.

In Chapter 1, the processes, challenges, and the future of twin-screw granulation (wet and melt granulation) for manufacturing oral tablets and capsules are reviewed. Four aspects of twin-screw granulation, including (1) granule formation mechanisms, (2) benefit over conventional batch process, (3) process control and monitoring, and (4) history, recent progress, and the future will be highlighted in this chapter.

In Chapter 2, the recent progress of twin-screw melt granulation (TSMG) will be reviewed. As TSMG is a solvent-free process, it is a preferable granulation method for a moisture-sensitive drug as compared to twin-screw wet granulation (TSWG). Therefore, this chapter focuses on the understanding of how the formulation and process impact the granule properties as well as the challenges of TSMG that is needed to be considered.

In Chapter 3, the effect of thermal binders (PEG, HPC, and Compritol), molecular weight, and binder particle size on the physicochemical properties of gabapentin (GABA), a thermally labile drug, in granules prepared using TSMG was investigated. It was found that higher degradation and crystal size reduction of GABA were observed in HPC-based formulation. Smaller particle size and lower molecular weight of HPC led to faster granule growth. The tableability of granules was insensitive to the variations in particle size and molecular weight of HPC.

In Chapter 4, the effect of screw profile and processing conditions on the process-induced transformation and chemical degradation of gabapentin was studied. It was found that both the granules size and gabapentin degradant level correlated positively with the specific rate, the ratio between feed rate and screw speed. At the higher specific rate, the barrel was filled to a greater extent, enhancing the compressive forces. This resulted in more interaction between the powder particles, facilitating the granule growth as well as generating the crystal size reduction which led to more degradation.

In Chapter 5, the difference of granulation behavior in two sizes of twin-screw extruder (Nano-16 and Micro-18) was investigated. It was observed that due to the difference in extruder geometries between the two extruders, correlations between granule properties and processing parameters are different. For Nano-16, DF was a critical parameter, where higher DF led to higher degradant levels and more compressible granules. For granules prepared using the Micro-18, SME was a critical parameter, where a higher SME led to higher degradant level and more compressible granules.

## Table of Contents

List of Tables .....	xiv
List of Figures .....	xv
Chapter 1: Processes, Challenges and the Future of Twin-screw Granulation for Manufacturing Oral Tablets and Capsules <sup>1</sup> .....	1
1.1 Abstract .....	1
1.2 Granule formation mechanisms :twin-screw continuous granulation .....	1
1.3 Twin-screw wet-granulation )TSWG( .....	3
1.4 Twin-screw melt-granulation )TSWG( .....	4
1.5 Benefits of twin-screw continuous granulation over batch granulation.....	5
1.6 Process control and monitoring .....	6
1.7 History, recent progresses and the future in pharmaceutical application .....	8
1.8 Conclusion .....	9
1.9 References.....	10
Chapter 2: Twin-Screw Melt Granulation: Current Progress and Challenges.....	12
2.1 Abstract.....	12
2.2 Introduction.....	12
2.2.1 Purposes of granulation.....	12
2.2.2 Advantages of melt granulation .....	13
2.2.3 Transformation from traditional batch to continuous twin-screw melt granulation .....	14
2.3 Twin-screw extruder .....	17
2.3.1 Conveying element .....	18
2.3.1 Mixing element .....	19



2.4 Granule formation mechanism during TSMG .....	21
2.5 Factors affecting the physical properties of granules.....	22
2.5.1 Formulation Composition .....	24
2.5.1.1 Binder properties.....	24
2.5.1.1.1 Binder Molecular Weight .....	26
2.5.1.1.2 Binder particle size.....	26
2.5.1.2 Binder and drug miscibility .....	27
2.5.2 Processing parameters.....	28
2.5.2.1 Feed rate and screw speed.....	28
2.5.2.2 Barrel temperature.....	30
2.5.2.3 Screw configuration .....	31
2.6 Binder distribution .....	33
2.7 Challenges of TSMG .....	35
2.7.1 Polymorphic transformation.....	35
2.7.2 Chemical degradation.....	37
2.8 Process analytical technology (PAT) in twin-screw melt granulation.....	39
2.9 Conclusion .....	40
2.10 References .....	42
Chapter 3: Effects of Thermal Binders on Chemical Stabilities and Tableability of Gabapentin Granules Prepared by Twin-Screw Melt Granulation <sup>2</sup> .....	49
3.1 Abstract.....	49
3.2 Introduction.....	50
3.3 Materials and Methods.....	54
3.3.1 Materials.....	54

3.3.2 Methods.....	55
3.3.2.1 Twin-screw melt granulation .....	55
3.3.2.2 Miscibility of Gabapentin with thermal binders .....	56
3.3.2.3 Granule size distribution .....	56
3.3.2.4 Image analysis using scanning electron microscope .....	56
3.3.2.5 Tabletability of melt-extruded granules.....	57
3.3.2.6 HPLC analysis of gabapentin and gabapentin-lactam of granules .....	57
3.3.2.7 Melt viscosity of thermal binders .....	58
3.3.2.8 FT-IR analysis.....	58
3.3.2.9 Particle size of gabapentin in melt-extruded granules .....	58
3.3.2.10 Time-of-flight secondary ion mass spectrometry (ToF- SIMS) .....	59
3.4 Results and Discussion .....	59
3.4.1 Selection of thermal binders and processing parameters .....	59
3.4.2 Effect of thermal binders on the properties of melt-extruded GABA granules .....	63
3.4.2.1 Tabletability of melt-extruded granules.....	63
3.4.2.2 Crystal form and crystallinity of GABA following TSMG ....	65
3.4.2.3 Chemical stability of GABA granules .....	67
3.4.3 Effect of excipient variability on the properties of HPC-based GABA granules.....	72
3.4.4 Distribution of thermal binder in HPC-based GABA granules .....	76
3.5 Conclusion .....	77
3.6 References.....	78

Chapter 4: Effect of Screw Profile and Processing Conditions on Physical Transformation and Chemical Degradation of Gabapentin during Twin-Screw Melt Granulation <sup>3</sup> .....	80
4.1 Abstract .....	80
4.2 Introduction .....	81
4.3 Materials and Methods .....	83
4.3.1 Materials .....	83
4.3.2 Methods .....	85
4.3.2.1 Twin-screw melt granulation .....	85
4.3.2.2 Granule size distribution .....	85
4.3.2.3 Tableability of melt-extruded granules .....	85
4.3.2.4 HPLC analysis of GABA and its degradant .....	86
4.3.2.5 Particle size of gabapentin in melt-extruded granules .....	87
4.3.2.6 FT-IR analysis .....	87
4.3.2.7 Powder X-ray diffraction (PXRD) .....	87
4.4 Results and Discussion .....	87
4.4.1 Effect of screw profile (kneading block) .....	88
4.4.2 Effect of processing condition on the physicochemical properties of GABA granules .....	90
4.4.2.1 Effect of screw speed and feed rate on GABA granule size ...	91
4.4.2.2 Effect of screw speed and feed rate on both polymorphic form stability and disorder of GABA crystals .....	93
4.4.2.3 Effect of screw speed and feed rate on GABA chemical stability .....	94
4.4.2.4 Effect of processing condition on the tableability of GABA granules .....	99

4.5 Conclusions.....	101
4.6 References.....	102
Chapter 5: Is the Melt Granulation Behavior Same between Leistritz Nano-16 and Micro-18 Extruders? .....	105
5.1 Abstract.....	105
5.2 Introduction.....	105
5.3 Material and methods.....	108
5.3.1 Material.....	108
5.3.2 Methods .....	108
5.3.2.1 Twin-screw melt granulation .....	108
5.3.2.2 Assay and impurity content .....	110
5.3.2.3 Enthalpy change during twin-screw melt granulation .....	111
5.3.2.4 Tableability of melt-extruded granules.....	112
5.3.2.5 Granule density .....	113
5.3.2.6 Binder distribution .....	114
5.3.2.7 Particle size of GABA in melt-extruded granules .....	114
5.4 Results and discussions.....	114
5.4.1 Scale-up from Nano-16 to Micro-18 .....	114
5.4.2 Correlation between processing parameters and chemical stability of GABA granules. Nano-16 vs. Micro-18.....	116
5.4.3 Offset between Degradant Content-SME Profiles at Different Feed Rates for the Micro-18 .....	119
5.4.4 Crystal form changes and particle size reduction of GABA .....	122
5.4.5 Physical properties of granules, Nano-16 vs. Micro-18 .....	123
5.4.5.1 Granule shape.....	123

5.4.5.2	Tabletability of GABA granules .....	124
5.5	Conclusion .....	127
5.6	References .....	128
	Bibliography .....	130
	Vita.....	141

## List of Tables

Table 2.1	Differences between batch vs. continuous melt granulation .....	16
Table 2.2	Formulation and process variables affecting the physical attributes of granules .....	23
Table 2.3	Polymers that is used as a binder in TSMG.....	25
Table 3.1	Summary of process setup and extrusion torque for twin-screw melt granulation. ....	55
Table 4.1	A list of extrusion runs and their processing conditions.....	84
Table 5.1	Differences of machine and screw geometry at kneading zone between Leistritz Nano-16 and Micro-18 extruders.....	106
Table 5.2	A list of extrusion runs and their processing condition. ....	110

## List of Figures

Figure 1.1	Illustration of various screw elements .....	2
Figure 1.2	Cross section view of TSE denoting different regions of mixing (courtesy of Leistritz).....	3
Figure 1.3	Illustration of a twin-screw wet granulation with flash drying )courtesy of Leistritz(.....	4
Figure 2.1	Schematic diagram of twin-screw melt granulation .....	18
Figure 2.2	Screw elements for the twin-screw extruder.....	18
Figure 2.3	Critical parameters of kneading elements: offset angle (W), the disc width (S). T and M indicates forwarding and reversing flow, respectively. K represent the material that passes over the element crest. ....	20
Figure 2.4	Granule formation mechanisms .....	21
Figure 2.5	Granule formation mechanism in batch melt granulation.....	22
Figure 2.6	(A) Binder distribution in gabapentin-HPC ELF granules samples at different zone of extruder analyzed byToF-SIMS. Blue color is indicative of HPC and red color is indicative of GABA. (B) The signal intensity of $C_2H_3O^-$ and $CH_2N^-$ on the surface of granules sampled along the screw from zone 1 to zone 3. ....	34
Figure 2.7	Schematic diagram demonstrating the major factors that contribute to the physicochemical instability during TSMG. ....	35
Figure 3.1	Chemical structures of (A) gabapentin (GABA), (B) polyethylene glycol 8000 (PEG 8000), (C) glycerol behenate (Compritol), and (D) hydroxypropyl cellulose (HPC). ....	53

Figure 3.2	DSC and TGA thermograms of gabapentin (GABA) drug substance. At the melting point temperature of GABA, TGA thermogram shows the 10% weight loss due to chemical degradation.....	54
Figure 3.3	DSC thermograms of physical mixtures containing gabapentin (GABA) and binders (10, 20, or 80%); ramp from 25°C to zone 2 processing temperature; hold at the processing temperature for 5 minutes; ramp further to 250°C; (A) GABA-PEG 8000 with a zone 2 processing temperature of 80°C; (B) GABA-Compritol with a zone 2 processing temperature of 100°C; (C) GABA-HPC ELF with a zone 2 processing temperature of 140°C.....	61
Figure 3.4	Hot-stage polarized light microscope of physical mixture (A) 80% GABA-20% PEG 8000, (B) 80% GABA-20% Compritol, and (C) 80% GABA-20% HPC ELF.....	63
Figure 3.5	Photo images (top row) of extrudate and scanning electron microscope images (bottom row) of milled granules containing 80% GABA and 20% of various binders. (A) PEG 8000, (B) Compritol, and (C) HPC ELF. ....	64
Figure 3.6	Compression profiles of blends containing 99% melt-extruded granules or physical mixture and 1% magnesium stearate; 11 mm in diameter, round, flat-faced tooling; 350 mg in tablet weight. ....	65
Figure 3.7	FTIR spectra of physical blends and melt-extruded GABA granules. PM: physical mixture, ME: melt-extruded granule. ....	66
Figure 3.8	Gabapentin-lactam profile of melt-extruded granules packaged with desiccant in induction-sealed HDPE bottle stored at 40°C/75% RH condition for 3 months. GABA drug substance was used as the control.....	67



Figure 3.9	Melt viscosity of binders as a function of shear rate at their respective zone 2 processing temperatures of three thermal binders. ....	69
Figure 3.10	Gabapentin-lactam profile of melt-extruded GABA granules processed at 90°C, 100°C and 110°C barrel temperature. ....	69
Figure 3.11	Particle size distribution of gabapentin (GABA) drug substance and GABA in melt-extruded granules (average of triplicate analyses). ....	70
Figure 3.12	Scanning electron microscope images (top row) and polarized light microscope images (bottom row) of GABA crystals in melt-extruded GABA granules (A) GABA drug substances (B) Compritol-based granule, (B) PEG 8000-based granule, and (C) HPC ELF-based granule. ....	70
Figure 3.13	Gabapentin-lactam content of melt-extruded 80% GABA-20% HPC ELF granules packaged in open containers stored at 40°C and various relative humidity conditions. ....	71
Figure 3.14	Size distribution of melt-extruded GABA granules based on different grades of HPC. Camsizer® was used in this analysis. ELF (40,000, 160 µm D <sub>50</sub> ); EXF (80,000, 50 µm D <sub>50</sub> ), and spray-dried EXF (80,000, 10 µm D <sub>50</sub> ). ....	72
Figure 3.15	Compression profiles of A) physical mixtures and B) melt-extruded granules based on HPC of different molecular weight and particle size. ELF (40,000, 160 µm D <sub>50</sub> ); EXF (80,000, 50 µm D <sub>50</sub> ), and spray-dried EXF (80,000, 10 µm D <sub>50</sub> ). ....	74
Figure 3.16	Gabapentin-lactam content of GABA drug substance and melt-extruded 80% GABA-20% HPC granules containing HPC of different particle sizes; processing conditions: 10 g/min feed rate, 100 rpm screw speed and four different barrel temperatures (90, 100, 110 and 120°C). ....	75

Figure 3.17	(A) ToF-SIMS image (500 $\mu\text{m}$ x 500 $\mu\text{m}$ ) of GABA-HPC ELF granules sampled at different processing zone. Blue color is indicative of HPC and red color is indicative of GABA. (B) the signal intensity of $\text{CH}_2\text{N}^-$ and $\text{C}_2\text{H}_3\text{O}^-$ of HPC EXF and GABA at different processing zones. ....	76
Figure 4.1	Chemical structure of (A) gabapentin (GABA) and (B) hydroxypropyl cellulose (HPC). ....	83
Figure 4.2	Barrel configuration and screw profile with open-end discharge (A) two 60° offset neutral kneading blocks, (B) two 30° offset forward kneading blocks. ....	84
Figure 4.3	Polymorphic transformation of GABA determined by (A) XRPD, and (B) FT-IR. Processed at 10 g/min and 100 rpm with 30° forward or 60° neutral kneading block. ....	89
Figure 4.4	Images of melt-extruded granules processed at various processing conditions; feed rate: 5 g/min, 7.5 g/min, or 10 g/min; screw speed: 100 rpm, 150 rpm, 200 rpm, or 300 rpm. ....	92
Figure 4.5	Correlation between granules size ( $D_{50}$ ) and specific rate of melt granulation process (n=3, means are reported). ....	92
Figure 4.6	ATR-FTIR spectra of GABA and HPC raw materials, their physical mixtures, and melt-extruded granules processed at different conditions. ....	93
Figure 4.7	XRD pattern of GABA-HPC physical mixture and melt-extruded granules processed at highest (0.10 g/min/rpm – 10 g/min at 100 rpm) and lowest (0.0167 g/min/rpm – 5 g/min at 300 rpm) specific rates (Q/N). ....	94

Figure 4.8	GABA-L content of melt-extruded GABA granules processed at various combination of screw speeds and feed rates (error bar represents the standard deviation of triplicate analyses).....	95
Figure 4.9	Relation between GABA-L content of melt-extruded GABA granules and system parameters of melt extrusion. (A) Specific mechanical energy, and (B) Specific rate. ....	96
Figure 4.10	Correlation between GABA-L content and the size of melt-extruded GABA granules.....	96
Figure 4.11	Particle size distribution of gabapentin (GABA) drug substance and GABA crystals in the melt-extruded granules at highest (0.10 g/min/rpm – 10 g/min at 100 rpm) and lowest (0.0167 g/min/rpm – 5 g/min at 300 rpm) specific rates.....	97
Figure 4.12	Correlation between D <sub>50</sub> of GABA crystals in the melt-extruded granules and specific rate (Initial GABA crystal size has D <sub>50</sub> of 65 µm) (n=3, mean values are reported). ....	97
Figure 4.13	(A) The percentage of GABA degradant and (B) CAMES beads breakage along the axial direction at the highest (0.10 g/min/rpm – 10 g/min at 100 rpm) and lowest (0.0167 g/min/rpm – 5 g/min at 300 rpm) specific rates. (n=3, mean value and standard deviation are reported) .....	99
Figure 4.14	(A) Compression profiles of physical mixture and melt-extruded granules processed at high and low degree of fill and (B) correlation between tensile strength of the tablets prepared at 100 MPa compression pressure and the tensile strength of tablet. (n=5, mean value and standard deviation are reported) .....	100

Figure 5.1	Barrel configuration, screw profile with open-end discharge, and barrel temperature of (A) Nano-16 (B) Micro-18 twin-screw extruder. ....	109
Figure 5.2	(A) Schematic diagram demonstrating enthalpy measurement using thermodynamic method and (B) Measured cumulative heat release of each material from isothermal microcalorimetry analyses. ....	111
Figure 5.3	Correlation between (A and C) %GABA-L and Degree of fill, (B and D) %GABA-L and SME of GABA granules processed using Nano-16 and Micro-18. ....	116
Figure 5.4	Correlation between degradant content and the temperature of GABA granules prepared using the Micro-18. ....	117
Figure 5.5	Apparent density of granules sampled along the barrel (A) Nano-16 (operated at the feed rate of 15 g/min, screw speed of 100 rpm) (B) Micro-18 (operated at the feed rate 64 g/min, screw speed of 100 rpm)....	118
Figure 5.6	Schematic diagram showing the energy balance at zone 5 (kneading zone).....	120
Figure 5.7	Amount of heat loss to the barrel during granulation process at various feed rates calculated by heat transfer method. Each line represents each feed rate operated at screw speed of 100 rpm (■), 200 rpm (□), and 300 rpm (▣).....	121
Figure 5.8	(A) The correlation between %GABA-L and specific mechanical energy (B) the correlation between %GABA-L and enthalpy difference between the material entering and exiting the barrel zone 5.....	122

Figure 5.9	Images of melt-extruded granules processed with (A) Nano-16 extruder at given feed rate of 15 g/min and (B) Micro-18 extruder at the feed rate of 64 g/min with increasing screw speed (100, 150, 200, 300 rpm). *AR is aspect ratio, $D^{F_{max}}$ is maximum diameter, and $D^{F_{min}}$ is minimum diameter.....	124
Figure 5.10	Correlation between process parameter and tensile strength of melt-extruded GABA tablets containing granules processed with (A) Nano-16 (B) Micro-18. ....	125
Figure 5.11	Binder distribution of melt-extruded GABA granules processed with Micro-18 at (A) high SME (0.18 kW.hr/kg, Run F16 in Table 5.2) and (B) low SME (0.06 kW.hr/kg,, Run F25 in Table 5.2). ....	126

# **Chapter 1: Processes, Challenges and the Future of Twin-screw Granulation for Manufacturing Oral Tablets and Capsules<sup>1</sup>**

## **1.1 ABSTRACT**

The majority of marketed tablets and capsules products are manufactured using granulation processes including wet, melt, and dry granulation. These granulation techniques are also used across many other industries, such as the food and polymer industries. Powders are granulated to prevent material segregation, and to improve powder properties (e.g., flowability and compressibility). While other industries transitioned wet and melt granulation from batch to continuous processes using twin-screw extruders in 1970s, the adoption of twin-screw granulation has been slow in pharmaceutical industry. As pharmaceutical scientists become more familiar with twin-screw granulation, and with the recent interest in continuous manufacturing, an increasing number of process patents and products utilizing twin-screw granulation platform is anticipated. This article highlights four aspects of twin-screw granulation (TSG): (a) granule formation mechanisms, (b) benefit over conventional batch processes, (c) process control and monitoring, and (d) history, recent progresses and the future.

## **1.2 GRANULE FORMATION MECHANISMS: TWIN-SCREW CONTINUOUS GRANULATION**

The twin-screw extruder (TSE) is available in a variety of configurations with the co-rotating, intermeshing, twin-screw extruder being the most commonly used for granulation applications. This design of the TSE is also considered “self-wiping”, because the opposing surface velocities inherent with the intermeshing motion leads to material removal from the surface.

---

<sup>1</sup> Kittikunakorn, N., DiNunzio, J. C., Martin, C., & Zhang, F. (2018). Processes, Challenges, and the Future of Twin-Screw Granulation for Manufacturing Oral Tablets and Capsules. *AAPS NewsMagazine*, Mar(Mar), 12-18.

I am the primary author of this work.

The screws consist of conveying and mixing elements (Figure 1.1). Conveying elements transfer material along the barrel, while mixing elements contribute to both distributive mixing and dispersive mixing during TSG. Distributive mixing involves division and recombination, while dispersive mixing involves planar mixing and extensional shear (stretching) (Todd, 2004). Depending on their geometry, mixing elements can be predominately distributive, predominately dispersive, or a balance of both. Images of representative conveying and mixing elements are shown in.

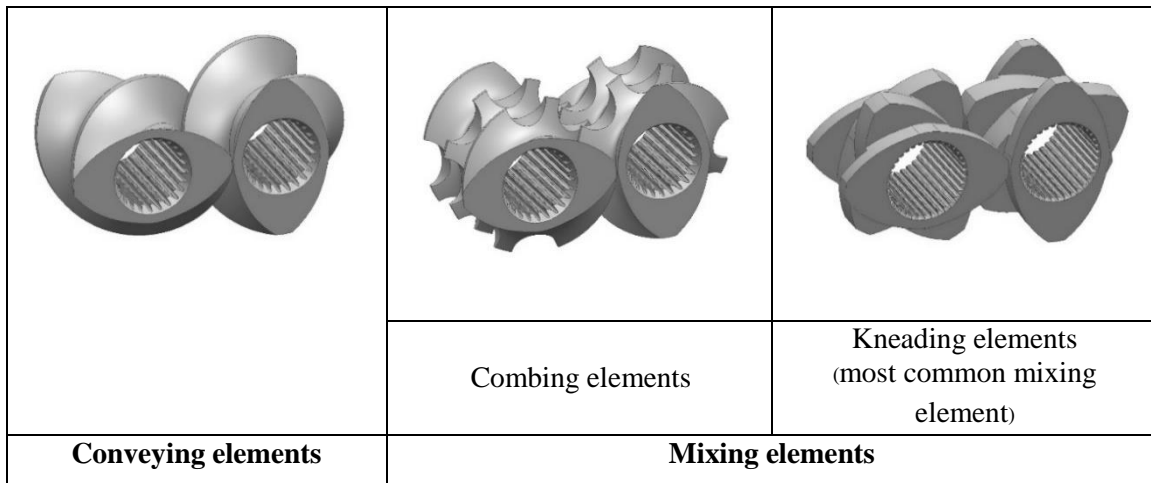


Figure 1.1 Illustration of various screw elements

The TSE is regarded as a small volume, continuous mixer. A 27 mm Leistritz extruder at 24 L/D configuration could operate at a production rate of 15 to 30 kg/hr. The total free volume inside the extruder at this configuration is only about 250 mL. This small mixing volume and corresponding mass transfer distance improves the product consistency by ensuring that all granules have similar shearing history. This is why the term “small volume” mixer is used to describe TSE. As shown in Figure 1.2, materials are bounded and divided into different regions by the screw flights and barrel wall . Depending on the location relative to the barrel and screw elements, materials experience different intensity of mixing .in different regions High-intensity mixing regions are highlighted in red, while regions of low-intensity mixing are in blue

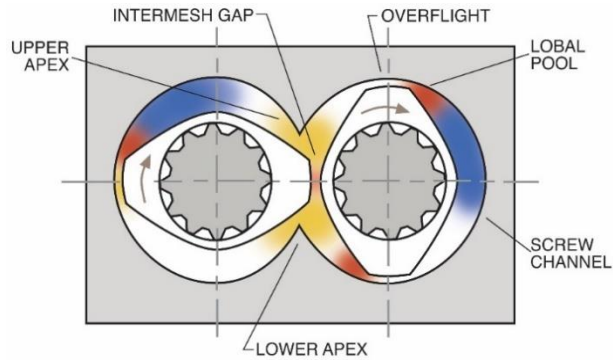


Figure 1.2 Cross section view of TSE denoting different regions of mixing )courtesy of Leistritz(

Twin-screw granulation has traditionally been divided into two categories: twin-screw wet-granulation (TSWG) and twin-screw melt-granulation (TSMG).

### 1.3 TWIN-SCREW WET-GRANULATION (TSWG)

In TSWG, granulation fluid (e.g., water or solvent, optionally containing a polymeric binder or foam) is introduced into the extruder via liquid injection port either as liquid or as foam (Sheskey, Keary, Clark, & Bahwinski, 2007). TSWG is mechanistically similar to batch high-shear wet granulation. As the granulation progresses along the barrel in TSWG, the powder blend undergoes wetting and nucleation, consolidation and coalescence, and attrition processes to transform into granules. Wetting and nucleation take place in conveying regions to form large, non-uniform agglomerates. These agglomerates are sheared, fractured, and compressed. As a result, consolidation and coalescence take place. Granules grow denser, stronger, and more uniform in mixing regions (Dhenge, Cartwright, Hounslow, & Salman, 2012a, 2012b).

Water or solvent can be removed from wet granules via different processes post granulation. Large-scale fluid-bed drying is still commonly used as a batch process to dry the wet granules prepared using TSWG. The ConsiGma™ continuous tableting system designed by GEA contains a segmented dryer consisting of multiple individual drying



modules. When drying endpoint (product temperature or residual moisture) is reached for one drying module, granules are discharged and a new pack of wet granules is loaded. Continuous dielectric (microwave) drying has also been utilized and was first disclosed in the continuous pharmaceutical granulation patent by scientists from Warner Lambert (Ghebre-Sellassie, I., Mollan, Pathak, Lodaya, & Fessehaie, 2002).

A continuous flash drying process has been developed by Leistritz (Figure 1.3). The drying process is begun in the extruder via a vent. After discharge, hot air is then used to drive off the remaining residual water and to transfer them into a mill for size reduction.

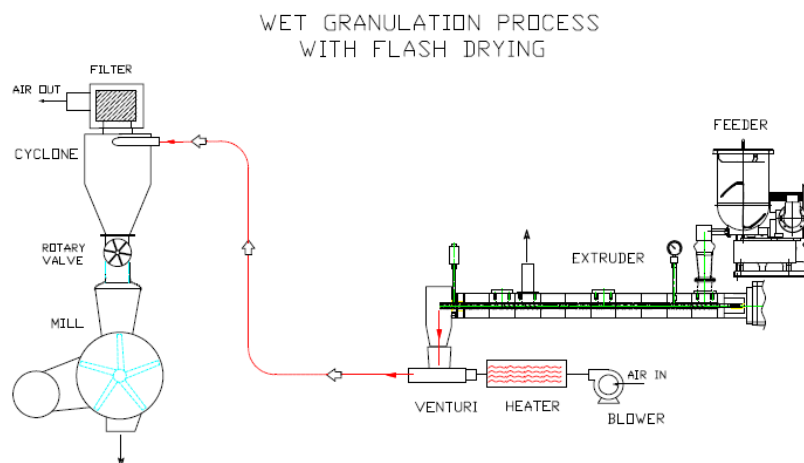


Figure 1.3 Illustration of a twin-screw wet granulation with flash drying (courtesy of Leistritz)

#### 1.4 TWIN-SCREW MELT-GRANULATION (TSWG)

As a solvent-free alternative to TSWG, twin-screw continuous melt-granulation (TSMG) uses thermal binder instead of liquid binder. The process is performed with a higher viscosity binder at elevated temperature. Melt granulation is especially suitable for drugs that undergo undesired physical or chemical changes in the presence of water or solvent (Lakshman et al., 2011a; Vasanthavada, Wang, Haefele, Lakshman, Mone, Tong, Joshi, & AT, 2011). There have been limited studies to investigate the mechanisms of melt granulation process. Due to the thermal and mechanical energy input, thermal

binders turn into low viscosity liquid (e.g., polyethylene glycol and glycerol behenate) or viscoelastic polymer melt (e.g., hydroxypropyl cellulose) inside the extruder barrel. Molten thermal binders bridge the powder particles together to form larger agglomerates. Coating of thermal binders on the surface of granules has been observed in the lab at the University of Texas using Time-of-Flight Secondary Ion Mass spectrometry for the surface composition analysis of granules (N. Kittikunakorn et al., 2017).

## **1.5 BENEFITS OF TWIN-SCREW CONTINUOUS GRANULATION OVER BATCH GRANULATION**

Batch high-shear granulators generally consist of mixing blades positioned inside large mixing chambers. The mixing and agglomeration occur at the high shear zones, such as those located between the tips of the rotating blades and the wall of mixing chamber for high shear granulator. On the other hand, for TSG, different stages of the granulation process take place at different screw segments.

Batch granulation is operated under the globally starved (the extruder barrel is at 30 to 70% filled during processing) and unpressurized condition. Even though the TSE is operated under globally starved conditions, processing section of a TSE consists of both starved (partially filled in conveying elements) and pressurized (fully filled in mixing elements) segments dictated by the screw elements (White & Bumm, 2010). Powder is randomly subjected to the high shear zone in a batch granulator, potentially resulting in non-uniform mixing dynamics. In TSG, the material is forced through a sequence of starved and pressurized zones. As a result, granules prepared using TSG have a more uniform mixing history, where incoming blend is processed in a principle of first-in, first-out with a given residence time distribution. This allows the system to be able to operate in a state of control and to ensure the consistent quality of granules (Chen, Zhu, Zhang, & Qiu, 2016; White & Bumm, 2010).

Three distinct advantages of TSG are (1) more homogeneous distribution of drug, excipient, and binder solution; (2) reduced level of binder solution to achieve desired granules; and (3) shorter processing time (Chen et al., 2016). Granulation time is on the

order of about 10 seconds for TSG. In comparison, granulation time for a batch process is on the order of minutes. This shorter processing time makes it feasible to explore high processing temperatures, that are not practical for batch process.

Beside the improved quality of granules, TSG provide the following benefits when utilized as a continuous process (Lodaya, Mayur, Mollan, & Ghebre-Sellassie, 2003).

1. Lower level of binder solution is needed
2. Smaller production facility and less capital investment
3. Modular construction allows flexibility in configuration of processing section
4. On-line and real-time monitoring of product quality rather than the post-production testing
5. More efficient manufacturing with shorter production cycle, and lower product cost
6. Simpler process optimization and scale up
7. Use of the same equipment train for a much broader production volume and quicker response to changes in market demand

## **1.6 PROCESS CONTROL AND MONITORING**

A TSE line consists of drive section (motor and gearbox), process section (barrel and screw), and electrical and control panel. TSE is starve-fed with output rate control by feeder. The energy required to transform the powder blend to granules predominately comes from the mechanical energy input by the motor via rotating screws into the material. Heat conducted from barrel can also play a significant role, especially for small-diameter extruder. Modular design of barrel and screw makes TSE an extremely versatile granulator. Screw elements and barrel design at any given segment can vary to accommodate various unit operations such as direct powder feeding, powder side stuffing, liquid injection, conveying, mixing, venting, and devolatilization (removal of water and solvents).

Key processing variables include screw speed, barrel temperature, and feed rate. Screw speed is controlled by a variable speed AC drive, motor, and gearbox. Generally, screw speed is set between 50 to 1000 rpm. Heating and cooling of barrel is controlled by cartridge heaters and cooling liquid such as a water/propylene glycol mixture. Temperatures also can be set by liquid temperature control units, as required in explosion proof rated environments. For wet granulation, barrel temperature is set at or slight above the ambient temperature. For melt granulation, barrel temperature is set above the melting and glass transition temperature of thermal binders, and is typically in the range of 80 to 130°C. Feeding of powder and binder solution is controlled using loss-in-weight powder feeder (with the entire feeder and material are continuously weighed, the feeder speed is adjusted automatically to achieve the target feed rate) and pump (gear or peristaltic pump for liquid and side-stuffer for foam), respectively. Twin-screw continuous granulation operates in an open-end discharge mode. A restraining plate or outboard bearing is used to prevent the screw from moving axially without obstructing the granule flow.

Precise process control to ensure consistent product quality requires the monitoring of the process parameters at different locations along the barrel. The parameters include temperatures, pressure, and torque. Thermocouple or infrared probe can be used to monitor the temperature of the material. Specific mechanical energy (SME), the amount of motor power input into each kg of material processed, could be derived from the motor torque readout. However, SME is not as critical as that for melt extrusion process, due to the lower energy-space, at which granulation operations are conducted. Because of multifactor nature of TSG process, multivariate analysis can be performed to understand the effect of processing variables and to identify key risk factors.

Process analytical technology (PAT) should be implement to monitor the properties of granules on-line and in real time. Raman and near infrared spectroscopy have been applied to monitor drug and water content. Acoustic emission is a non-invasive tool to monitor the granule size distribution (Markarian, Jennifer, 2017). Granule

monitoring technologies, such as the Eyecon™ imaging system, can also be used to assess granulation characteristics (Kumar et al., 2015a).

## **1.7 HISTORY, RECENT PROGRESSES AND THE FUTURE IN PHARMACEUTICAL APPLICATION**

The food and polymer industries were dominated by products manufactured by high-shear batch granulation into the 1960s. The transition to TSG to enable continuous manufacturing in 1970s was based on the improved “product uniformity” and “mixing quality” (Martin, 2016). Application of TSWG to prepare pharmaceutical dosage forms was first reported by Gamlen and Eardly in 1986 to improve compaction properties of acetaminophen. Granules containing 80% acetaminophen were prepared. The granulation process was significantly facilitated with the presence of hypromellose in binder solution (Gamlen, M. J. & Eardley, C., 1986). In 2002, Ghebre-Sellasie and his colleagues at Warner Lambert filed the first patent on continuous pharmaceutical wet granulation using TSE. The inventor disclosed a continuous granulation line consisted of twin-screw granulation, milling (optional), microwave drying, and dry milling. The process was successfully demonstrated at 15 kg per hour output rate (Ghebre-Sellassie, I. et al., 2002).

A significant amount of research in TSWG was pioneered by Dhenge’s research team at University of Sheffield, United Kingdom and Thompson’s research team at McMaster University, Canada. They have conducted extensive study in the granule formation mechanisms, effect of screw design, and effect of processing parameters (e.g., liquid-to-solid ratio, location of liquid injection, binder concentration, and degree of fill) (Dhenge et al., 2012a, 2012b; Dhenge et al., 2010; Thompson, 2015b).

Eucreas® tablets, immediate-release tablet of metformin and vildagliptin, is the first commercial product prepared using TSMG. The product was developed at Novartis. Metformin hydrochloride granules are prepared using TSMG. Hydroxypropyl cellulose is used as the thermal binder. The temperature of the extruded granules is about 140 to 160 °C (above the softening temperature of hydroxypropyl cellulose and below the melting point of metformin) (Lakshman et al., 2011a).

From a theoretical perspective, it is possible that melt granulation is a viable alternative to roller compaction process. Roller compaction (RC) is the most common granulation process to manufacture oral dosage forms. However, the well-recognized problems of RC include (1) a limited ability to accommodate very low or very high doses, (2) irregularly-shaped granules and generation of fine particles, that negatively affect flowability and potentially content uniformity, and (3) poor mechanical properties of granules for tableting (Miller, 2005). Granules prepared with TSWG often have improved flow and compaction properties relative to RC. For TSMG, the particle “rolling” inside the extruder also has a spheronization effect on the granules. The coating of particles with molten binders during the extrusion process significantly improves the compaction properties of the granules (N. Kittikunakorn et al., 2017).

## **1.8 CONCLUSION**

The adoption, implementation, and expanded applications of twin-screw granulation and the potential to integrate into continuous manufacturing systems in the pharmaceutical industry resembles what occurred in the food and polymer industry 5 decades ago. Valuable knowledge, technical expertise, and manufacturing experience gained in these industries would allow for expeditious adoption and implementation of this established processing technology to replace existing batch granulation processing. With the concerted efforts and commitment from the pharmaceutical industry, equipment suppliers, excipients companies, and regulatory agencies around the advancement of continuous manufacturing, the “evolution” of twin-screw continuous granulation is expected to continue.

## 1.9 REFERENCES

- Chen, B., Zhu, L., Zhang, F., & Qiu, Y. (2016). Process Development and Scale-Up Twin-Screw Extrusion. In Y. Qiu, Y. Chen, G. G. Z. Zhang, L. Yu, & R. V. Mantri (Eds.), *Developing Solid Oral Dosage Forms: Pharmaceutical Theory and Practice* (Second;2;2nd; ed.). US: Academic Press.
- Dhenge, R. M., Cartwright, J. J., Hounslow, M. J., & Salman, A. D. (2012a). Twin screw granulation: Steps in granule growth. *International Journal of Pharmaceutics*, 438(1), 20-32. doi:<https://doi.org/10.1016/j.ijpharm.2012.08.049>
- Dhenge, R. M., Cartwright, J. J., Hounslow, M. J., & Salman, A. D. (2012b). Twin screw wet granulation: Effects of properties of granulation liquid. *Powder Technology*, 229(Supplement C), 126-136. doi:<https://doi.org/10.1016/j.powtec.2012.06.019>
- Dhenge, R. M., Fyles, R. S., Cartwright, J. J., Doughty, D. G., Hounslow, M. J., & Salman, A. D. (2010). Twin screw wet granulation: Granule properties. *Chemical Engineering Journal*, 164(2), 322-329. doi:<https://doi.org/10.1016/j.cej.2010.05.023>
- Gamlen, M. J., & Eardley, C. (1986). Continuous Extrusion Using a Raker Perkins MP50 (Multipurpose) Extruder. *Drug Development and Industrial Pharmacy*, 12(11-13), 1701-1713. doi:10.3109/03639048609042604
- Ghebre-Sellassie, I., Mollan, M. J., Pathak, N., Lodaya, M., & Fessehaie, M. (2002). U.S. Patent 2304392A.
- Kumar, A., Dhondt, J., De Leersnyder, F., Vercruyssen, J., Vanhoorne, V., Vervaeke, C., . . . Nopens, I. (2015a). Evaluation of an in-line particle imaging tool for monitoring twin-screw granulation performance. *Powder Technology*, 285(Supplement C), 80-87. doi:<https://doi.org/10.1016/j.powtec.2015.05.031>
- Lakshman, J. P., Kowalski, J., Vasanthavada, M., Tong, W. Q., Joshi, Y. M., & Serajuddin, A. T. (2011a). Application of melt granulation technology to enhance tableting properties of poorly compactible high-dose drugs. *J Pharm Sci*, 100(4), 1553-1565. doi:10.1002/jps.22369
- Lodaya, M., Mollan, M., & Ghebre-Sellassie, I. (2003). Twin-screw wet granulation. In I. Ghebre-Sellassie & C. Martin (Eds.), *Pharmaceutical Extrusion Technology* (pp. 323-344): CRC Press.
- Markarian, J. (2017). Scaling Up a Continuous Granulation Process. *Pharmaceutical Technology*, 41(9), 30-31.
- Martin, C. (2016). Twin Screw Extruders as Continuous Mixers for Thermal Processing: a Technical and Historical Perspective. *AAPS PharmSciTech*, 17(1), 3-19. doi:10.1208/s12249-016-0485-3
- Miller, R. W. (2005). Roller Compaction Technology. In D. M. Parikh (Ed.), *Handbook of Pharmaceutical Granulation Technology* (2 ed., pp. 159-190): CRC Press.
- N. Kittikunakorn, D. White, T. Listro, C. Martin, X. Feng, & F. Zhang. (2017). Granulation mechanisms and the effect of processing conditions on physicochemical properties of gabapentin granules prepared by continuous twin-screw extrusion. *AAPS PharmSciTech* (Abstract AM-17-1742).

- Sheskey, P., Keary, C., Clark, D., & Bahwinski, K. (2007). Scale-up trials of foam-granulation technology : high shear. *Pharmaceutical Technology Europe*, 19(9), 37-46.
- Thompson, M. R. (2015b). Twin screw granulation – review of current progress. *Drug Development and Industrial Pharmacy*, 41(8), 1223-1231. doi:10.3109/03639045.2014.983931
- Todd, D. B. (2004). Mixing of Highly Viscous Fluids, Polymers, and Pastes. In S. M. Kresta, V. A. Atiemo-Obeng, E. L. Paul, & V. Atiemo-Obeng (Eds.), *Handbook of Industrial Mixing : Science and Practice* (pp. 987-1024): John Wiley & Sons, Incorporated.
- Vasanthavada, M., Wang, Y., Haeefe, T., Lakshman, J. P., Mone, M., Tong, W., . . . AT, M. S. (2011). Application of melt granulation technology using twin-screw extruder in development of high-dose modified-release tablet formulation. *J Pharm Sci*, 100(5), 1923-1934. doi:10.1002/jps.22411
- White, J. L., & Bumm, S. H. (2010). Perspectives on the Transition from Batch to Continuous Mixing Technologies in the Compounding Industry. *International Polymer Processing*, 25(5), 322-326. doi:10.3139/217.2293



## **Chapter 2: Twin-Screw Melt Granulation: Current Progress and Challenges**

### **2.1 ABSTRACT**

Twin-screw melt granulation (TSMG) is a new alternative method for granulation that offers several advantages over wet and dry granulation methods. TSMG has been rapidly gaining interest over recent years in the pharmaceutical industry. Since it is an inherently continuous process with controlled temperature and shear history, TSMG produces products with more consistent quality compared to the batch process. Studies have been conducted to study how various formulation and processing parameters influence granulation behavior and granule properties; however, there are still challenges that require a better mechanistic understanding to be overcome.

This review article summarizes the current progress of TSMG, highlighting how various formulation and process parameters affect the physicochemical properties of granules. The challenges related to the process-induced physicochemical changes of drug substances are also discussed.

### **2.2 INTRODUCTION**

#### **2.2.1 Purposes of granulation**

Granulation is an essential process applied across different industries such as the pharmaceutical, plastics, chemical, and food industries. Granulation involves size enlargement of fine powders in which small particles are agglomerated and compacted into larger sizes (Ennis, 2010). In the pharmaceutical industry, granulation processes are applied to manufacture the majority of tablet and capsule products. The primary purposes of pharmaceutical granulation are (1) to improve the flowability of powder formulations (Cartwright, Robertson, D'Haene, Burke, & Hennenkamp, 2013), (2) to enhance the tableability of powder formulations, especially blends containing high-dose, poorly

compressible drug (Lakshman et al., 2011a), (3) to improve the homogeneity between drug substance and other excipients in the formulation, (4) to control the particle size distribution to prevent the segregation of the material during downstream processing, and (5) to enhance or regulate the dissolution of drug (Ennis, 2010).

### **2.2.2 Advantages of melt granulation**

Granulation processes can be categorized as wet, melt, or dry granulation. Each process has benefits and limitations. For wet granulation, undesired moisture-induced physicochemical transformations can occur. These changes include chemical degradation and polymorph changes of drug substance and changes in hardness and dissolution during storage (Lakshman et al., 2011a; Shanmugam, 2015). Dry granulation, also known as roller compaction, has a limited ability to process very low and high doses. Granules prepared with dry granulation have lower tableability than their respective powder blends (Sun, C. & Himmelsbach, 2006). Irregularly shaped granules and large amount of fines typically generated during dry granulation negatively impact the flowability and content uniformity (Kittikunakorn, N., DiNunzio, Martin, & Zhang, 2018).

Melt granulation offers several advantages over wet and dry granulation, as it is solvent-free and the granules it produces have superior tableability (Batra, A., Desai, D., & Serajuddin, A. T., 2017). Melt granulation is particularly suitable for moisture-sensitive or highly water-soluble drugs. Melt granulation has been successfully applied at the commercial scale to granulate metformin (Eucras<sup>TM</sup> tablet) in order to overcome the challenges associated with wet granulation. Being freely soluble in water, a significant portion of metformin is solubilized in binder solution. The solubilized metformin does not fully recrystallize following drying. During storage and tableting, moisture in the ambient environment induces the crystallization of amorphous metformin inside the granules that results in poor flowability (Lakshman et al., 2011a).

In melt granulation, nucleation of fine powders is facilitated by softened or molten thermal binders (Grymonpré et al., 2017). Softening or melting of thermal binders is attributed to conducted heat or frictional heating during the process (Steffens & Wagner,

2019a). Following nucleation, granule growth is promoted by the coalescence of large nuclei. Granules are subsequently kneaded and consolidated by applied mechanical forces (Ennis, 2010). The granules are cooled down to room temperature to allow bridge formation of solidified binder (Vervaet & Remon, 2010). Enrichment of the particle surface with highly compressible thermal binders has been demonstrated to effectively improve the tableability of poorly compressible formulations (Lakshman et al., 2011a; Shi, Limin & Sun, Changquan Calvin, 2010).

### **2.2.3 Transformation from traditional batch to continuous twin-screw melt granulation**

Despite its multiple advantages over wet and dry granulation, melt granulation has not been widely used due to its challenges associated with process control and process-induced physicochemical changes. Melt granulation is traditionally performed in batch processes using high-shear granulators equipped with a heating jackets (Schäfer & Mathiesen, 1996b) or using fluid-bed granulators (Veliz Moraga et al., 2015). The poor and non-uniform temperature control in these batch processes limits their granulation performance. Binder selection is limited to only low melting-point thermal binders such as polyethylene glycol. Chemical decomposition of formulations can occur due to exposure to the elevated temperatures for extended periods. To achieve better process control and more consistent product quality, melt granulation based on twin-screw extrusion has been gaining popularity in the pharmaceutical industry over the past 15 years. Recent advancements in melt granulation using twin-screw extruder have been driven by the pharmaceutical industry's growing interest in continuous manufacturing and by the distinctive mixing mechanisms of twin-screw extruder, which could potentially overcome the challenges associated with batch melt granulation.

Twin-screw extrusion was invented in the early 1970s for compounding plastics. Since then, the process has been broadly adopted in other industries such as the food, pharmaceutical, and chemical industries. In the pharmaceutical industry, twin-screw extrusion has been used for a wide range of applications including the preparation of

amorphous solid dispersions for bioavailability enhancement, long-acting implants, abuse-deterrent opioid formulations, and granules. In the pharmaceutical industry, twin-screw granulation (TSG) was first applied by Gamlen and Eardley in 1986 to produce paracetamol granules using a wet granulation process (Gamlen, M. J. & Eardley, C., 1986). In 1987, Lindberg used twin-screw extruder to prepare effervescent paracetamol granules via wet granulation (Lindberg, Tufvesson, Holm, & Olbjer, 1988; Lindberg, Tufvesson, & Olbjer, 1987). Since Warner-Lambert's patent filing on TSG-based continuous pharmaceutical granulation in 2002, TSG has gained popularity as an alternative for traditional batch granulation (Ghebre-Sellassie, Isaac, Matthew J. Mollan, Pathak, Lodaya, & Fessehaie, 2002).

The advantages of twin-screw melt granulation (TSMG) over batch melt granulation are summarized in Table 2.1 The heating in TSMG is more efficient than that of batch granulation originates from both the heat conducted from the barrel and from the frictional heat generated between particles or at particle-screw/barrel contact surfaces. This distinctive heating mechanism of TSMG allows uniform heating to take place locally and minimizes the formulation's exposure to elevated temperatures for extended period of time. Efficient heating during TSMG also enables the use of high melting point thermoplastic polymers (e.g. hydroxypropyl cellulose, hydroxypropyl methylcellulose, methacrylate copolymer, and copovidone) as thermal binders (Batra, A. et al., 2017). In addition, the consistency in product quality is improved due to the small mixing volume inside the extruder, enabling efficient mass and heat transfer (Lodaya, M. & Thompson, 2018). The material is forced to pass through a series of starved zones (partially filled in conveying elements) and pressurized zones (fully filled in mixing elements) in the principle of first-in, first-out. This ensures that all granules experience similar shear history and are uniformly mixed inside the extruder (White & Bumm, 2010).

Table 2.1 Differences between batch vs. continuous melt granulation

	<b>Batch melt granulation</b>	<b>Continuous twin-screw melt granulation</b>
Equipment	High-shear granulator with jacketed mixing vessel	Twin-screw extruder
Binder	Low melting point thermal binder (e.g., PEG or wax)	Both low melting point thermal binder (e.g., PEG or wax) and thermoplastics binder (e.g., HPC, HPMC, or PVP)
Mechanism of heating	Heat conducted by the heated vessel	1. Viscous and frictional heat dissipation by screws 2. Heat conducted by heated barrel
Mechanism of mixing	Mixing by rotating blade	Dispersive and distributive mixing (more extensive and effective)
Processing time	10-20 minutes	10 seconds to 2 minutes
Drug uniformity	Typical of a batch process	Significantly more uniform
Process monitoring and control	Difficult to implement advanced control strategies	Advanced control strategies can be implemented to ensure all critical quality attributes are within specification rather than process variables operating at steady state.

TSMG has been applied to the preparation of a wide range of drug delivery systems, including immediate-release (Lakshman et al., 2011a), sustained-release (Patil, Tiwari, Upadhye, Vladyka, & Repka, 2015; Vaingankar & Amin, 2017), modified-release (Keen et al., 2015), and taste-masking dosage forms (Upadhye, Vladyka, Repka, Park, & Tiwari, 2017). Furthermore, TSMG can efficiently improve tabletability even with low amounts of thermal binder to the extent that tablets containing up to 90% drug substance have been successfully manufactured using a TSMG process. High drug loading is especially beneficial for high-dose drugs since this leads to smaller tablets (Lakshman et al., 2011a; Vasanthavada, Wang, Haeefe, Lakshman, Mone, Tong, Joshi, & AT, 2011). Eucreas<sup>TM</sup> is one of the commercial products prepared using TSMG to produce the granules of metformin-HPC for immediate-release tablets to overcome the

problem related to the solubilization of metformin during wet granulation process (Lakshman et al., 2011a).

### **2.3 TWIN-SCREW EXTRUDER**

The pharmaceutical industry typically uses co-rotating, fully intermeshing, twin-screw extruders in which two parallel screw shafts rotate in the same direction (Giles, 2005). The fully intermeshing characteristic is considered to render the screws self-wiping, such that the flight of one screw wipes material from another screw as material is conveyed down the length of the barrel (DiNunzio, Zhang, Martin, & McGinity, 2012). Self-wiping eliminates the stagnation of the material on the screw surface and barrel wall and is desirable for pharmaceutical processing to maintain drug stability. The length of the processing section is commonly defined by the L/D ratio, which is the ratio of length (L) to the diameter (D) of the barrel (Seem et al., 2015). Extruders with L/D ratio less than 40 are commonly used for pharmaceutical processing (DiNunzio et al., 2012). Extruder barrels are heated using internal cartridge heaters and are cooled with circulating water or oil (Martin, 2013b). The screws arranged on the screw shaft are housed and fit in the bore of the barrel, creating confined space between the screw and barrel wall. This confined space ensures that consistent shear is applied on the material and improves the mixing efficiency, resulting in a more consistent product (Keleb, Vermeire, Vervaet, & Remon, 2004).

Specific functionality can be utilized along the barrel, allowing multiple-unit operations such as feeding, venting, liquid injection, and devolatilization to be conducted in a single extruder. The upstream of the barrel is typically used as a feed zone in which the material is introduced into the extruder (Figure 2.1). Gravimetric or volumetric feeders are used to precisely control the feed rate. Feeding to extruders in pharmaceutical processes is normally conducted in a starve-fed mode where the rate of material feeding into the extruder is less than the processing capability of the extruder (Douroumis, 2012).

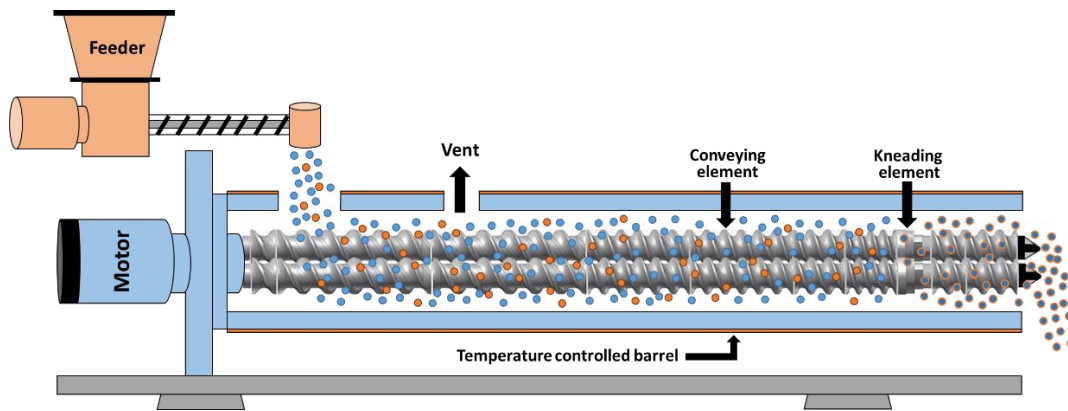


Figure 2.1 Schematic diagram of twin-screw melt granulation

There are mainly three types of screw elements used in granulation: conveying elements, kneading elements, and combing elements (Figure 2.2).

Conveying element	Mixing element	
	Kneading element	Combing element

Figure 2.2 Screw elements for the twin-screw extruder.

### 2.3.1 Conveying element

Conveying elements are mainly used to transfer the material in the forward or reverse direction. They are available in various pitches, with pitch referring to the length between the flights along the element. Narrow-pitch conveying elements exhibit the slowest conveying capacity and the highest degree of fill of channel volume (Giles, 2005). On the other hand, wide pitch conveying elements provide the highest conveying capacity and operate at a lower degree of fill. They are typically used in the feed zone or the devolatilization zone of the extruder (Todd, 1998b). In addition, the pitch length

influences the residence time. As the pitch length decreases, the residence time increases, and it takes more revolutions to convey material over the same axial distance (Ziegler & Aguilar, 2003). Since the conveying element is partially filled, the residence time in this zone is only affected by screw speed. An increase in feed rate, however, will result in a higher degree of fill without changing the residence time in this element (Giles, 2005).

### **2.3.1 Mixing element**

#### **Kneading element**

Kneading elements are used in the mixing zone to apply high-shear mechanical energy to materials via distributive and dispersive mixing. Distributive mixing divides and recombines material without changing its morphology. The materials are uniformly distributed without the particles being broken down. In comparison, dispersive mixing generates shear stress and extensional stress to overcome the cohesive forces of the agglomerates. Dispersive mixing can change the morphology of material and can lead to particle size reduction (Ghebre-Sellassie, Isaac, Martin, Zhang, & Dinunzio, 2018). Kneading elements are composed of individual kneading discs which are offset at specific offset angles (e.g., 30°, 45°, 60°, and 90°). Mixing performance is dictated by both offset angle (W) and disc width (S) (Figure 2.3). Larger offset angles lead to an increase in the opening between discs, thereby reducing the transport force (forwarding flow, T) and increasing the backflow (reversing flow, M). As a result, it reduces the conveying capacity and creates high pressure and compaction which improves the mixing performance (Andersen, 2018). The other aspect of kneading element geometry that plays an important role in mixing performance is the disc width. Narrow kneading disc width reduces shear in the kneading gaps as the material can more easily flow around the disc. As the disc width increases, the material flow is split into fewer streams which reduces the distributive mixing. However, the intensity of dispersive mixing (K) increases as the materials are prone to spread in the axial direction over the crest region as a result of the forces from discs upstream and downstream (Andersen, 2018; Todd, 1998b). Kneading elements usually operate fully filled. Therefore, the residence time in the kneading



element sections can be varied by adjusting the feed rate, but it is not affected by the screw speed.

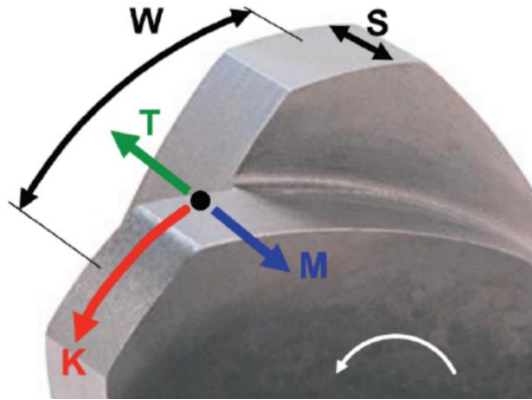


Figure 2.3 Critical parameters of kneading elements: offset angle (W), the disc width (S). T and M indicates forwarding and reversing flow, respectively. K represent the material that passes over the element crest.

### **Combing element**

Combing elements are conveying elements with a series of cuts on their flights to create distributive mixing. The conveying capacity and mixing performance of combing elements are between those of conveying and kneading elements. They offer mixing with less mechanical shear stress applied to the material (Thompson, 2015a). Combing elements are used preferably in twin-screw wet granulation because they can be used to facilitate liquid binder distribution in the solid powder bed or to de-agglomerate the granules following kneading elements (Djuric, Dejan, 2008). However, combing elements might not generate enough shear to melt particular binders in TSMG.

## 2.4 GRANULE FORMATION MECHANISM DURING TSMG

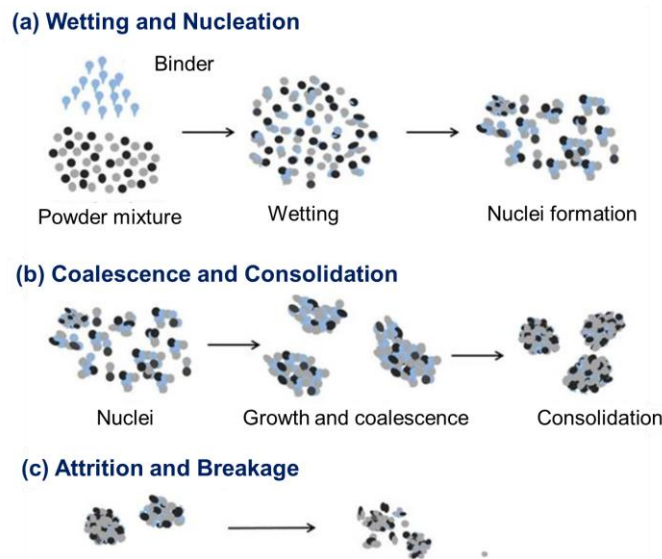


Figure 2.4 Granule formation mechanisms

Granulation consists of three processes: (1) wetting and nucleation, (2) coalescence and consolidation, and (3) attrition and breakage as shown in Figure 2.4 (Yinghe He, Lian X. Liu, James D. Litster, & Kayrak-Talay, 2010). The binder viscosity plays a crucial role in the wetting and nucleation process during TSMG (Monteyne, T., Heeze, Liza, et al., 2016). In batch melt granulation processes using high shear granulators, the granulation mechanism was described as either immersion or distribution as shown in Figure 2.5 (Schæfer, 2001). The distribution mechanism is favored when the binder viscosity is low or when the binder particles are smaller than solid particles being granulated. The immersion mechanism, on the other hand, is dominant when the binder viscosity is high or when the binder particles are relatively large compared to the solid particles.

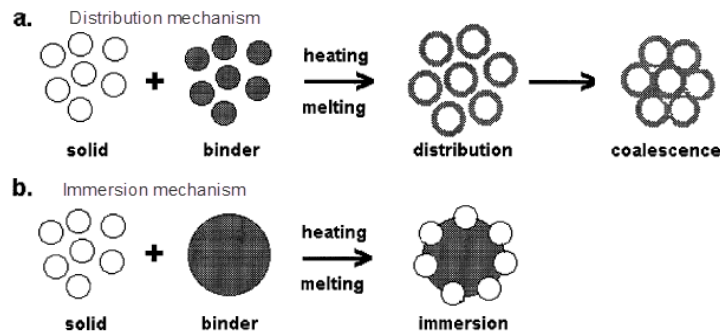


Figure 2.5 Granule formation mechanism in batch melt granulation.

Twin-screw extrusion provides superior mechanical mixing and control of heat and mass transfer compared to high shear granulation. It was suggested that the granulation mechanism in the extruder starts off with an immersion mechanism followed by a distribution mechanism (Mu & Thompson, 2012). At the initial stage of granulation, the high binder viscosity restricts the spread of the binder. The solid particles are captured by the softened binder particles. Once the material is exposed to higher temperatures and more intensive mixing, binder viscosity significantly drops and promotes the distribution of binder on the solid surface particles.

## 2.5 FACTORS AFFECTING THE PHYSICAL PROPERTIES OF GRANULES

Several formulation and process parameters (Table 2.2) can impact granulation behavior during TSMG and subsequently granule properties (Monteyne, Vancoillie, Remon, Vervaet, & De Beer, 2016b). Various factors that significantly affect the physical properties of granules are discussed in this section.

Table 2.2 Formulation and process variables affecting the physical attributes of granules

Factors	Observation	References
Formulation composition		
Binder properties		
<ul style="list-style-type: none"> <li>Binder molecular weight</li> </ul>	Provide two opposing effects: <ol style="list-style-type: none"> <li>Low MW binder promotes the binder distribution, facilitating the granule growth.</li> <li>Smaller granules are formed with lower MW of binder as a result of weak and fragile granules which easy to break.</li> </ol>	(Kittikunakorn, Nada, Koleng, Listro, Calvin Sun, & Zhang, 2019; Liu, Y., Thompson, & O'donnell, 2018)
<ul style="list-style-type: none"> <li>Binder particle size</li> </ul>	<b>Crystalline binder (e.g. PEG):</b> Solid particles are captured on the surface of binder droplet. The larger binder size is used, the large granules are formed. <b>Amorphous binder (e.g. HPC):</b> Binder with larger particle size requires longer time to get soften, thus small granules and fines are generated.	(Kittikunakorn, Nada et al., 2019; Mu & Thompson, 2012; Schæfer & Mathiesen, 1996a)
Drug-binder miscibility	<b>Miscible system:</b> Less processing temperature is required due to plasticizing effect. Drug-binder interaction hinders the polymer movement which restrict the binder distribution. <b>Immiscible system:</b> Higher processing temperature is required. Binder distribution largely depends on the binder viscosity.	(Monteyne, T., Heeze, L., Mortier, S. T., Oldorp, K., Nopens, I., et al., 2016; Monteyne, T., Heeze, Liza, et al., 2016)
Process parameters		
Feed rate and screw speed	Variation of feed rate and screw speed changes the degree of fill and SME, which can be strongly correlate with granules properties. However, different result can be observed, depending on machine variables.	(Kittikunakorn, N., Sun, & Zhang, 2019; Liu, Y., Thompson, & O'donnell, 2018; Monteyne, T., Vancoillie, J., et al., 2016b)
Processing temperature	Processing temperature is typically set at higher than $T_m$ and $T_g$ of the binder. Higher temperature decreases (amorphous) binder viscosity, resulting in improved binder distribution. No significant effect is observed when crystalline binder is used.	(Monteyne, T., Vancoillie, J., et al., 2016b)
Screw configuration	Conveying element generates porous and fragile granules. More compacted and stronger granules are generated with kneading element. The larger offset angle and the wider disc width is used, the higher dispersive mixing is generated.	(Djuric, Dejan & Kleinebudde, 2008; Mu & Thompson, 2012; Van Melkebeke, B., Vervaet, & Remon, 2008; Vercruysse et al., 2012)

## **2.5.1 Formulation Composition**

### **2.5.1.1 Binder properties**

Binders are usually added to formulations to overcome undesirable properties of granules and tablets such as poor compressibility or inadequate granule strength. Binders accomplish this by improving the cohesiveness to the powder, thereby creating strong inter-particulate bonding to form granules. The polymers that can be used as a binder for TSMG are broadly categorized into two groups, hydrophilic and hydrophobic binders (Table 2.3). Binder selection is generally based on the formulation requirement. Hydrophilic binders such as polyethylene glycol (PEG), polyvinyl pyrrolidone (PVP), hydroxypropyl cellulose (HPC), and hydroxypropyl methylcellulose (HPMC) are used for immediate-release formulation. Hydrophobic binders such as ethylcellulose (EC) and waxes are used for modified release dosage forms. For immediated-release dosage forms, hydrophilic binders can be classified into two types: low-melting point binders with low viscosity (e.g. PEG) and thermoplastic binders with high viscosity (e.g. HPC, HPMC). In batch melt granulation processes, the selection of binders is limited to the low-melting point thermal binders. Due to the distinctive melting and mixing mechanisms of TSMG, thermoplastic binders with high melting points or glass transition temperatures can be used (Batra, A. et al., 2017).

Typically, the processing temperature is set above  $T_m$  or  $T_g$  of the polymeric binders but below  $T_m$  of the drug substance to maintain the drug in its crystalline state in order to minimize physicochemical changes. Distribution of molten binders on the surface of solid particles is driven by both mixing and compaction during TSMG. Different binders or the same binder with different particle sizes or molecular weights may exhibit different thermomechanical behavior under the elevated temperature and shear stress, resulting in different granules properties.

Table 2.3 Polymers that is used as a binder in TSMG.

Polymer	Grade	T <sub>g</sub> (°C)	T <sub>m</sub> (°C)
<b>Hydrophilic polymer</b>			
Polyethylene glycol (PEG)	PEG 400 <sup>1,3</sup>	-	53
	PEG 3350 <sup>2,7,10</sup>	-	62
	PEG 4000 <sup>3</sup>	-	65
	PEG 8000 <sup>2,10,17</sup>	-	63
Polyethylene oxide	PEO 1M <sup>5,6,9</sup>		65-70
Poloxamer	Kolliphor® P407 <sup>19</sup>	-	56
	Kolliphor® P188 <sup>9</sup>	-	52-57
Polyvinyl caprolactam-polyvinyl acetate-polyethylene glycol graft copolymer	Soluplus® <sup>1,4,13,14,16</sup>	70	-
Polyvinylpyrrolidone	Kollidon® 12 PF <sup>9</sup>	72	-
	Kollidon® 30 <sup>9</sup>	160	-
Vinylpyrrolidone-vinyl acetate copolymer	Kollidon® VA64 <sup>9,14</sup>	108	-
Hydroxypropyl cellulose	Klucel® ELF <sup>17</sup>	120	-
	Klucel® EXF <sup>9,17,18</sup>	120	-
	Klucel® EF <sup>7</sup>	120	-
	Klucel® HF <sup>11</sup>	130	-
Hydroxypropylmethyl cellulose	HPMC K4M, Affinisol™ 4M <sup>5,14</sup>	96	-
	Affinisol™ 15LV <sup>14</sup>	97	-
	HPMC K100M <sup>11</sup>	175	-
Methylacrylate copolymer	Eudragit® EPO <sup>9,14</sup>	45-53	-
	Eudragit® L100-55 <sup>9</sup>	110	-
Hydrophilic thermoplastic polyurethane (TPU)	Tecophilic™ (SP60D60) <sup>12</sup>	-	71
<b>Hydrophobic polymers</b>			
Glyceryl behenate	Compritol® ATO 888 <sup>5,8,17</sup>	-	70
Glyceryl palmitostearate	Precirol® ATO5 <sup>5</sup>	-	52
Stearic acid <sup>6</sup>		-	69
Ethyl cellulose	Ethocel® <sup>7,11</sup>	133	-
Hydrophobic thermoplastic polyurethane (TPU)	Tecoflex™ (EG72D) <sup>12</sup>	-	55

<sup>1</sup> (Monteyne, T., Vancoillie, J., et al., 2016b), <sup>2</sup> (Mu & Thompson, 2012), <sup>3</sup> (Van Melkebeke, Barbara, Vermeulen, Vervae, & Remon, 2006), <sup>4</sup> (Monteyne, T., Heeze, Liza, et al., 2016), <sup>5</sup> (Tan, David Cheng Thiam et al., 2014), <sup>6</sup> (Monteyne, T., Adriaenssens, P., et al., 2016), <sup>7</sup> (Patil et al., 2015), <sup>8</sup> (Keen et al., 2015), <sup>9</sup> (Batra, A. et al., 2017), <sup>10</sup> (Weatherley, Sharleen, Mu, Thompson, Sheskey, & O' Donnell, 2013), <sup>11</sup> (Vasanthavada, Wang, Haefele, Lakshman, Mone, Tong, Joshi, & AT, 2011), <sup>12</sup> (Verstraete et al., 2016), <sup>13</sup> (Monteyne, Tinne et al., 2016), <sup>14</sup> (Grymonpré et al., 2017), <sup>15</sup> (Xu, Nahar, Dave, Bates, & Morris, 2018), <sup>16</sup> (Monteyne, T., Heeze, L., Mortier, S. T., Oldorp, K., Nopens, I., et al., 2016), <sup>17</sup> (Kittikunakorn, Nada et al., 2019), <sup>18</sup> (Kittikunakorn, N., Sun, C. C., et al., 2019), <sup>19</sup> (Steffens & Wagner, 2019a)

#### **2.5.1.1.1 Binder Molecular Weight**

The binder molecular weight was reported to exhibit two opposing effects on the granule size. On one hand, lower molecular weight results in weak and fragile granules which are more susceptible to breakage during the attrition and breakage steps. On the other hand, the low molecular weight facilitates granule growth by exhibiting more efficient spreading on the surface of solid particles during the wetting and nucleation steps. Therefore, the overall effect of binder molecular weight on the granule size is dependent on the formulation and the process.

Larger caffeine-HPMC granules were observed when HPMC of higher molecular weight was used (HPMC 4M) (Liu, Y., Thompson, & O'donnell, 2018). Higher viscosity resulted in stonger bridges between solid powders, thereby generating larger granules. Consistent results were observed by Mu & Thompson, in which the granule size of lactose increased with higher molecular weights of PEG (PEG 3350 vs PEG 8000) (Mu & Thompson, 2012). The opposite effect was found in gabapentin-HPC granules, in which larger granules were formed when HPC of a lower molecular weight grade (Klucel® ELF) was used due to the more efficient binder distribution. (Kittikunakorn, Nada et al., 2019). However, in terms of the effect of binder molecular weight on the tableability of granules, no significant difference was observed when different molecular weights of PEG (Mu & Thompson, 2012) and HPC (Kittikunakorn, Nada et al., 2019) were used.

#### **2.5.1.1.2 Binder particle size**

The effect of binder particle size on the properties of TSMG granules has been reported. Mu and Thompson observed that the final granule size of lactose becomes larger with an increasing particle size of PEG, suggesting that the immersion mechanism is dominant (Mu & Thompson, 2012). With this mechanism, once the solid binder melts, nuclei of solid powders are captured on the surface of binder droplet. The larger particle size of binder creates larger binder droplets. Therefore, a positive correlation is observed between binder particle size and final granule size (Mu & Thompson, 2012). However,

the opposite effect was observed with thermoplastic binder (e.g., HPC) in which binder of larger particle sizes requires longer residence times inside the barrel to soften. Therefore, when HPC of larger particle size was used (Klucel® EF), more fines or under-granulated granules were obtained as compared to the formulations consisting of finer HPC (Klucel® EXF). In both studies, the particle size of binders had no effect on the tabletability of gabapentin granules.

#### **2.5.1.2 Binder and drug miscibility**

Even though twin-screw extruder is used for both TSMG and hot-melt extrusion (HME), the objectives of these two processes are different. HME requires good miscibility between drug and polymer melt in order to form a drug-polymer solution. Polymer typically accounts for more than 65% of the formulation in HME (Huang, Mao, Williams, & Yang, 2016). In contrast, the objective of TSMG is to form granules using molten polymer as a binder to facilitate the nucleation and agglomeration of solid particles. The miscibility between drug and polymer should be minimized to prevent the physicochemical changes resulted from the solubilization of drug in polymer melt. The miscibility between drug and binder can be determined using differential scanning calorimetry analysis (Kittikunakorn, Nada et al., 2019; Monteyne, T., Heeze, Liza, et al., 2016), Hanson solubility parameters, and Flory-Huggins solubility parameters (Monteyne, T., Vancoillie, J., et al., 2016b). The level of binder is typically below 20% in TSMG process (Lakshman et al., 2011a).

Monteyne et al. examined the effect of miscibility on processability and granule formation (Monteyne, T., Vancoillie, J., et al., 2016b). Formulations (e.g. metoprolol-Soluplus®, acetaminophen-HPC) with good drug-binder miscibility can be processed at lower processing temperatures and with less specific mechanical energy. This is attributed to the plasticization of binder by the solubilized drug. In miscible systems, granule growth is more readily promoted when the nuclei collide. The nuclei are subsequently deformed and kneaded under the intensive mechanical mixing. However, the interaction between drug and polymer restricts the movement of nuclei to be close



together. This phenomenon hinders the polymer chain to flow independently which results in poor binder distribution. The binder is distributed in discontinuous patches rather than forming a continuous binder film, as confirmed by Rheoscope analysis. As a result, the lower strength of granules is produced (Monteyne, T., Heeze, L., Mortier, S. T., Oldorp, K., Nopens, I., et al., 2016).

On the other hand, immiscible systems (e.g. gabapentin-HPC, caffeine-Soluplus®) require higher processing temperatures (above  $T_m$  or  $T_g$  of the polymer) due to the lack of plasticization. Because of the absence of strong drug-binder interaction, a continuous binder film is formed instead of a discontinuous network in the case of miscible system. The distribution of binder on the primary solid particles in an immiscible system largely depends on the binder viscosity. At higher barrel temperatures, the binder viscosity decreases, which facilitates binder distribution and granule growth (Monteyne, T., Heeze, L., Mortier, S. T., Oldorp, K., Nopens, I., et al., 2016).

## 2.5.2 Processing parameters

### 2.5.2.1 Feed rate and screw speed

Feed rate and screw speed are critical parameters that affect the physicochemical properties of granules. Varying feed rate and screw speed can alter the system parameters such as residence time, degree of fill, and specific mechanical energy (SME) (Todd, 1998b). Quality attributes of granules are highly correlated with these systems parameters. These parameters are often kept constant during process scale-up. Degree of fill represents the present volume occupied by the material out of the total free volume inside the barrel. SME represents the amount of energy generated by the motor that inputs into each kilogram of the material processed (Martin, 2013b). The relationship of screw speed and feed rate with SME is represented by the following equation:

$$SME = \frac{kW (motor\ rating) \times \%Torque \times \frac{RPM\ running}{max\ RPM} \times 0.97 (gear\ efficiency)}{Feed\ rate (\frac{kg}{hr})} \quad \text{Equation 2.1}$$

An increase in screw speed and a decrease in feed rate result in higher SME and lower degree of fill. Similar SME and degree of fill can be achieved by using

combinations of different screw speeds and feed rates. Different correlations between processing parameters and granule quality attributes have been reported in literature. One possible explanation might be the differences in screw profile and screw geometry used in the studies. Screw profile and screw geometry play critical roles in determining the granulation behaviors and mechanisms. Higher degree of fill, achieved with high feed rates and low screw speeds, generate larger and stronger granules in small size extruders (e.g., Leistritz Nano-16 mm), while the opposite result was found in larger extruders (e.g., Leistritz Micro-18 mm). Kittikunakorn et al., examined the difference in the granule mechanisms between the Leistritz Nano-16 and the Leistritz Micro-18. The Leistritz Nano-16, commonly used in the early stages of formulation development, exhibits smaller free volume and narrower over-flight gaps. The Leistritz Micro-18 has a higher free volume which is usually used to support phases 1 through 3 clinical trials (0.5 to 4 kg per hour production rate). Due to its narrower kneading discs (2.5 mm in width), the Nano-16 does not provide efficient dispersive mixing to melt thermal binders. Therefore, higher barrel temperatures and higher degree of fill are required to form granules using the Nano-16, as these conditions allow greater axial compaction and more efficient heating by the barrel. At higher degree of fill, better interlocking between the primary particles was achieved. Consequently, larger granules with better tabletability are produced. A similar correlation was also found in granules processed by using the Prism Eurolab 16 twin-screw extruder (Monteyne, T., Vancoillie, J., et al., 2016b).

Conversely, the opposite correlation between processing parameters and granule properties was observed in the Leistritz Micro-18. The kneading discs for the Leistritz Micro-18 are wider (5 mm) and provide more intensive dispersive mixing. As a result, the energy required to melt HPC is predominately provided by the dispersive mixing of kneading elements. The extent of dispersive mixing is quantified by SME. Higher feed rates with the constant screw speed lower the specific mechanical energy applied to the material, resulting in fragile granules of low tabletability. Similar observations were reported in TSMG of caffeine-HPMC granules using a Leistritz ZSE-HP 27 mm extruder (Liu, Y., Thompson, & O'donnell, 2018). Larger and stronger granules were generated at

lower feed rates at a fixed screw speed, which was attributed to high SME generated under this condition. The mechanical energy induces the interaction between particles, facilitating binder distribution and granule growth. Therefore, granules with improved tableability are prepared at high SME conditions (low feed rate and high screw speed). However, high SME imposed on the material potentially affects the physicochemical stability of drug substance as high energy can break down drug crystals and promote amorphization or polymorphic transformation (Kittikunakorn, N., Sun, C. C., et al., 2019). Therefore, SME should be optimized to be sufficient to achieve the strong granules but not too high as to cause the undesirable properties of granules.

#### **2.5.2.2 Barrel temperature**

Barrel temperature is one of the critical processing parameters during TSMG as the heat transfer between the barrel and formulation can play a significant role in granulation formation. Barrel temperature is usually set above the melting point and glass transition temperature of the polymer but below the melting point of crystalline drug. For semi-crystalline binders with low melting points and low melt viscosities (e.g., PEG, waxes), no significant influence on the granule (caffeine-PEG granules) properties was observed as the binder abruptly changes from solid to liquid once the barrel temperature exceeded their melting points (Monteyne, T., Vancoillie, J., et al., 2016b). However, for thermoplastic binders with high molecular weights (e.g., Soluplus®, HPC, HPMC), the effect of barrel temperature is significant. At higher barrel temperature, the improved binder distribution due to lower melt viscosity induced faster agglomeration of the nuclei, which promoted granule growth and increased granule strength. Larger and less friable granules (caffeine-soluplus® granules) were then obtained at higher barrel temperature (Monteyne, T., Vancoillie, J., et al., 2016b).

However, the physicochemical instability of drugs must be considered when choosing a barrel temperature. High barrel temperatures might lead to undesired physicochemical changes of drug substances. Therefore, to achieve granule growth with minimal physicochemical instability, binders of lower melt viscosity should be used since

they require lower processing temperatures to melt. Pre-plasticized or in-situ plasticization commonly used in the HME process to decrease the polymer melt viscosity could be applied in melt granulation process to minimize drug degradation (Repka et al., 2007).

#### **2.5.2.3 Screw configuration**

One distinctive feature of twin-screw granulation is the modular screw design. The sequence of different conveying and mixing elements could be designed to meet specific process needs. Studies have showed that screw configuration can have a significant effect on the size, strength, structure, and temperature of granules (Batra, A. et al., 2017; Mu & Thompson, 2012). Since the conveying elements do not provide intensive shear force, porous and friable granules are typically formed with conveying elements alone (Djuric, Dejan & Kleinebudde, 2008). Wide pitch conveying elements are positioned under the feed and vent zones to transfer the material. Narrow-pitch conveying elements are normally positioned upstream of kneading elements to pre-compact the material prior to its entry into the mixing zone (Todd, 1998b). In the mixing zone, mechanical energy is converted via dispersive and distributive mixing into the thermal energy needed to soften or melt the binders (Vercruysse et al., 2012). This results in an increase in granule temperature. The mixing also promotes the consolidation of nuclei and facilitates binder distribution. As a result, dense and strong granules are formed (Seem et al., 2015). However, very dense granules might not be desirable as the granules resist deformation upon compression, resulting in a deterioration of granules tableability. Moreover, longer disintegration time and slower drug release might occur due to the restriction of the water penetration into dense granules (Vercruysse et al., 2012). Modification of the conveying element located after the mixing zone can also impact the final granule properties. If a narrow-pitch conveying element is used, further breakage and attrition can occur, and the milling process after granulation can be avoided (Van Melkebeke, Barbara et al., 2006). On the other hand, wide pitch conveying elements positioned after the mixing zone can quickly transfer the material out of the extruder after

granule formation which can reduce the exposure time of material to high temperatures. However, oversized granules might be obtained, and a milling process might be required to achieve the optimal granule size.

It was reported that even one mixing zone was sufficient to prepare granules with uniform binder distribution (Van Melkebeke, B. et al., 2008). Mu and Thompson characterized the properties of granules prepared with different screw configurations which were composed of conveying elements with an incremental number of mixing zones consisting of two 60° kneading elements. These three different screw configurations varied the level of mechanical stress and the retention time during the process. Oversized granules with fewer fines are generated as the number of mixing zones increases. However, after the granule growth reached certain threshold, further addition of mixing zones did not result in any significant difference in granule growth (comparable fraction of large granules) (Mu & Thompson, 2012).

Offset angle and the disc width are the key parameters that control the mixing performance of kneading elements. The larger the offset angle and the wider the disc width, the more aggressive the mixing. Thompson and Sun found larger offset angles of kneading elements resulted in higher torque during the granulation process and yielded dense and large granules. This is attributed to the increased shear and extensional stress as the material was squeezed through the openings between the discs and intermeshing region. However, the effect of the offset angle was found to be less significant as the degree of fill decreased (Thompson & Sun, 2010). The disc width strongly influenced the friability and density of granules, in which thicker discs lead to more compacted granules with higher tensile strength (Thompson & Sun, 2010; Van Melkebeke, B. et al., 2008). It was also found that, if conveying elements were added after the kneading elements, breakage and attrition of oversized granules will be observed, suggesting that the granule size can be controlled by modifying the conveying elements position post kneading block (Van Melkebeke, B. et al., 2008). More intense mixing and higher granule temperature can negatively impact the stability of drug substance. Therefore, the screw configuration should be optimized to provide sufficient mechanical energy to facilitate binder

distribution and granule growth without being too aggressive to decrease the physicochemical stability of drug substance.

## **2.6 BINDER DISTRIBUTION**

Improved tableability of granules prepared using TSMG is attributed to the modification of the granule surface by highly compressible thermal binders. Therefore, binder distribution in the granules is critical to their tableability (Steffens & Wagner, 2019a).

Binder distribution within the TSMG granules has been investigated using various techniques. Confocal Raman microscopy was applied to examine the binder distribution of imatinib mesylate-HPC granules. Each component showed different Raman spectra which were mapped and differentiated with different colors. The Raman mapping confirmed the crystalline state of imatinib mesylate and the thin layer of HPC distributed on the surface of drug crystals. This unique spatial distribution of drug and binder resulted in higher tableability and lower friability (Vasanthavada, Wang, Haefele, Lakshman, Mone, Tong, Joshi, & AT, 2011). Near-infrared chemical imaging analysis was applied to visualize binder distribution in cross sections of caffeine-Soluplus® granules. The shear force during granulation led to the “squeeze-out” (enrichment) of Soluplus® onto the granule surface. The distribution of Soluplus® became more uniform under higher barrel temperature. (Monteyne, T., Heeze, Liza, et al., 2016). Scanning electron microscopy coupled with energy-dispersive X-ray was utilized to probe the binder distribution in dicalcium phosphate-poloxamer granules. Carbon mapping was used to visualize the distribution of poloxamer in the granules due to the absence of carbon atoms in dicalcium phosphate. The binder distribution study results showed a positive correlation between binder distribution uniformity and tableability (Steffens & Wagner, 2019a).

Time-of-flight secondary ion mass spectrometry (ToF-SIMS) was applied in our lab to construct the binder distribution map of gabapentin-HPC granules. With a shallow analysis depth around 1 nm, ToF-SIMS is highly sensitive in analyzing the chemical

composition of granule surfaces by detecting the time-of-flight of secondary ions generated from bombarding the granule surface with a primary ion pulse (Furudate et al., 2015). Gabapentin (GABA) and HPC signal are differentiated based on the specific mass-to-charge ratio ( $m/z$ ) of each component. As shown in Figure 2.6, an increase of HPC signal ( $C_2H_3O^-$ ) and a decrease of GABA ( $CH_2N^-$ ) signal intensity indicate the enrichment of HPC on the surface of gabapentin granules. This surface modification resulted in the improved tabletability of gabapentin (Kittikunakorn, Nada et al., 2019).

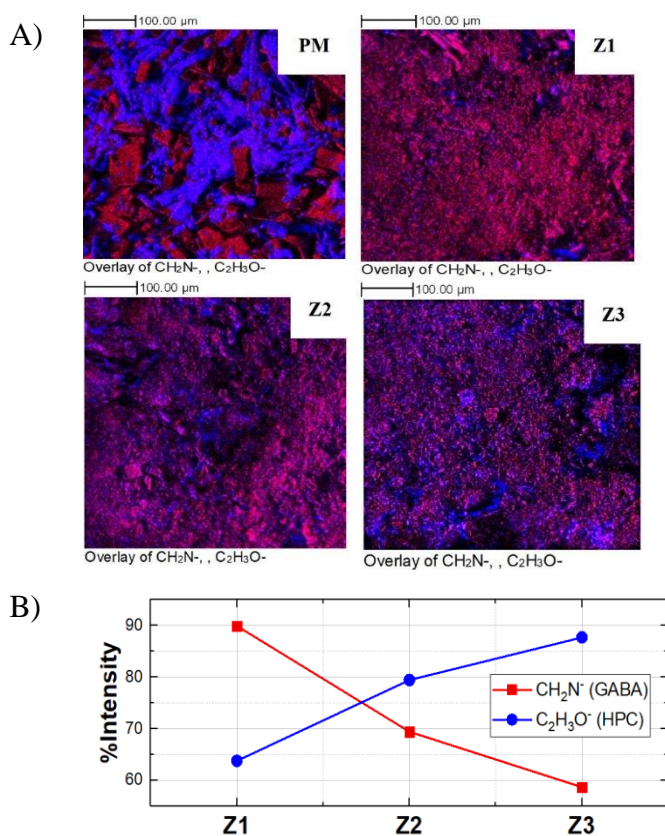


Figure 2.6 (A) Binder distribution in gabapentin-HPC ELF granules samples at different zone of extruder analyzed byToF-SIMS. Blue color is indicative of HPC and red color is indicative of GABA. (B) The signal intensity of  $C_2H_3O^-$  and  $CH_2N^-$  on the surface of granules sampled along the screw from zone 1 to zone 3.

## 2.7 CHALLENGES OF TSMG

The major challenge of TSMG is undesired physicochemical changes of drug substance. During TSMG, formulations are exposed to both elevated temperatures and high mechanical energy. Undesired changes include particle size reduction, polymeric transformation, chemical degradation, and amorphization. All these changes are dependent on the processing conditions (screw speed, feed rate, and barrel temperature), screw configuration and drug-binder miscibility as shown in Figure 2.7.

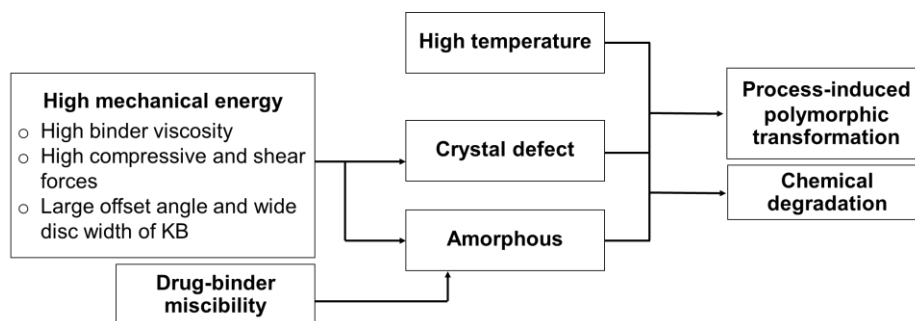


Figure 2.7 Schematic diagram demonstrating the major factors that contribute to the physicochemical instability during TSMG.

### 2.7.1 Polymorphic transformation

TSMG involves both thermal stress and mechanical stress generated from the barrel and frictional viscous dissipation during the process. The machine consists of variable configurations of screw elements which provides different mechanical stress profile. However, the shear stress is mainly generated by the kneading element (Andersen, 2018). During TSMG, the metastable form might be generated and remain stable inside the barrel via kinetic trapping and relaxation mechanism (Morris, Griesser, Eckhardt, & Stowell, 2001). Upon the existing of the extruder, the metastable form should thermodynamically relax to its stable form. However, depending on the cooling rate and the molecular interaction between drug and polymer, the metastable form might be trapped in the granules.



Polymorphic transformation of drug substance can lead to physicochemical stability changes. For example, the conversion of acetaminophen form I (monoclinic) to form II (orthorhombic) during TSMG has been reported, in which form II showed improved tabletability due to the sliding planes present in the orthorhombic form, causing fragmentation and plastic deformation under high compression pressure (Grymonpré et al., 2016; Maniruzzaman et al., 2014). The polymorphic transformation of Indomethacin was also found during TSMG with PEG 3350 as the binder. Indomethacin converted from the stable  $\gamma$  form to a mixture of the amorphous state and the metastable  $\alpha$  form, in which the amorphous will subsequently undergo the recrystallization back to the metastable  $\alpha$  form during the cooling. It was found that the thermal stress was the dominant factor that stimulates the polymorphic transition of indomethacin (Xu et al., 2018). (Otsuka, Otsuka, & Kaneniwa, 1994).

Multiple variables during the process, including formulation and processing conditions, can significantly impact the extent of polymorphic transformation. The influence of binder on the polymorphic transformation has been observed by Monteyne et al. Conversion of caffeine anhydrous form II to I was detected during TSMG with Soluplus®. As the Soluplus® level was increased from 5% to 30%, the onset temperature of the polymorphic conversion shifted to a lower temperature (120 to 110°C). It was explained that the polymer acts as an impurity which absorbed on the surface of drug crystal. Polymer, therefore, can disturb the crystal arrangement at the molecular level, causing polymorphic transformation (Monteyne, Tinne et al., 2016; Tiwary, 2007). The conversion of gabapentin form II to form IV was found in TSMG of gabapentin-HPC based granules when using 60° trilobed kneading elements (Leistritz Nano-16). 60° trilobed kneading elements functions as neutral elements in which there is no conveying capacity to transfer the material forward. Such elements exhibit aggressive dispersive mixing. The material was imposed on intense thermal and mechanical stress, causing the conversion of polymorph to metastable form (form IV) which was more stable under the stress condition. Upon exiting the extruder, due to rapid cooling, the metastable form of

gabapentin was then trapped inside the granules following the process and highly susceptible to further chemical degradation (Kittikunakorn, N., Sun, C. C., et al., 2019).

### **2.7.2 Chemical degradation**

Another challenge of TSMG is the potential chemical degradation of drug substance. The chemical instability of drug substance is attributed to various factors, including (1) melting of the drug and subsequent degradation, (2) solubilization of drug in molten binders, (3) amorphous form generated following the processes which is susceptible to degradation, and (4) crystal size reduction of drug substance. As previously discussed, thermal and mechanical stress during TSMG can induce the transition from the crystalline form to the metastable or amorphous form of the drug substance. Even though some drug molecules are not susceptible to polymorphic transformation, partially amorphization or disordered crystal lattices can occur under high mechanical stress. The amorphous or crystal defects exhibit high free energy which substantially accelerates chemical degradation due to the greater molecular mobility (Yoshioka & Aso, 2007).

The interaction between drug and polymer is one of the factors that can promote amorphization upon elevated temperatures and high mechanical stress during TSMG. Drug molecules can fully or partially dissolve in the polymer melt if they are miscible and subsequently undergo chemical degradation (Alexis, 2005). For a drug with good chemical stability, such as metformin, the dissolution of the drug in polymer melt might be less concerning in terms of chemical stability. However, dissolved drug in polymer melt can potentially change the physical properties, such as compressibility, flowability or dissolution of granules (Hou et al., 2019). In addition, the recrystallization of dissolved drug can occur upon storage, leading to variation of the physical properties of granules. Therefore, to minimize the amorphization, thermal binders that are immiscible with drug would be preferred.

Binder viscosity also impacts the chemical degradation during TSMG. Higher barrel temperature and higher mixing energy are required to soften or melt thermoplastic binders. Drug crystals in the formulation are therefore exposed to higher thermal and

mechanical stresses as well, causing amorphization and particle size reduction. The effect of three thermal binders, including HPC, PEG 8000 and Compritol, on the physicochemical properties of gabapentin granules was evaluated in our study. Due to the high melt viscosity of HPC as compared to PEG8000 and Compritol, a significant size reduction of gabapentin in HPC-based formulation from 63  $\mu\text{m}$  to 10  $\mu\text{m}$  was observed which predominately occurred over the kneading block. The crystal defect of gabapentin was also observed by using scanning electron microscopy (SEM) showing the roughness of crystal surface. The generated crystal defect is normally a region that exhibits higher free energy and greater molecular mobility, which can serve as sites for initiation of chemical reactions (Newman & Zografi, 2014). Therefore, the higher crystal defects are generated, leading to the faster degradation kinetics in the granules (Kittikunakorn, Nada et al., 2019).

Processing parameters, including feed rate and screw speed, also contribute to chemical degradation during TSMG as they can alter the residence time, degree of fill, and mechanical energy input to the material (Kittikunakorn, N., Sun, C. C., et al., 2019). Increasing screw speed and decreasing feed rate generally increase the specific mechanical energy applied to the material. For amorphous solid dispersion by hot-melt extrusion (HME), there was a positive correlation between SME and degradation, as observed in formulations of meloxicam and copovidone (Haser, Abbe, Huang, Siyuan, Listro, Tony, White, David, & Zhang, Feng, 2017a). However, the observed correlation between processing conditions and chemical degradation in TSMG differed depending on the extruder geometry. Degree of fill was found to positively correlate with chemical degradation of GABA granules processed in small extruders (Leistritz Nano-16) due to the high axial compaction force. Crystal size reduction was found in granules processed at high degree of fill which corresponds to higher chemical degradation due to an increase in the specific surface and crystal defect (Kittikunakorn, N., Sun, C. C., et al., 2019). Granule formation in larger extruders (Leistritz Micro-18), on the other hand, was predominantly based on the mechanical energy generated at the kneading element as increasing screw speed or decreasing feed rate. The degradation level positively

correlated with SME. The higher SME was, the more crystal defect or amorphization occurred, subsequently leading to more chemical degradation.

Screw configuration also plays a critical role that contributes to the chemical degradation during TSMG. High compressive and shear forces are predominately generated at the kneading element which corresponds to particle size reduction and the high degradation level. However, narrow-pitch conveying element located prior to kneading element was also reported to introduce compressive force to the material as a result of an increased degree of fill in the screw channel (Kittikunakorn, Nada et al., 2019). Therefore, to decrease the chemical degradation, screw design with the minimization of packing should be considered. This includes avoiding the use of highly aggressive kneading elements in the mixing zone and a long length of narrow-pitch conveying elements. Also, large-pitch conveying elements located after the mixing zone is preferred to minimize the thermal stress by efficiently transferring granules out of the extruder.

## **2.8 PROCESS ANALYTICAL TECHNOLOGY (PAT) IN TWIN-SCREW MELT GRANULATION**

One of the main drives behind the pharmaceutical industry's interest in TSMG is the benefits TSMG provides as a continuous process. Process data (also known as soft sensor), such as extrusion torque, barrel temperature, and barrel heating and cooling duration can be used for predicting granule quality. Several techniques have been recently developed and utilized for in-time monitoring of granule quality attributes such as granule size, granule temperature, flow properties, content uniformity, and solid-state properties (Fonteyne et al., 2012). Various imaging techniques can be used to characterize size, shape, and surface roughness of granules prepared using TSMG. Eyecon<sup>TM</sup> 3D Particle Characterizer was used to monitor TSMG granules (Kumar et al., 2015b; Liu, H. et al., 2019). This technique is based on high-speed imaging using illumination pulses to capture the movement of the particles, providing surface morphology, shape, and size information of granules. Spatial Filter Velocimetry has been

applied in other granulation processes such as fluidized bed wet granulation (Burggraeve et al., 2010), high-shear wet granulation, and twin-screw wet granulation (Madarász et al., 2018). The process could be readily adapted in TSMG process. In spatial filter velocimetry, the size and velocity of the granules are measured as the particles pass through a laser beam and cast shadows onto a linear array of optical fibers. Photometric stereo imaging (FlashSizer FS3D) technique was used to simultaneously evaluate the granule size distribution, granule shape, and surface roughness. The granules are illuminated with light sources from different incident angles to create 3D surfaces with a photometric approach. The three-dimensional features of the surface images created are then used in particle size analysis. The surface roughness is evaluated based on the different intensity of the grey level in the images (Fonteyne et al., 2012).

Raman spectroscopy and Near-Infrared Spectroscopy (NIR) are two PAT tools commonly used to determine the content uniformity (Fonteyne et al., 2016; Harting & Kleinebudde, 2018) and solid-state properties (Fonteyne et al., 2012). Raman spectroscopy measured the light scattered from a sample by using the laser light as an excitation source, while NIR measures the transmittance of electromagnetic radiation at the wavelength in the range of 780 to 2500 nm after interacted and absorbed by the sample. The fingerprint spectra obtained from both techniques reveal the chemical composition at the atomic scale and can be used to quantify the concentration and the solid-state properties of APIs. Raman and NIR spectroscopy for real-time process monitoring typically provided a huge number of spectra. Multivariate data analysis is applied to process and develop the model to interpret the data from the raw spectra (Otsuka, Mouri, & Matsuda, 2003). Infrared sensors can be used to measure granule temperature.

## **2.9 CONCLUSION**

TSMG is a technique that has rapidly gained popularity recently as an alternative method for granulation. To transition from the traditional batch process to the continuous process might still require an extensive understanding of how formulation and process

variables can affect the quality attributes of granules. Several studies have been conducted in an effort to provide a more mechanistic understanding and to show the potential for adoption and implementation of this technique. However, despite the several advantages offered by TSMG, because the process involves elevated temperatures and intensive high shear, the challenges related to physicochemical instability of drug substances still need to be considered and addressed. Several in-line monitoring techniques and PAT have to be employed due to the complexity of the system to visualize the active process. Moreover, modeling of the TSMG is another area that needs to be developed for process understanding, optimization, and scale-up. Ultimately, despite the challenges that need to be overcome, TSMG still remains an attractive technique that shows a great potential for the granulation process.

## 2.10 REFERENCES

- Alexis, F. (2005). Factors affecting the degradation and drug-release mechanism of poly(lactic acid) and poly[(lactic acid)-co-(glycolic acid)]. *Polymer International*, 54, 36-46. doi:10.1002/pi.1697
- Andersen, P. G. (2018). *Fundamentals Of Twin-Screw Compounding: Kneading Block Performance Characteristics*. Paper presented at the SPE International Conference.
- Batra, A., Desai, D., & Serajuddin, A. T. (2017). Investigating the Use of Polymeric Binders in Twin Screw Melt Granulation Process for Improving Compactibility of Drugs. *J Pharm Sci*, 106(1), 140-150. doi:10.1016/j.xphs.2016.07.014
- Burggraeve, A., Van Den Kerkhof, T., Hellings, M., Remon, J. P., Vervaet, C., & De Beer, T. (2010). Evaluation of in-line spatial filter velocimetry as PAT monitoring tool for particle growth during fluid bed granulation. *European Journal of Pharmaceutics and Biopharmaceutics*, 76(1). doi:10.1016/j.ejpb.2010.06.001
- Cartwright, J. J., Robertson, J., D'Haene, D., Burke, M. D., & Hennenkamp, J. R. (2013). Twin screw wet granulation: Loss in weight feeding of a poorly flowing active pharmaceutical ingredient. *Powder Technology*, 238, 116-121. doi:<https://doi.org/10.1016/j.powtec.2012.04.034>
- DiNunzio, J. C., Zhang, F., Martin, C., & McGinity, J. W. (2012). Melt extrusion. In R. O. Williams Iii, A. B. Watts, & D. A. Miller (Eds.), *Formulating Poorly Water Soluble Drugs* (1. ed.). New York, NY: AAPS Advances in the Pharmaceutical Sciences, Springer New York.
- Djuric, D. (2008). *Continuous Granulation with a Twin-Screw Extruder* (Vol. 1): Cuvillier Verlag.
- Djuric, D., & Kleinebudde, P. (2008). Impact of screw elements on continuous granulation with a twin-screw extruder. *Journal of Pharmaceutical Sciences*, 97(11), 4934-4942. doi:10.1002/jps.21339
- Douroumis, D. (2012). *Hot-melt extrusion pharmaceutical applications*. Chichester, West Sussex, U.K: Wiley.
- Ennis, B. J. (2010). Theory of Granulation: An Engineering Perspective. In D. M. Parikh. (Ed.), *Handbook of pharmaceutical granulation technology* (Vol. 3): New York : Informa Healthcare USA.
- Fonteyne, M., Soares, S., Vercruysse, J., Peeters, E., Burggraeve, A., Vervaet, C., . . . De Beer, T. (2012). Prediction of quality attributes of continuously produced granules using complementary pat tools. *European Journal of Pharmaceutics and Biopharmaceutics*, 82(2), 429-436. doi:10.1016/j.ejpb.2012.07.017
- Fonteyne, M., Vercruysse, J., De Leersnyder, F., Besseling, R., Gerich, A., Oostra, W., . . . De Beer, T. (2016). Blend uniformity evaluation during continuous mixing in a twin screw granulator by in-line NIR using a moving F-test. *Analytica Chimica Acta*, 935, 213-223. doi:<https://doi.org/10.1016/j.aca.2016.07.020>
- Furudate, T., Kurasako, Y., Takata, E., Morishita, T., Miwa, A., Suzuki, R., & Terada, K. (2015). Possibility of monitoring granulation by analyzing the amount of

- hydroxypropylcellulose, a binder on the surface of granules, using ToF-SIMS. *International Journal of Pharmaceutics*, 495(2), 642-650. doi:10.1016/j.ijpharm.2015.09.060
- Gamlen, M. J., & Eardley, C. (1986). Continuous Extrusion Using a Raker Perkins MP50 (Multipurpose) Extruder. *Drug Development and Industrial Pharmacy*, 12(11-13), 1701-1713. doi:10.3109/03639048609042604
- Ghebre-Sellassie, I., Martin, C. E., Zhang, F., & Dinunzio, J. (2018). *Pharmaceutical extrusion technology* (2 ed. Vol. 217). Boca Raton, Florida ;: CRC Press.
- Ghebre-Sellassie, I., Matthew J. Mollan, J., Pathak, N., Lodaya, M., & Fessehaie, M. (2002). U.S. Patent 2304392A.
- Giles, H. F. (2005). *Extrusion : the definitive processing guide and handbook / by Harold F. Giles, Jr., John R. Wagner, Jr., Eldridge M. Mount, III*. Norwich, NY: William Andrew Pub.
- Grymonpré, W., De Jaeghere, W., Peeters, E., Adriaenssens, P., Remon, J. P., & Vervaet, C. (2016). The impact of hot-melt extrusion on the tableting behaviour of polyvinyl alcohol. *International Journal of Pharmaceutics*, 498(1-2). doi:10.1016/j.ijpharm.2015.12.020
- Grymonpré, W., Verstraete, G., Vanhoorne, V., Remon, J. P., De Beer, T., & Vervaet, C. (2017). Downstream processing from melt granulation towards tablets : in-depth analysis of a continuous twin-screw melt granulation process using polymeric binders. *European Journal of Pharmaceutics and Biopharmaceutics*, 124. doi:10.1016/j.ejpb.2017.12.005
- Harting, J., & Kleinebudde, P. (2018). Development of an in-line Raman spectroscopic method for continuous API quantification during twin-screw wet granulation. *European Journal of Pharmaceutics and Biopharmaceutics*, 125, 169-181. doi:<https://doi.org/10.1016/j.ejpb.2018.01.015>
- Haser, A., Huang, S., Listro, T., White, D., & Zhang, F. (2017a). An approach for chemical stability during melt extrusion of a drug substance with a high melting point. *International Journal of Pharmaceutics*, 524(1-2), 55-64. doi:10.1016/j.ijpharm.2017.03.070
- Hou, H. H., Rajesh, A., Pandya, K. M., Lubach, J. W., Muliadi, A., Yost, E., . . . Nagapudi, K. (2019). Impact of Method of Preparation of Amorphous Solid Dispersions on Mechanical Properties: Comparison of Coprecipitation and Spray Drying. *Journal of Pharmaceutical Sciences*, 108(2), 870-879. doi:<https://doi.org/10.1016/j.xphs.2018.09.008>
- Huang, S., Mao, C., Williams, R. O., & Yang, C.-Y. (2016). Solubility Advantage (and Disadvantage) of Pharmaceutical Amorphous Solid Dispersions. *Journal of Pharmaceutical Sciences*, 105(12), 3549-3561. doi:10.1016/j.xphs.2016.08.017
- Keen, J. M., Foley, C. J., Hughey, J. R., Bennett, R. C., Jannin, V., Rosiaux, Y., . . . McGinity, J. W. (2015). Continuous twin screw melt granulation of glyceryl behenate: Development of controlled release tramadol hydrochloride tablets for improved safety. *Int J Pharm*, 487(1-2), 72-80. doi:10.1016/j.ijpharm.2015.03.058



- Keleb, E. I., Vermeire, A., Vervaet, C., & Remon, J. P. (2004). Extrusion Granulation and High Shear Granulation of Different Grades of Lactose and Highly Dosed Drugs: A Comparative Study. *Drug Development and Industrial Pharmacy*, 30(6), 679-691. doi:10.1081/DDC-120039338
- Kittikunakorn, N., DiNunzio, J., Martin, C., & Zhang, F. (2018). Processes, Challenges and Futures in Twin-screw Continuous Granulation for Manufacturing Oral Tablets and Capsules. *Cover article AAPS Newsmagazine*. 12-18, Mar 2018, 12-18.
- Kittikunakorn, N., Koleng, J. J., Listro, T., Calvin Sun, C., & Zhang, F. (2019). Effects of thermal binders on chemical stabilities and tableability of gabapentin granules prepared by twin-screw melt granulation. *International Journal of Pharmaceutics*, 559, 37-47. doi:<https://doi.org/10.1016/j.ijpharm.2019.01.014>
- Kittikunakorn, N., Sun, C. C., & Zhang, F. (2019). Effect of screw profile and processing conditions on physical transformation and chemical degradation of gabapentin during twin-screw melt granulation. *European Journal of Pharmaceutical Sciences*, 131, 243-253. doi:<https://doi.org/10.1016/j.ejps.2019.02.024>
- Kumar, A., Dhondt, J., De Leersnyder, F., Vercruysse, J., Vanhoorne, V., Vervaet, C., . . . Nopens, I. (2015b). Evaluation of an in-line particle imaging tool for monitoring twin-screw granulation performance. *Powder Technology*, 285, 80-87. doi:<https://doi.org/10.1016/j.powtec.2015.05.031>
- Lakshman, J. P., Kowalski, J., Vasanthavada, M., Tong, W. Q., Joshi, Y. M., & Serajuddin, A. T. (2011a). Application of melt granulation technology to enhance tableting properties of poorly compactible high-dose drugs. *J Pharm Sci*, 100(4), 1553-1565. doi:10.1002/jps.22369
- Lindberg, N. O., Tufvesson, C., Holm, P., & Olbjer, L. (1988). Extrusion of an Effervescent Granulation with a Twin Screw Extruder, Baker Perkins MPF 50 D. Influence on Intragranular Porosity and Liquid Saturation. *Drug Development and Industrial Pharmacy*, 14(13), 1791-1798. doi:10.3109/03639048809151987
- Lindberg, N. O., Tufvesson, C., & Olbjer, L. (1987). Extrusion of an Effervescent Granulation with a Twin Screw Extruder, Baker Perkins MPF 50 D. *Drug Development and Industrial Pharmacy*, 13(9-11), 1891-1913. doi:10.3109/03639048709068698
- Liu, H., Ricart, B., Stanton, C., Smith-Goettler, B., Verdi, L., O'Connor, T., . . . Yoon, S. (2019). Design space determination and process optimization in at-scale continuous twin screw wet granulation. *Computers & Chemical Engineering*, 125. doi:10.1016/j.compchemeng.2019.03.026
- Liu, Y., Thompson, M. R., & O'donnell, K. P. (2018). Impact of non-binder ingredients and molecular weight of polymer binders on heat assisted twin screw dry granulation. *International Journal of Pharmaceutics*, 536(1), 336-344. doi:10.1016/j.ijpharm.2017.11.061
- Lodaya, M., & Thompson, M. (2018). Continuous Oral Solid Dose Manufacture. In I. Ghebre-Sellassie, C. Martin, F. Zhang, & J. DiNunzio (Eds.), *Pharmaceutical Extrusion Technology* (2 ed.): CRC Press.

- Madarász, L., Nagy, Z. K., Hoffer, I., Szabó, B., Csontos, I., Pataki, H., . . . Marosi, G. (2018). Real-time feedback control of twin-screw wet granulation based on image analysis. *International Journal of Pharmaceutics*, 547(1), 360-367. doi:<https://doi.org/10.1016/j.ijpharm.2018.06.003>
- Maniruzzaman, M., Islam, M. T., Moradiya, H. G., Halsey, S. A., Slipper, I. J., Chowdhry, B., . . . Douroumis, D. (2014). Prediction of Polymorphic Transformations of Paracetamol in Solid Dispersions. *Journal of Pharmaceutical Sciences*, 103(6), 1819-1828. doi:10.1002/jps.23992
- Martin, C. (2013b). Twin Screw Extrusion for Pharmaceutical Processes. In M. A. Repka, N. Langley, & J. DiNunzio (Eds.), *Melt Extrusion Materials, Technology and Drug Product Design, AAPS Advances in the Pharmaceutical Sciences Series*, 9 (1st ed. 2013. ed., pp. 47-79). New York, NY: Springer New York.
- Monteyne, T., Adriaenssens, P., Brouckaert, D., Remon, J. P., Vervaet, C., & De Beer, T. (2016). Stearic acid and high molecular weight PEO as matrix for the highly water soluble metoprolol tartrate in continuous twin-screw melt granulation. *Int J Pharm*, 512(1), 158-167. doi:10.1016/j.ijpharm.2016.07.035
- Monteyne, T., Heeze, L., Mortier, S. T., Oldorp, K., Nopens, I., Remon, J. P., . . . De Beer, T. (2016). The use of rheology to elucidate the granulation mechanisms of a miscible and immiscible system during continuous twin-screw melt granulation. *Int J Pharm*, 510(1), 271-284. doi:10.1016/j.ijpharm.2016.06.055
- Monteyne, T., Heeze, L., Mortier, S. T. F. C., Oldörp, K., Cardinaels, R., Nopens, I., . . . De Beer, T. (2016). The use of Rheology Combined with Differential Scanning Calorimetry to Elucidate the Granulation Mechanism of an Immiscible Formulation During Continuous Twin-Screw Melt Granulation. *Pharmaceutical Research*, 33(10), 2481-2494. doi:10.1007/s11095-016-1973-6
- Monteyne, T., Heeze, L., Oldörp, K., Vervaet, C., Remon, J.-P., & De Beer, T. (2016). Vibrational spectroscopy to support the link between rheology and continuous twin-screw melt granulation on molecular level: A case study. *European Journal of Pharmaceutics and Biopharmaceutics*, 103, 127-135. doi:10.1016/j.ejpb.2016.03.030
- Monteyne, T., Vancoillie, J., Remon, J. P., Vervaet, C., & De Beer, T. (2016b). Continuous melt granulation: Influence of process and formulation parameters upon granule and tablet properties. *Eur J Pharm Biopharm*, 107, 249-262. doi:10.1016/j.ejpb.2016.07.021
- Morris, K. R., Griesser, U. J., Eckhardt, C. J., & Stowell, J. G. (2001). Theoretical approaches to physical transformations of active pharmaceutical ingredients during manufacturing processes. *Advanced Drug Delivery Reviews*, 48(1), 91-114. doi:[https://doi.org/10.1016/S0169-409X\(01\)00100-4](https://doi.org/10.1016/S0169-409X(01)00100-4)
- Mu, B., & Thompson, M. R. (2012). Examining the mechanics of granulation with a hot melt binder in a twin-screw extruder. *Chemical Engineering Science*, 81, 46-56. doi:10.1016/j.ces.2012.06.057

- Newman, A., & Zografi, G. (2014). Critical Considerations for the Qualitative and Quantitative Determination of Process-Induced Disorder in Crystalline Solids. *Journal of Pharmaceutical Sciences*, 103(9), 2595-2604. doi:10.1002/jps.23930
- Otsuka, M., Mouri, Y., & Matsuda, Y. (2003). Chemometric evaluation of pharmaceutical properties of antipyrine granules by near-infrared spectroscopy. *AAPS PharmSciTech*, 4(3), 142-148. doi:10.1208/pt040347
- Otsuka, M., Otsuka, K., & Kaneniwa, N. (1994). Relation Between Polymorphic Transformation Pathway During Grinding and the Physicochemical Properties of Bulk Powders for Pharmaceutical Preparations. *Drug Development and Industrial Pharmacy*, 20(9), 1649-1660. doi:10.3109/03639049409050205
- Patil, H., Tiwari, R. V., Upadhye, S. B., Vladyka, R. S., & Repka, M. A. (2015). Formulation and development of pH-independent/dependent sustained release matrix tablets of ondansetron HCl by a continuous twin-screw melt granulation process. *Int J Pharm*, 496(1), 33-41. doi:10.1016/j.ijpharm.2015.04.009
- Repka, M. A., Battu, S. K., Upadhye, S. B., Thumma, S., Crowley, M. M., Zhang, F., . . . McGinity, J. W. (2007). Pharmaceutical Applications of Hot-Melt Extrusion: Part II. *Drug Development and Industrial Pharmacy*, 33(10), 1043-1057. doi:10.1080/03639040701525627
- Schäfer, T. (2001). Growth mechanisms in melt agglomeration in high shear mixers. *Powder Technology*, 117(1), 68-82. doi:10.1016/S0032-5910(01)00315-1
- Schäfer, T., & Mathiesen, C. (1996a). Melt pelletization in a high shear mixer. IX. Effects of binder particle size. *International Journal of Pharmaceutics*, 139(1), 139-148. doi:[http://dx.doi.org/10.1016/0378-5173\(96\)04548-6](http://dx.doi.org/10.1016/0378-5173(96)04548-6)
- Schäfer, T., & Mathiesen, C. (1996b). Melt pelletization in a high shear mixer. VII. Effects of product temperature. *International Journal of Pharmaceutics*, 134(1-2), 105-117. doi:10.1016/0378-5173(95)04455-8
- Seem, T. C., Rowson, N. A., Ingram, A., Huang, Z., Yu, S., de Matas, M., . . . Reynolds, G. K. (2015). Twin screw granulation — A literature review. *Powder Technology*, 276(C), 89-102. doi:10.1016/j.powtec.2015.01.075
- Shanmugam, S. (2015). Granulation techniques and technologies: recent progresses. *BioImpacts : BI*, 5(1), 55-63. doi:10.15171/bi.2015.04
- Shi, L., & Sun, C. C. (2010). Transforming Powder Mechanical Properties by Core/Shell Structure: Compressible Sand. *Journal of Pharmaceutical Sciences*, 99(11), 4458-4462. doi:<https://doi.org/10.1002/jps.22172>
- Steffens, K. E., & Wagner, K. G. (2019a). Improvement of tabletability via twin-screw melt granulation: Focus on binder distribution. *International Journal of Pharmaceutics*, 570. doi:10.1016/j.ijpharm.2019.118649
- Sun, C., & Himmelsbach, M. W. (2006). Reduced tabletability of roller compacted granules as a result of granule size enlargement. *Journal of Pharmaceutical Sciences*, 95(1), 200-206. doi:10.1002/jps.20531
- Tan, D. C. T., Chin, W. W. L., Tan, E. H., Hong, S., Gu, W., & Gokhale, R. (2014). Effect of binders on the release rates of direct molded verapamil tablets using

- twin-screw extruder in melt granulation. *International Journal of Pharmaceutics*, 463(1), 89-97. doi:10.1016/j.ijpharm.2013.12.053
- Thompson, M. R. (2015a). Twin screw granulation - review of current progress (Vol. 41, pp. 1223-1231): Informa Healthcare.
- Thompson, M. R., & Sun, J. (2010). Wet granulation in a twin-screw extruder: Implications of screw design. *Journal of Pharmaceutical Sciences*, 99(4), 2090-2103. doi:10.1002/jps.21973
- Tiwary, A. (2007). Crystal habit changes and dosage form performance. *Encyclopedia of Pharmaceutical Technology*, 820-833.
- Todd, D. B. (1998b). *Plastics Compounding Equipment and Processing*. Munich: Hanser
- Upadhye, S. B., Vladyka, p. R. R. S., Repka, M. A., Park, J.-b., & Tiwari, R. V. (2017).
- Vaingankar, P., & Amin, P. (2017). Continuous melt granulation to develop high drug loaded sustained release tablet of Metformin HCl. *Asian Journal of Pharmaceutical Sciences*, 12(1), 37-50. doi:<https://doi.org/10.1016/j.ajps.2016.08.005>
- Van Melkebeke, B., Vermeulen, B., Vervaet, C., & Remon, J. P. (2006). Melt granulation using a twin-screw extruder: A case study. *International Journal of Pharmaceutics*, 326(1-2), 89-93. doi:10.1016/j.ijpharm.2006.07.005
- Van Melkebeke, B., Vervaet, C., & Remon, J. P. (2008). Validation of a continuous granulation process using a twin-screw extruder. *International Journal of Pharmaceutics*, 356(1-2), 224-230. doi:10.1016/j.ijpharm.2008.01.012
- Vasanthavada, M., Wang, Y., Haefele, T., Lakshman, J. P., Mone, M., Tong, W., . . . AT, M. S. (2011). Application of melt granulation technology using twin-screw extruder in development of high-dose modified-release tablet formulation. *J Pharm Sci*, 100(5), 1923-1934. doi:10.1002/jps.22411
- Veliz Moraga, S., Villa, M. P., Bertín, D. E., Cotabarren, I. M., Piña, J., Pedernera, M., & Bucalá, V. (2015). Fluidized-bed melt granulation: The effect of operating variables on process performance and granule properties. *Powder Technology*, 286, 654-667. doi:10.1016/j.powtec.2015.09.006
- Vercruysse, J., Córdoba Díaz, D., Peeters, E., Fonteyne, M., Delaet, U., Van Assche, I., . . . Vervaet, C. (2012). Continuous twin screw granulation: influence of process variables on granule and tablet quality. *European Journal of Pharmaceutics and Biopharmaceutics*, 82(1). doi:10.1016/j.ejpb.2012.05.010
- Verstraete, G., Mertens, P., Grymonpré, W., Van Bockstal, P. J., De Beer, T., Boone, M., . . . Vervaet, C. (2016). A comparative study between melt granulation/compression and hot melt extrusion/injection molding for the manufacturing of oral sustained release thermoplastic polyurethane matrices. *International Journal of Pharmaceutics*, 513(1-2). doi:10.1016/j.ijpharm.2016.09.072
- Vervaet, C., & Remon, J. P. (2010). Mlet granulation. In D. M. Parikh. (Ed.), *Handbook of pharmaceutical granulation technology* (Vol. 3): New York : Informa Healthcare USA.

- Weatherley, S., Mu, B., Thompson, M. R., Sheskey, P. J., & O' Donnell, K. P. (2013). Hot-Melt Granulation in a Twin Screw Extruder: Effects of Processing on Formulations with Caffeine and Ibuprofen. *Journal of Pharmaceutical Sciences*, 102(12), 4330-4336. doi:10.1002/jps.23739
- White, J. L., & Bumm, S. H. (2010). Perspectives on the Transition from Batch to Continuous Mixing Technologies in the Compounding Industry. *International Polymer Processing*, 25(5), 322-326. doi:10.3139/217.2293
- Xu, T., Nahar, K., Dave, R., Bates, S., & Morris, K. (2018). Polymorphic Transformation of Indomethacin during Hot Melt Extrusion Granulation: Process and Dissolution Control. *Pharmaceutical Research*, 35(7), 1-15. doi:10.1007/s11095-017-2325-x
- Yinghe He, Lian X. Liu, James D. Litster, & Kayrak-Talay, D. (2010). Scale-up Considerations in Granulation. In D. M. Parikh. (Ed.), *Handbook of pharmaceutical granulation technology* (Vol. 3): New York : Informa Healthcare USA.
- Yoshioka, S., & Aso, Y. (2007). Correlations between molecular mobility and chemical stability during storage of amorphous pharmaceuticals (Vol. 96, pp. 960-981). Hoboken: Wiley Subscription Services, Inc., A Wiley Company.
- Ziegler, G. R., & Aguilar, C. A. (2003). Residence time distribution in a co-rotating, twin-screw continuous mixer by the step change method. *Journal of Food Engineering*, 59(2-3), 161-167. doi:10.1016/S0260-8774(02)00453-3

## **Chapter 3: Effects of Thermal Binders on Chemical Stabilities and Tabletability of Gabapentin Granules Prepared by Twin-Screw Melt Granulation<sup>2</sup>**

### **3.1 ABSTRACT**

The effect of thermal binders on the physicochemical properties of gabapentin, a thermally labile drug, in granules prepared using twin-screw melt granulation was investigated in this study. Hydroxypropyl cellulose (HPC), a thermoplastic high molecular-weight binder, was compared against conventional low molecular-weight semi-crystalline thermal binders PEG 8000 and Compritol. Both the chemical degradation and polymorph form change of gabapentin were analyzed. The effects of particle size and molecular weight of HPC on the properties of granules were also studied. To overcome the high melt viscosity of HPC, higher barrel temperatures and higher specific mechanical energy were required to attain suitable granules. As a result, higher levels of gabapentin degradant were observed in HPC-based formulations. However, gabapentin form change was not observed in all formulations. Smaller particle size and lower molecular weight of HPC led to faster granule growth. The tabletability of granules was insensitive to the variations in particle size and molecular weight of HPC. Gabapentin crystal size reduction, HPC size reduction, and HPC enrichment on granule surface were observed for HPC-based granules.

---

<sup>2</sup> Kittikunakorn, N., Koleng, J. J., Listro, T., Calvin Sun, C., & Zhang, F. (2019). Effects of thermal binders on chemical stabilities and tabletability of gabapentin granules prepared by twin-screw melt granulation. *International Journal of Pharmaceutics*, 559, 37-47.  
I am the primary author of this work.

## 3.2 INTRODUCTION

The majority of marketed pharmaceutical tablets and capsules are manufactured using granulation processes, such as wet, melt, and dry granulation. Powders are granulated to prevent material segregation and to improve powder properties (e.g., flowability and tableability) (Iveson, Simon M., Litster, Hapgood, & Ennis, 2001; Kittikunakorn, N., DiNunzio, Martin, & Zhang, 2018). All three granulation techniques are also used across many other industries, such as the food and plastics industries. Melt granulation offers several advantages over wet granulation and dry granulation, because it is solvent free and can effectively improve the tableability of the granule (Batra, A. et al., 2017). During melt granulation, the enlargement of granules is facilitated by molten thermal binders, which solidify upon cooling after exiting the granulator. Pharmaceutical melt granulation is traditionally carried out in batch-process equipment, such as high-shear granulator equipped with heating jacket, and fluid-bed granulator.

In pursuit of better process control and more consistent product quality, other industries, such as metallurgy and energetic materials gradually transitioned from batch to continuous melt granulation using twin-screw extruders in early 1970s (Dombe, Mehilal, Bhongale, Singh, & Bhattacharya, 2015). In contrast, the adoption of twin-screw melt granulation (TSMG) has been slow in the pharmaceutical industry. However, with the introduction of twin-screw granulation technology (Gamlen, M. & Eardley, C., 1986) in 1986 and the first disclosed patent of the twin-screw granulation (US patent 6,499,984 B1) by the Warner-Lambert company, the TSMG technique has gained attention as an alternative method to wet and dry granulation (Ghebre-Sellassie, I. et al., 2002). Renewed interest in twin-screw melt granulation by both pharmaceutical companies and regulatory agencies are also driven by the increased interest in continuous manufacturing of pharmaceutical products (Lee, 2017).

TSMG operates under different principles and offers many advantages over batch melt granulation. Even though the TSMG operates under globally starved conditions (the extruder barrel is 30 to 70 percent filled during processing), the processing section of a twin-screw extruder consists of both starved (partially filled in conveying elements) and

pressurized (fully filled in mixing elements) segments, dictated by the screw elements (White & Bumm, 2010). In comparison, powder is always under the globally starved and is unpressurized conditions and randomly subjected to the high shear zone in a batch granulator, potentially resulting in non-uniform mixing dynamics. In TSMG, the material is forced through a sequence of starved and pressurized zones in accordance to the screw element design. As a result, granules prepared using TSMG have a more uniform mixing history, where incoming blend is processed in a principle of first-in, first-out with a given residence time distribution. This allows the system to operate in a state of control and to ensure the consistent quality of granules (Chen et al., 2016; White & Bumm, 2010). Process analytical technology (PAT) could be implemented to monitor the properties of granules on line and in real time during TSMG. For example, Raman and near infrared spectroscopy have been applied to monitor drug content uniformity (Paudel, Rajjada, & Rantanen, 2015). Acoustic emission is used to monitor the granule size distribution (Markarian, J., 2017). Granule monitoring technologies, such as the Eyecon® imaging system, were also used to assess granule size distribution (Kumar et al., 2015b).

The TSMG process is more versatile and can process a wider range of powder compositions than batch melt granulation. During TSMG, powder blends are heated by not only the heat conducted from the barrel but also the viscous or frictional heat dissipation from the mixing by rotating screws, making it feasible to use high melting point (or softening-point) thermoplastic materials, such as hydroxypropyl cellulous (HPC), methacrylate copolymers, and copovidone (Batra, A. et al., 2017).

TSMG has been applied to prepare a wide range of dosage forms, such as immediate release tablet (Lakshman et al., 2011b), modified release tablets (Vasanthavada, Wang, Haefele, Lakshman, Mone, Tong, Joshi, & Serajuddin, 2011), wax matrix granules (Keen et al., 2015), and water-dispersible granules (Van Melkebeke, Barbara et al., 2006). TSMG provided a robust manufacturing process with highest compactibility and lowest friability that were not sensitive to changes in atmospheric moisture level. The process can decrease tablet sizes of high-dose drugs and combination



products by decreasing the need for relatively large amounts of excipients generally used to overcome physicochemical limitations of drug substances (Lakshman et al., 2011b). Vasanthavada and his colleagues demonstrated that the level of drug release retardant could be reduced with TSMG process. This unique advantage of TSMG for modified release tablets is particularly beneficial for high-dose drug (Vasanthavada, Wang, Haefele, Lakshman, Mone, Tong, Joshi, & Serajuddin, 2011). In Keen and Van Melkebeke's studies, extrudates granules were used as the final dosage forms with desired drug release characteristics without further processing (Keen et al., 2015; Van Melkebeke, Barbara et al., 2006). Studies have been carried out to investigate the effect of thermal binder type (Batra, A. et al., 2017), thermal binder level (Lakshman et al., 2011b), screw profile, and processing conditions on the properties of granules (Weatherley, S., Mu, Thompson, Sheskey, & O'Donnell, 2013). All these studies focused primarily on the flow and compaction properties of the granules. In general, the level of binders required to achieve desired compactability is low (5-20%) for TSMG formulations.

The mechanisms of granule formation have also been studied (Monteyne, T., Heeze, L., Mortier, S. T., Oldorp, K., Cardinaels, R., et al., 2016). Spectroscopic analysis revealed drug-polymer interactions which constrain the polymer to flow independently. As a result, the binder distribution step, which generally follows the immersion step, was hindered. This insight assisted the understanding of the granule properties. Inhomogeneous granules were produced due to large initial nuclei or adhesion of multiple smaller nuclei. Consequently, a higher granulation temperature was required in order to get the binder more homogeneously distributed within the granules (Monteyne, T., Heeze, L., Mortier, S. T., Oldorp, K., Cardinaels, R., et al., 2016). Since powder blends are exposed to high thermal and mechanical stresses during TSMG, the chemical degradation and the polymorphic transformation of the drug substance is a potential challenge to successful manufacturing. However, the effects of formulation composition on the chemical and physical stabilities of drugs during TSMG have rarely been investigated, if at all.

The main objective of this study was to investigate the effect of thermal binders on the stabilities (physical and chemical) and tableability of melt-extruded granules. Gabapentin (GABA), a thermally labile drug, was used as the model compound. Three types of thermal binders were investigated: PEG 8000 (low-melting point hydrophilic binder), Compritol (low-melting point hydrophobic binder), and HPC (thermoplastic binder) (Figure 3.1). As a high-dose drug (600 or 800 mg unit dose) with poor compaction properties, commercial GABA tablets are manufactured using high-shear or fluid-bed granulation process. GABA is thermally labile and undergoes an intramolecular cyclization dehydration reaction to yield gabapentin-lactam upon melting at 174°C (Figure 3.2). The rate of GABA degradation is not only a function of temperature but also GABA crystallinity. Spray-dried amorphous solid dispersions of GABA in HPC at 10% and 20% drug loadings completely degraded within one week of storage in induction-sealed HDPE bottles placed at 40°C/75% RH. In comparison, only less than 0.1% crystalline GABA drug substance degraded under the same condition. GABA was also chosen because it undergoes polymorphic transition at elevated temperatures (Hsu, C. H., Ke, W. T., & Lin, S. Y., 2010).

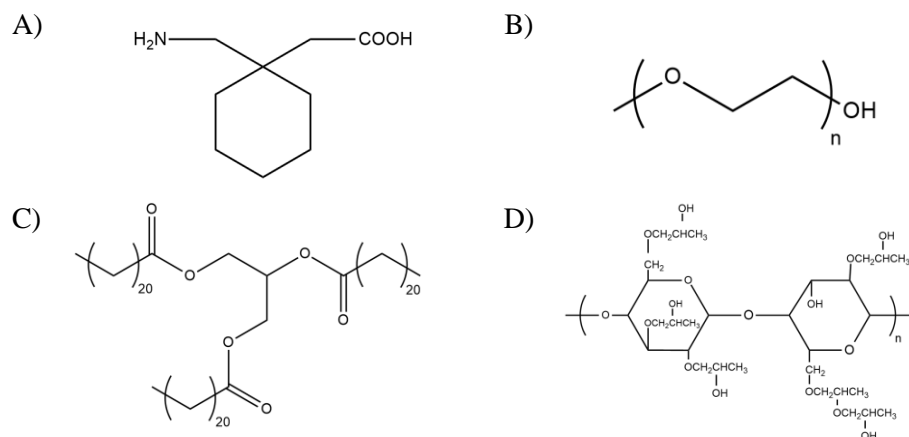


Figure 3.1 Chemical structures of (A) gabapentin (GABA), (B) polyethylene glycol 8000 (PEG 8000), (C) glycerol behenate (Compritol), and (D) hydroxypropyl cellulose (HPC).

The second objective was to investigate the effect of HPC variability on the physicochemical properties of TSMG GABA granules. HPC is available from Ashland Chemical in a variety of grades that differ in molecular weight and particle size. The

effects of these physical attributes of HPC on GABA chemical stability and granule tableability were investigated. The third objective was to study the spatial arrangement of HPC and GABA in the GABA TSMG granules. Time-of-flight secondary ion mass spectrometry was applied to determine the distribution of GABA and HPC on the surface of the granules.

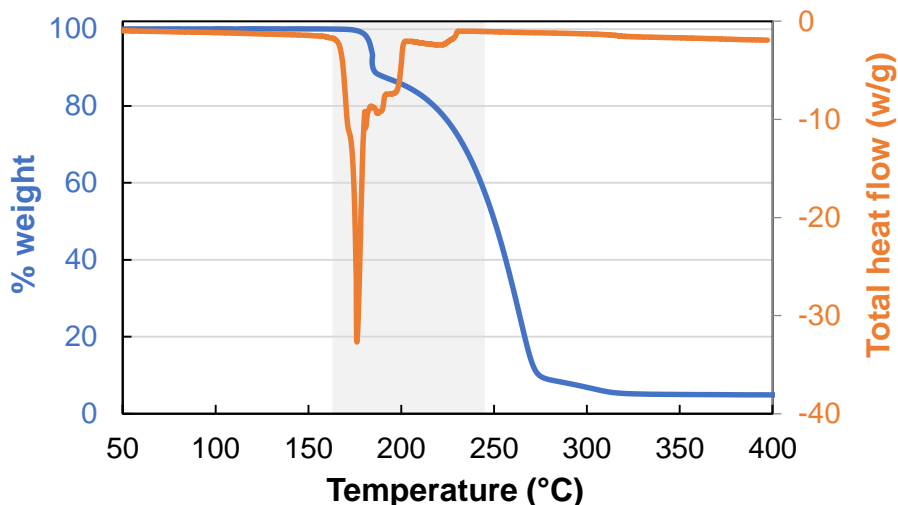


Figure 3.2 DSC and TGA thermograms of gabapentin (GABA) drug substance. At the melting point temperature of GABA, TGA thermogram shows the 10% weight loss due to chemical degradation.

### 3.3 MATERIALS AND METHODS

#### 3.3.1 Materials

Gabapentin was purchased from ShenZhen Nexconn Pharmatechs (Shenzhen, China). Hydroxy propyl cellulose (Klucel® ELF and Klucel® EXF) was kindly donated by Ashland Inc. (Wilmington, DE). Polyethylene glycol (PEG 8000) was obtained from Spectrum Chemical (New Brunswick, NJ). Glyceryl behenate (Compritol) was supplied from Gattefosse (Saint-Priest, France). All other chemicals were of ACS grade or of higher purity.

### 3.3.2 Methods

#### 3.3.2.1 Twin-screw melt granulation

A physical mixture consisting of 80% (w/w) GABA and 20% (w/w) binder was prepared in a Turbula® Shaker-Mixer (Glen Mills, Clifton, NJ) for ten minutes. All granulation experiments were performed on a Leistritz Nano-16 co-rotating twin-screw extruder (American Leistritz Extruder Corp., Somerville, New Jersey) with an open-end discharge configuration. A 12 mm twin-screw volumetric feeder (Model MT-1, Brabender Technologies, Ontario, Canada) was used to meter the powder blend into the extruder. Screw configuration, processing parameters, and extrusion torque are summarized in Table 3.1. The feeding zone was cooled with water. Zones 1 and 2 were set at equal temperatures. Zone 3 was set at a lower temperature to allow the granules to cool down prior to exiting the barrel and before cooling at ambient conditions.

Table 3.1 Summary of process setup and extrusion torque for twin-screw melt granulation.

Formulation	Barrel temperature (°C)			Feed rate (g/min)	Screw speed (rpm)	Torque (Nm)
	Zone 1	Zone 2	Zone 3			
80%GABA+20% Compritol	80	80	40	10	100	0.7-1.0
80%GABA+20% PEG 8000	90	90	60	10	100	1.8-2.0
80%GABA+20% HPC	120	120	70	10	100	5.0-5.2

GFA X-XX-XX Co-rotating conveying screw-trilobal screw-pitch length (mm)-screw length (mm)  
 KB X-X-XX-XX Kneading block-number of kneading segment-screw length (mm)-the angle (°)  
 0d to 26d Length to diameter ratio (total barrel length is 420 mm, barrel diameter is 16 mm)

### **3.3.2.2 Miscibility of Gabapentin with thermal binders**

Gabapentin-binder miscibility was analyzed using differential scanning calorimetry and hot-stage polarized light microscopy. A differential scanning calorimeter (DSC Q20, TA Instruments, New Castle, DE, USA) was used to determine the depression of GABA's melting point in drug-binder mixtures. Mixtures with GABA content ranging from 10 to 80% were prepared using mortar and pestle. About 5 mg of mixture was sealed in a hermetic aluminum pan with a pin hole pierced through the lid. Samples were heated at 5 °C/min to the respective Zone 2 processing temperature during TSMG for each binder and held for 5 minutes prior to heating to 250°C at 20°C/minute.

The physical mixtures consisting of 80% GABA and 20% of different binders were heated on a hot-stage placed under a polarized light microscope (BX-53, Olympus, Waltham, MA) to the respective Zone 2 processing temperature of TSMG. The changes in the size and shape of GABA crystals were monitored in real-time. Images were taken with a QICAM digital camera (QImaging, BC, Canada) with Q capture software (Ver. 2.0.13, QImaging, BC, Canada).

### **3.3.2.3 Granule size distribution**

Granule size distribution was characterized using Retch Camsizer® Dynamic Image Analyzer apparatus (V.4.2.1., Haan, Germany). Approximately 10 g of granules were poured into the feeder of the instrument. The granules were then dropped in front of the measuring cameras to record the particle size with an image rate of 100% (1:1) and a display interval of 50. The covered area of the image recorded by CCD-Basic and CCD-Zoom, which was included in the measurement, was set at 2%. The measured particle size range was between 53 µm - 4000 µm. The control level for fast forward and the starting level for measurement of the feeder were set at 65 and 55, respectively.

### **3.3.2.4 Image analysis using scanning electron microscope**

The morphology of GABA crystals and granules was analyzed using a scanning electron microscope (SEM, Zeiss Supra40, USA). Prior to imaging, samples were distributed on carbon tapes fixed to the aluminum sample holders and sputter coated with

platinum/palladium to achieve 12 nm thickness. Samples were analyzed under vacuum with the electron beam operating at 5 kv.

Melt-extruded GABA granules were initially dispersed in solvents that do not dissolve GABA but easily dissolve thermal binders. Acetone was used for GABA-PEG 8000 and GABA-HPC granules, while chloroform was used for GABA-Compritol granules. The dispersions were stirred with magnetic stirrer for at least 2 hours to dissolve thermal binders. Dispersed GABA crystals were collected using centrifugation method. The crystals were dried at ambient conditions prior to SEM analysis.

### **3.3.2.5 Tableability of melt-extruded granules**

Granules prepared using TSMG were milled using a conical mill (Quadro Comil, U5-0516, Ontario, Canada). A 0.032-inch, round-hole screen and a square impeller at 1000 rpm were used for all formulations. Granules between 250 µm to 850 µm (20 to 60 mesh) were collected and mixed with 1% magnesium stearate for 3 minutes in a Turbula® Shaker-Mixer (Glen Mills, Clifton, NJ). Tablets (350±5 mg) were compressed with a manual tablet compression machine (MTCM-I, Globe pharma, NJ, USA) using 11 mm flat-faced round tooling. Tablet diametrical breaking strength, thickness and diameter (n=5) were recorded and the tensile strength (MPa) of the tablets was calculated using equation 3.1:

$$TS = \frac{2F}{\pi DH} \quad \text{Equation 3.1}$$

where F, D and H denote the tablet breaking force (N), tablet diameter (mm) and tablet thickness (mm), respectively.

### **3.3.2.6 HPLC analysis of gabapentin and gabapentin-lactam of granules**

GABA and GABA-latam content of the granules was analyzed with a Thermo Scientific Dionex UltiMate 3000 HPLC System (Thermo Scientific, Sunnyvale, CA, USA). Chromeleon software (Version 6.80, Thermo Scientific, Sunnyvale, CA, USA) was used to process all chromatography data. An Inertsil® ODS-2, C18 reverse phase HPLC column (4.6 x 150 mm, with 5-µm packing, GL Sciences Inc., Japan) was used. The mobile phase consisted of water, acetonitrile, and methanol at a 60:30:10 ratio. An

isocratic flow at 0.8 mL/min was used. The analysis wavelength was 210 nm. The retention time of GABA and GABA-lactam was approximately 32 and 12.8 min, respectively. Purified water was used as the extraction medium. The nominal concentration of GABA was 5 mg/mL. Samples were sonicated and filtered through a 0.45  $\mu\text{m}$  Nylon membrane prior to HPLC analysis. The injection volume was 20  $\mu\text{L}$ . The LOD and LOQ of GABA-lactam were 0.03 and 0.08  $\mu\text{g/mL}$ , respectively.

### **3.3.2.7 Melt viscosity of thermal binders**

The melt viscosity of the binders was determined using a melt rheometer (AR2000, TA Instruments, New Castle, DE, USA) with a 25 mm ETC steel plate. The viscosity of PEG 8000, Compritol ATO888, and HPC ELF was measured at temperatures of 80, 90, and 120°C (corresponding to extrusion barrel Zone 2 temperatures), respectively, with the shear rate ranging from 100 to 1000  $\text{s}^{-1}$ . Normal force was between 10 and 15 N. The sample was equilibrated at the target temperature for 3 min before each measurement.

### **3.3.2.8 FT-IR analysis**

FT-IR analysis was performed to determine the polymorphic form of GABA in the physical mixture and granules using a Thermo Nicolet iS50 spectrometer (ThermoFisher Scientific, Waltham, MA) equipped with an attenuated total reflection accessory. Sample was placed on the germanium crystal surface, compressed using the built-in pressure tower to achieve uniform contact between the solid and the crystal. The samples were analyzed at room temperature with the following setting: 4000–600  $\text{cm}^{-1}$ , 64 scans, resolution of 4  $\text{cm}^{-1}$ . The peak positions were determined using OMNIC software peak picking function (ThermoFisher Scientific, Waltham, MA).

### **3.3.2.9 Particle size of gabapentin in melt-extruded granules**

The particle size of GABA in the TSMG granules was determined using a laser diffraction method. The granules were first dispersed in a solvent that practically does not dissolve GABA but easily dissolves thermal binders to prepare concentrated GABA

dispersions. The dispersions were stirred with magnetic stirrer for at least 2 hours to dissolve thermal binders. Acetone was used for GABA-PEG 8000 and GABA-HPC granules, while chloroform was used for GABA-Compritol granules. The size of the resulting dispersed GABA crystals was measured using a laser diffraction size analyzer (Sympatec Helos equipped with an R3 lens and a cuvette dispersing system, Sympatec GmbH, Germany). The corresponding solvent (acetone or chloroform) was used as a blank solution in the cuvette and stirred with magnetic stir bar to prevent the sedimentation of GABA during analysis. Concentrated GABA dispersions were added drop-wise until the light obscuration reached 10-25%. Data was then collected every 100 ms for 10 seconds.

#### **3.3.2.10 Time-of-flight secondary ion mass spectrometry (ToF-SIMS)**

The distribution of GABA and binder on the surface of the granules was determined using Time-of-flight secondary ion mass spectrometry (ToF-SIMS) (ION-TOF GmbH, Germany). A sample was placed on carbon tape fixed to the sample plate. The operating conditions consisted of a 30 keV  $\text{Bi}^{3+}$  analysis beam and a 500 eV Cs sputter beam. The sample was sputtered with Cs for 400 sec prior to collecting the data. A 500 x 500  $\mu\text{m}$  area of each sample was raster scanned at a resolution of 256 x 256 pixels. Specific ion peaks for each component were determined. GABA and HPC were identified using the spectrum of  $\text{CH}_2\text{N}^-$  ( $m/z = 28$ ) and  $\text{C}_2\text{H}_3\text{O}^-$  ( $m/z = 43$ ) peaks, respectively. The measured intensity of the  $\text{CH}_2\text{N}^-$  and  $\text{C}_2\text{H}_3\text{O}^-$  peaks was represented by brightness in the images. Binder distribution map was constructed by overlaying the intensity map of  $\text{CH}_2\text{N}^-$  (representing GABA) and  $\text{C}_2\text{H}_3\text{O}^-$  (representing HPC).

### **3.4 RESULTS AND DISCUSSION**

#### **3.4.1 Selection of thermal binders and processing parameters**

Because of the challenges posed by high-dose, poor tableability, and thermal instability of GABA, formulation composition and TSMG process must be designed to improve the compaction properties of GABA while maintaining its chemical and physical



stability. Thermal binders were selected based on two criteria: (1) low melting point for semi-crystalline materials or glass transition temperature for amorphous binders, and (2) poor miscibility with GABA. These types of thermal binders would allow the processing at lower temperatures and lower mechanical stress, which correspond to lower tendency of physical and chemical changes in GABA.

Amorphization of GABA from mechanical milling substantially accelerated GABA degradation (Zong, Z. X. et al., 2011). We have observed that spray-dried GABA dispersion consisting of 60% HPC and 40% GABA completely degraded following 2 weeks storage at 40 °C/75%RH. It is reasonable to expect that GABA dissolved in binder during TSMG that does not crystallize also degrades at a faster rate than crystalline GABA. Thus, our goal is to minimize the amorphization and crystal defects of GABA during TSMG. We hypothesize that good miscibility between GABA and thermal binders leads to poor chemical stability of GABA. Although this effect is of practical importance, the effect of drug-binder miscibility during TSMG on the chemical stability of drug has not been reported. Depending on the solubility of drug in molten binder, formulation blends for TSMG have been classified into miscible and immiscible systems (Monteyne, T., Heeze, L., Mortier, S. T., Oldorp, K., Cardinaels, R., et al., 2016). It has been demonstrated that the miscibility between drugs and thermal binders significantly affects the extrusion conditions (e.g., torque) and granule properties (e.g., size distribution and friability).

All three thermal binders, PEG 8000, Compritol, and HPC, are free-flowing powders at ambient conditions but melt or soften at elevated temperatures during TSMG. Both PEG 8000 and Compritol are commonly used semi-crystalline binders in TSMG with melting points of 60 and 73°C, respectively (Mu & Thompson, 2012; Tan, D. C. T. et al., 2014). PEG 8000 is water-soluble while Compritol is water-insoluble. In comparison, HPC is a thermoplastic polymer with a glass transition temperature of about 20°C (Rials & Glasser, 1988). Because of the high melt viscosity of HPC, powder blends containing HPC as a thermal binder can only be granulated by a twin-screw extruder and not by a high shear granulator. TSMG using HPC as the thermal binder has been used to

manufacture metformin granules in Eucreas™ commercial tablets (Lakshman et al., 2011b). HPC is available in a wide range of molecular weights (40,000 – 1,150,000) and two particle sizes (regular grind with 250 µm mean particle size and fine grind with 50 µm mean particle size). The HPC ELF, a low molecular weight (40,000) and a regular grind grade, was used in the current study. The effects of excipient variability were also investigated using HPC of different molecular weight and particle sizes.

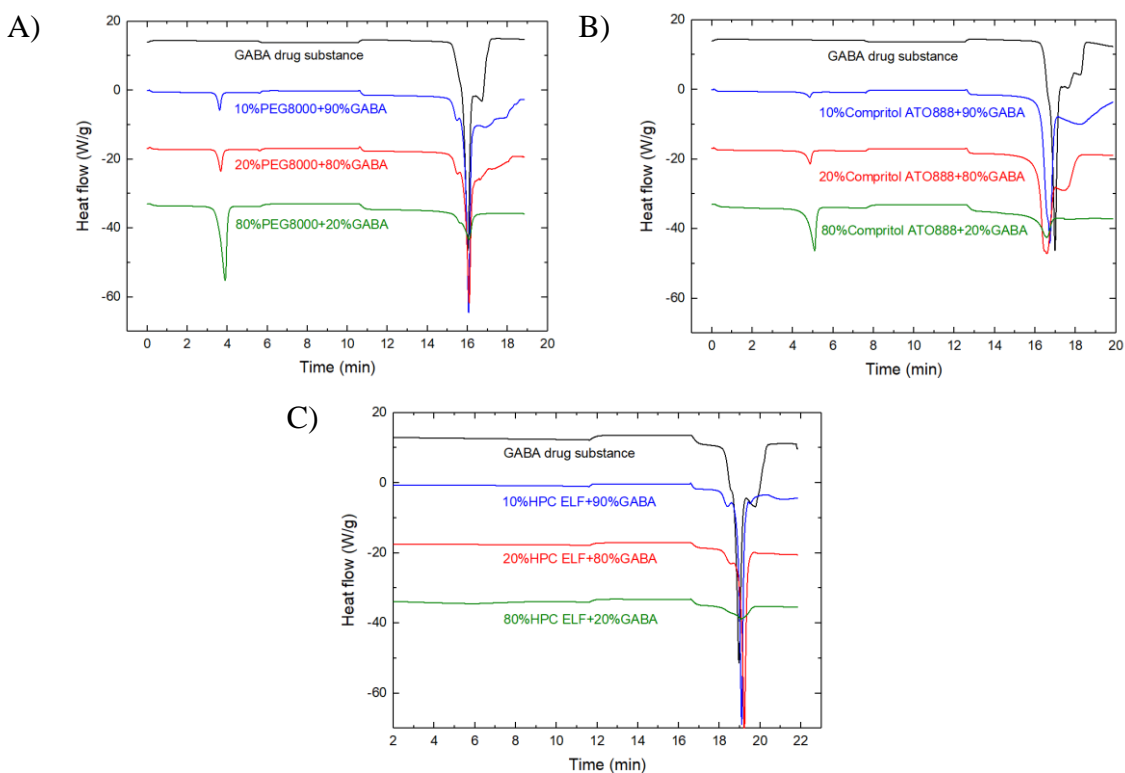


Figure 3.3 DSC thermograms of physical mixtures containing gabapentin (GABA) and binders (10, 20, or 80%); ramp from 25°C to zone 2 processing temperature; hold at the processing temperature for 5 minutes; ramp further to 250°C; (A) GABA-PEG 8000 with a zone 2 processing temperature of 80°C; (B) GABA-Compritol with a zone 2 processing temperature of 100°C; (C) GABA-HPC ELF with a zone 2 processing temperature of 140°C.

TSMG was carried out at the Zone 2 barrel temperatures of 80, 90, and 120°C for PEG 8000, Compritol, and HPC ELF-based formulations, respectively. For PEG 8000

and Compritol, the barrel temperature was set at about 20°C above the melting points of the thermal binders to ensure their complete melting. For HPC ELF, the barrel temperature was set at 100°C above the glass transition temperature to ensure sufficient agglomeration.

Drug-polymer interaction during TSMG is identical to that during hot-melt extrusion (HME) for amorphous solid dispersion. The primary goals of hot-melt extrusion are to dissolve drug in a polymer melt and to keep drug in the amorphous state after extrusion to improve drug dissolution. In contrast, the primary goal of TSMG is particle agglomeration, where drug dissolution in polymer melt should be minimized during TSMG to avoid gross physical and chemical instability, as mentioned for GABA.

Miscibility and dissolution of drug in melt binder can be quantified using melting point depression analysis via DSC. Melting point depression results from the reduced thermodynamic activity of the drug in the presence of the excipients relative to the activity of the pure crystalline drug. Hence, the drug in the amorphous drug-polymer mixture has a chemical potential equal to that of the crystalline drug at a temperature lower than the melting temperature of the pure drug (Marsac, Li, & Taylor, 2009). The greater the extent of melting point depression, the greater GABA solubility in molten binder. No significant melting point depression of GABA was observed with any binder upon temperature ramping at 10°C/min (data not shown). Additional DSC analysis was performed by holding the drug-binder binary mixtures at the barrel temperature (Zones 1 and 2) for 5 minutes to allow more time for GABA dissolution, if any. However, no thermal event was observed during this holding time and still no (PEG and HPC) or only slight (Compritol) melting point depression was observed in the subsequent temperature ramping beyond the melting temperature of GABA (Figure 3.3). Thus, GABA is immiscible with all three thermal binders.

Hot-stage polarized light microscopic experiments, performed by heating and holding the drug-binder binary mixtures at elevated temperatures, also did not show any sign of GABA crystal dissolution, since GABA crystal did not undergo visible changes in size and shape (Figure 3.4).

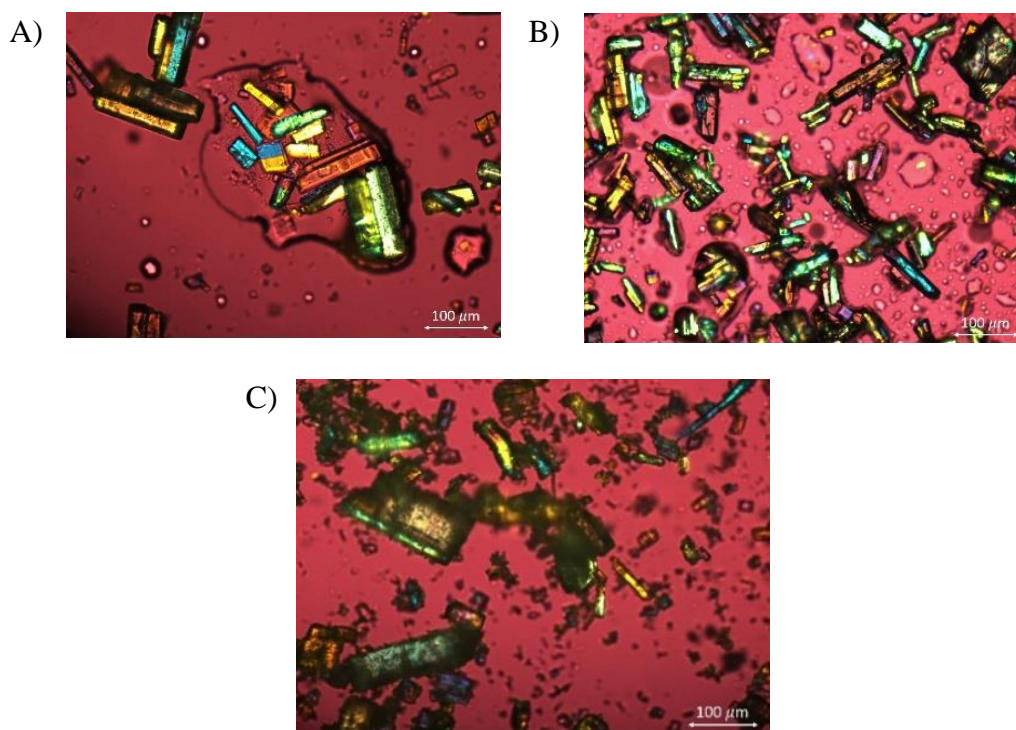


Figure 3.4 Hot-stage polarized light microscope of physical mixture (A) 80% GABA-20% PEG 8000, (B) 80% GABA-20% Compritol, and (C) 80% GABA-20% HPC ELF.

### 3.4.2 Effect of thermal binders on the properties of melt-extruded GABA granules

The effects of thermal binder on the tableability of granules, crystal form, and crystallinity of GABA, and the chemical stability of GABA using different process parameters (Table 3.1) are discussed in the following sections.

#### 3.4.2.1 Tableability of melt-extruded granules

The size and shape of the TSMG GABA granules were highly dependent on the type of thermal binder (Figure 3.5). Compritol-based granules were the smallest with most granules smaller than 425  $\mu\text{m}$ . GABA-PEG 8000 granules were ribbon-like. GABA-HPC granules were spherical with a size range of 100  $\mu\text{m}$  to 2 mm. The size and shape of extrudates are affected by both the screw configuration and processing conditions. Following the granulation as the result of dispersive mixing in the kneading section, GABA-HPC and GABA-Compritol formulation were broken down by the

narrow-pitch conveying element and the extrudates were granular. In comparison, the ribbon-shaped extrudate was observed for GABA-PEG 8000 formulation. It was hypothesized that GABA-PEG 8000 granules did not fully solidify in the conveying section post kneading.

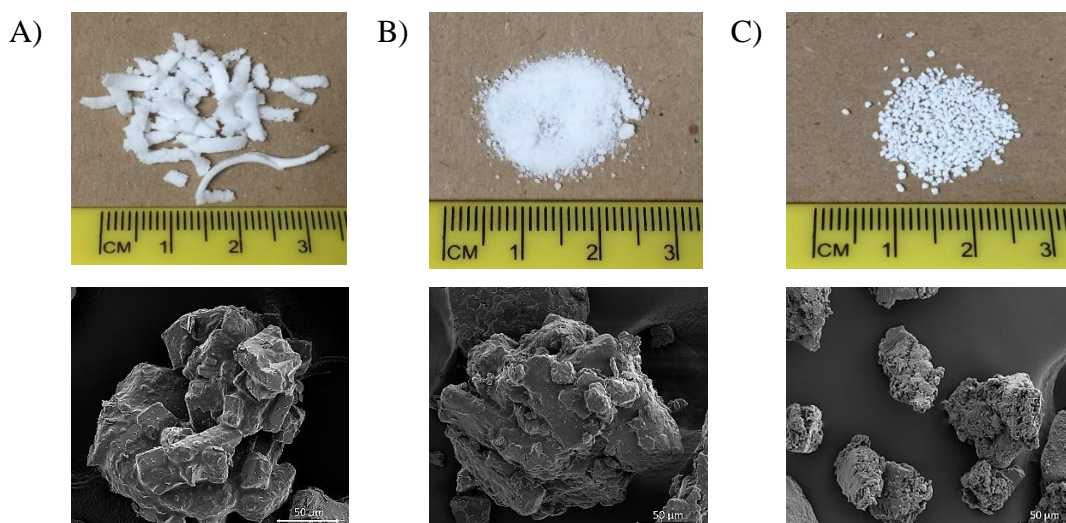


Figure 3.5 Photo images (top row) of extrudate and scanning electron microscope images (bottom row) of milled granules containing 80% GABA and 20% of various binders. (A) PEG 8000, (B) Compritol, and (C) HPC ELF.

Tabletability, tablet tensile strength as a function of compaction pressure, for milled and lubricated granules is presented in Figure 3.6. HPC ELF is the most effective in improving the tabletability of GABA. The desired tensile strength of 2.0 MPa (Osei-Yeboah, F. & Sun, C. C., 2015b), is attained over the entire pressure range investigated (35–125 MPa). In contrast, tablets containing Compritol-based granules never reached 2.0 MPa, while the tabletability of GABA-PEG 8000 granules was in between. The superior tabletability of HPC-based granules over that of PEG 8000 and Compritol-based granules is attributed to the superior plasticity of HPC.

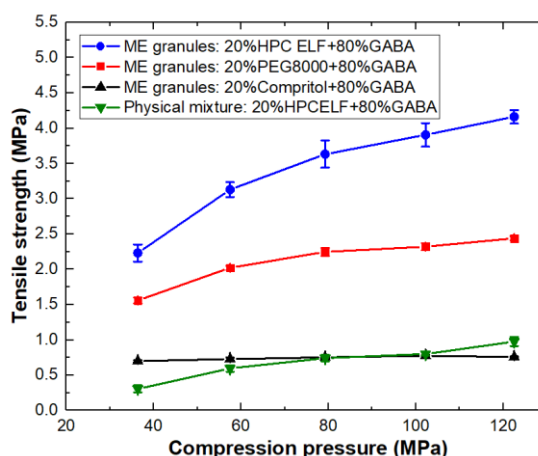


Figure 3.6 Compression profiles of blends containing 99% melt-extruded granules or physical mixture and 1% magnesium stearate; 11 mm in diameter, round, flat-faced tooling; 350 mg in tablet weight.

The tableability of TSMG granules containing 20% HPC was much improved over the corresponding physical mixture (Figure 3.6). This could be attributed to the unique spatial distribution of HPC ELF in the granules, where GABA crystals were surface coated by HPC as discussed in a later section. Such polymer coating is extremely effective in improving powder tableability (Osei-Yeboah, F. & Sun, C. C., 2015a).

#### 3.4.2.2 Crystal form and crystallinity of GABA following TSMG

In all four of its known crystal forms, GABA is zwitterionic and forms extensive networks of hydrogen bonds between  $\text{-NH}_3^+$  and  $\text{-COO}^-$  groups of neighboring molecules. Form I is a monohydrate, and the other three forms are anhydrous. GABA Form II, the most stable anhydrous form, is used in the current study.

Crystal form conversion of drug and excipient induced by thermal and mechanical stresses during TSMG has been reported (Liu, Y., Thompson, & O'Donnell, 2018). The potential changes of GABA crystal form were investigated using an FT-IR and XRD techniques, where polymorphic changes can be revealed by the emergence of new peaks, a shift in the position of the existing peaks, or a change in the shape of peaks in FTIR spectra or XRD diffraction pattern. The same conclusion was reached with both

techniques. Only FTIR data is discussed here. The spectral region from 1700 to 1500  $\text{cm}^{-1}$  is indicative of GABA polymorphs, where the peak at 1615  $\text{cm}^{-1}$  is the characteristic band of C=O stretching vibration of the ionized carboxylic group and the peak at 1546  $\text{cm}^{-1}$  is from N-H scissoring vibration of  $\text{NH}_3^+$  group. Compared to Form II, the C=O peak in forms III and IV shifts to a higher wave number, the N-H peak shifts to a lower wave number, and a new strong peak becomes present in the middle. IR band in the 1500-1300  $\text{cm}^{-1}$  region can be attributed to the asymmetric carboxylate band or  $\text{CH}_2$  deformation band (Hsu, C. H. et al., 2010). No significant change in the characteristic peaks of GABA Form II at 1615, 1546, 1475, 1420, 1400 and 1300  $\text{cm}^{-1}$  was observed for all TSMG granules prepared in this work (Figure 3.7). Thus, GABA form II remained stable during TSMG. The same observation was made for PEG 8000 and Compritol-based granules (data not presented).

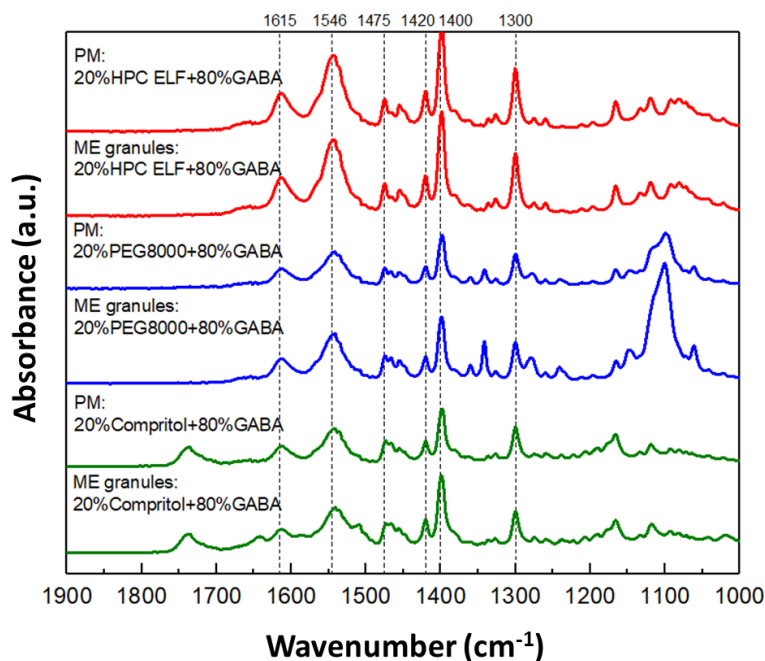


Figure 3.7 FTIR spectra of physical blends and melt-extruded GABA granules. PM: physical mixture, ME: melt-extruded granule.

It was reported that amorphization of GABA resulting from mechanical milling substantially accelerated GABA degradation (Zong, Z. X. et al., 2011). However,

amorphous GABA content was not detected in the granules using DSC and XRD because GABA is a fast crystallizer. In fact, amorphous GABA could not be prepared by spray drying. Melt quenching methods also did not work because of the significant degradation of GABA upon melting. Of course, these methods may not be sufficiently sensitive to detect a small amount of amorphous content in a crystalline sample. Although GABA chemical stability data indicated the presence of lattice defects or amorphous GABA in the melt-extruded granules, they were at a level too low to be detected by these analytical tools.

### 3.4.2.3 Chemical stability of GABA granules

During milling using a planetary mill, a longer milling duration corresponded to a higher level of GABA-Lactam post milling and faster degradation during storage (Zong, Z. X. et al., 2011). Chemical degradation of GABA under an elevated temperature was also reported (Hsu, C. H. et al., 2010). Since GABA was exposed to both elevated thermal and mechanical stresses during TSMG, the chemical stability of GABA during TSMG and the storage was monitored in this study.

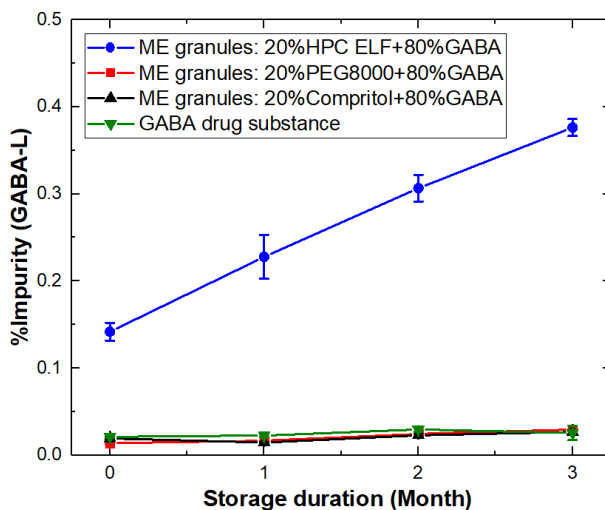


Figure 3.8 Gabapentin-lactam profile of melt-extruded granules packaged with desiccant in induction-sealed HDPE bottle stored at 40°C/75% RH condition for 3 months. GABA drug substance was used as the control.



Gabapentin-lactam (GABA-L) level after TSMG and at different time points under stressed conditions is presented in Figure 3.8. For storage stability testing, 1 g melt-extruded granules were packaged with 1 g desiccant in induction-sealed 20 cc HDPE bottles stored at 40 °C/75% RH for 3 months. As-received GABA drug substance contained 0.02% GABA-L. For PEG 8000 and Compritol-based granules, the level of GABA-L after TSMG or during the 3 months storage did not increase. In contrast, GABA-L level elevated to 0.14% for HPC ELF-based granules immediately following TSMG and then increased linearly to 0.38% over 3 months storage.

The poorer chemical stability of HPC ELF-based granules was likely attributed to both higher thermal and mechanical stresses during TSMG. Thermal stress during melt granulation originated from the heat conducted from extruder barrel. Mechanical stress resulted from the mixing by co-rotating screws. Mechanical stress also translated to thermal stress via frictional and viscous heat dissipation. Due to the high viscosity of binder melt, HPC ELF-based formulation had to be processed under a higher barrel temperature in order to achieve sufficient powder agglomeration, which corresponded to a higher level of thermal stress to GABA. The specific mechanical energy (SME) is the amount of power generated by the motor which is input into the material. SME can be calculated using Equation 3.2:

$$SME = \frac{KW \text{ (motor rating)} \times \% \text{ Torque} \times \frac{RPM \text{ running}}{RPM \text{ max}} \times 0.97 \text{ (gear box efficiency)}}{\text{Feed Rate} \left( \frac{kg}{hr} \right)} \quad \text{Equation 3.2}$$

Under the current processing conditions, SME for HPC ELF-based formulation (3.78 kW/kg/hr) was 3-6 times of that for PEG 8000 (1.78 kW/kg/hr) or Compritol (0.62 kW/kg/hr)-based formulations. Thus, the mechanical stress to GABA is correspondingly higher in the HPC ELF-based granules, which is attributed to the higher melt viscosity of HPC than PEG 8000 and Compritol at their respective processing barrel temperatures (Figure 3.9). The peak shear and minimum channel shear rate in the current study were calculated to be 1674 and 70 sec<sup>-1</sup>, respectively by using equation 3.3:

$$\text{Shear rate} = \frac{\pi \times \text{Screw diameter} \times \text{screw speed (rpm)}}{\text{Overflight gap} \times 60} \quad \text{Equation 3.3}$$

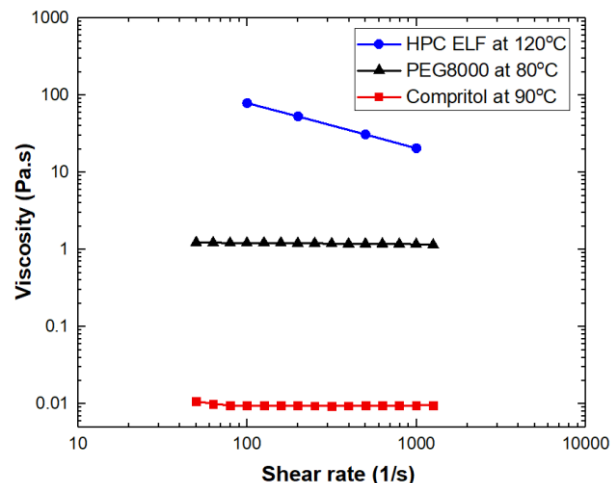


Figure 3.9 Melt viscosity of binders as a function of shear rate at their respective zone 2 processing temperatures of three thermal binders.

In this shear rate region, melt viscosity of HPC ELF is much greater than that of PEG 8000 and Compritol. Both PEG 8000 and Compritol are Newtonian fluids with constant viscosity (about 0.02 and 1 Pa.s for PEG 8000 and Compritol, respectively) across the entire range of shear rate. In contrast, melt viscosity of HPC ELF decreased with increasing shear rate (from 100 Pa.s to 20 Pa.s when the shear rate increased from 100 to 1000  $\text{sec}^{-1}$ ).

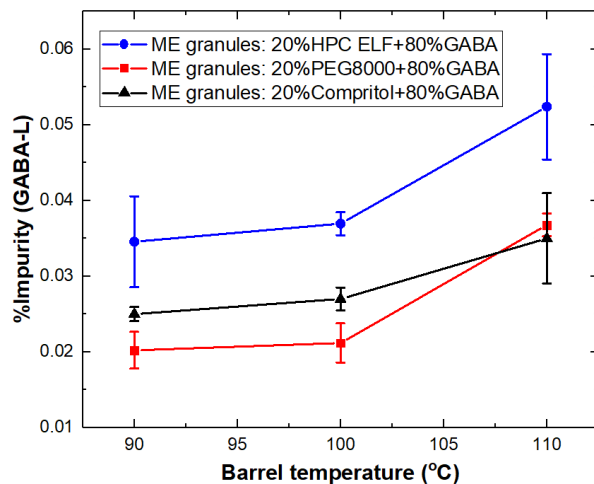


Figure 3.10 Gabapentin-lactam profile of melt-extruded GABA granules processed at 90°C, 100°C and 110°C barrel temperature.

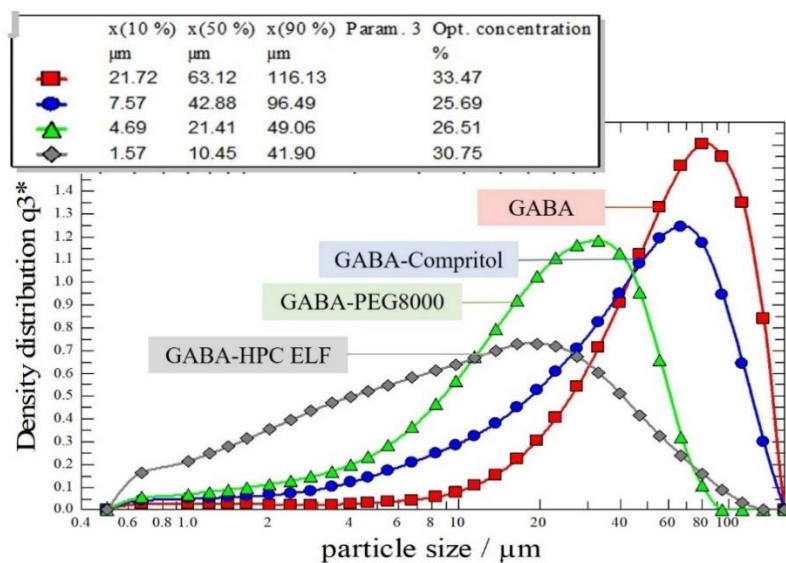


Figure 3.11 Particle size distribution of gabapentin (GABA) drug substance and GABA in melt-extruded granules (average of triplicate analyses).

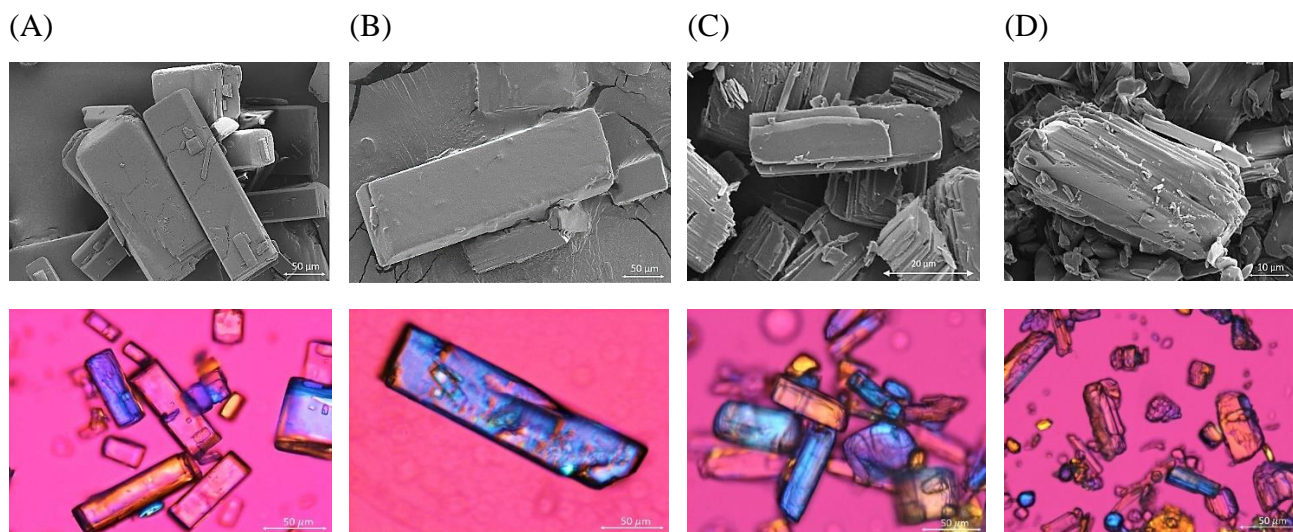


Figure 3.12 Scanning electron microscope images (top row) and polarized light microscope images (bottom row) of GABA crystals in melt-extruded GABA granules (A) GABA drug substances (B) Compritol-based granule, (B) PEG 8000-based granule, and (C) HPC ELF-based granule.

To further investigate the effect of binder melt viscosity, TSMG for all three formulations was carried out at the same barrel temperature so that the amount of heat conducted from the barrel was similar. In such case, the impurity level was higher for HPC ELF-based granules across all temperatures (Figure 3.10). The differences may be attributed largely to the different mechanical stresses in these cases. The higher mechanical stresses during HPC ELF-based process were also demonstrated by the more significant size reduction and surface defect of GABA crystals in the GABA-HPC ELF granules.  $D_{50}$  of the as-received GABA (63.1  $\mu\text{m}$ ) was reduced to 42.9, 21.4 and 10.5  $\mu\text{m}$  in PEG, Compritol, and HPC-based granules, respectively (Figure 3.11). This is corroborated by SEM and polarized light microscopy analyses of GABA crystals extracted from granules (Figure 3.12), which show both smaller GABA particles and more visible defects. GABA crystals in PEG and Compritol-based granules exhibited smooth surfaces and sharp edges, while fragmentation and rough surfaces were observed with GABA crystals from HPC ELF-based granules.

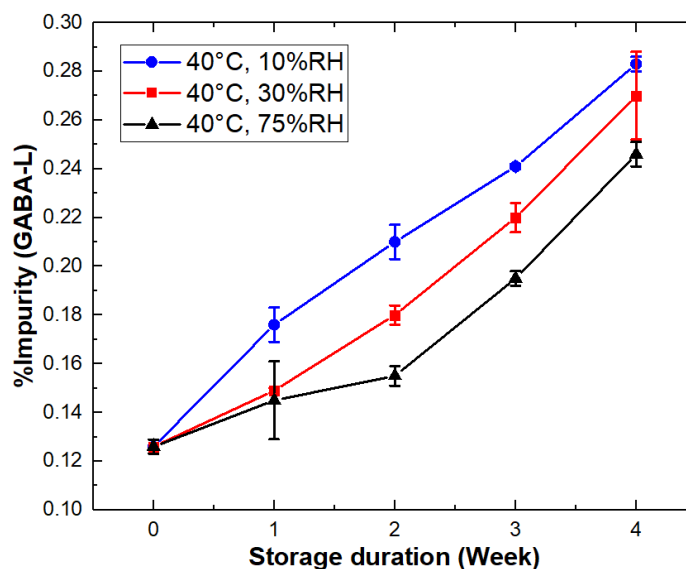


Figure 3.13 Gabapentin-lactam content of melt-extruded 80% GABA-20% HPC ELF granules packaged in open containers stored at 40°C and various relative humidity conditions.

The role of crystal defects on degradation of GABA in GABA-HPC ELF granules was also probed by comparing degradation kinetics at different humidity in open container, where higher humidity always corresponds to lower degradation (Figure 3.13). This is because more

available water at a higher humidity can facilitate faster recrystallization of amorphous GABA, or healing of crystal defects. Similar effects of RH on chemical stability was observed with ball milled GABA (Zong, Z. X. et al., 2011).

### 3.4.3 Effect of excipient variability on the properties of HPC-based GABA granules

Granulation consists of three processes: (1) wetting and nucleation, (2) consolidation and growth, and (3) attrition and breakage. All these three processes are impacted by the molecular weight and particle size of thermal binder. It is therefore important to understand the effects of excipient variability on the properties of HPC-based GABA granules.

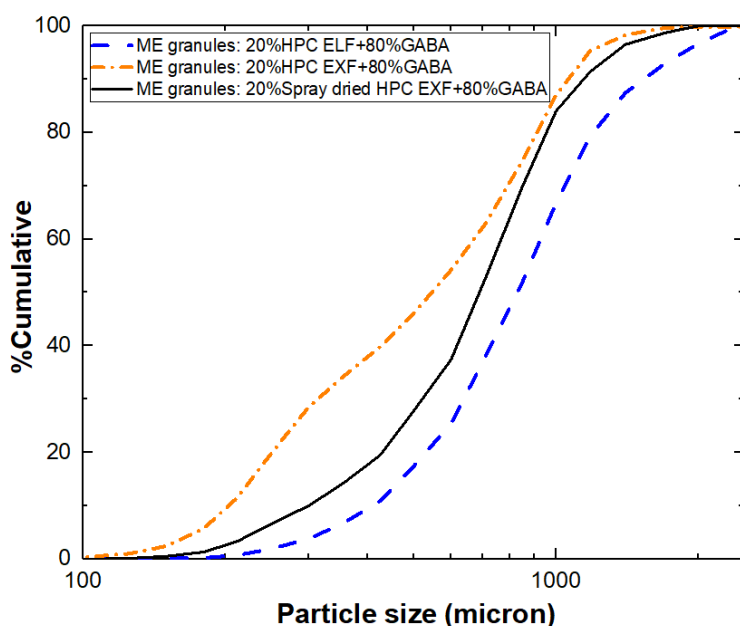


Figure 3.14 Size distribution of melt-extruded GABA granules based on different grades of HPC. Camsizer® was used in this analysis. ELF (40,000, 160  $\mu\text{m}$  D<sub>50</sub>); EXF (80,000, 50  $\mu\text{m}$  D<sub>50</sub>), and spray-dried EXF (80,000, 10  $\mu\text{m}$  D<sub>50</sub>).

HPC is available from Ashland chemical in a variety of grades with different molecular weights (40,000 – 1,150,000) and mean particle sizes (250  $\mu\text{m}$  for the regular grind grade and 50  $\mu\text{m}$  for the fine grind grade). Three different grades of HPC, EXF (80,000 MW, 50  $\mu\text{m}$  D<sub>50</sub>), spray-dried EXF (prepared in our lab, 80,000 MW, 10  $\mu\text{m}$  D<sub>50</sub>), and ELF (40,000 MW, 160  $\mu\text{m}$  D<sub>50</sub>), were used.

HPC EXF and spray-dried EXF were used to study the effect of HPC particle size. The use of spray-dried HPC EXF led to larger extruded granules, with  $D_{50}$  and  $D_{90}$  increased from 547 and 1049  $\mu\text{m}$  to 825 and 1336  $\mu\text{m}$ , respectively (Figure 3.14). During TSMG, “molten or softened” HPC must wet and spread on to the surface of GABA crystals to induce nucleation and growth of granules. With the compression arising from the axial pressure, the consolidation and growth mainly took place in the kneading segment. The intensive dispersive and distributive mixing in the kneading segment created progressively stronger granules, that steadily became more resistant to any further deformation-attempting consolidation (Iveson, S. M., Litster, & Ennis, 1996). Spray-dried HPC EXF provided higher specific surface area for wetting and nucleation, which also enhanced “consolidation and growth” to made granules sufficiently stronger to resist “attrition and breakage”. As a result, the melt-extruded granules were larger with HPC of finer particle size.

It was also observed that melt-extruded GABA granules were larger with lower molecular weight HPC. Thermal binder molecular weight affects all three processes of granulation. Molecular weight has two opposing effects on the size of the granules. On one hand, lower molecular weight binder has a lower melt viscosity and is easier to spread onto the surface of GABA crystals, which leads to more efficient “wetting and nucleation” and “consolidation and growth” processes. On the other hand, lower molecular weight binder leads to weaker particle-particle bridges, and thus higher extent of “attrition and breakage” during granulation and more friable granules. Consequently, granule size can be either larger or smaller when lower molecular weight binder is used. The overall impact of polymer molecular weight depends on which one of these two counteracting effects is more dominant. For examples, higher molecular weight of hypromellose led to larger granules (Liu, Y., Thompson, & O'Donnell, 2018), while the opposite effect by polyethylene glycol molecular weight was observed (Mu & Thompson, 2012). In our study, larger granules were obtained when lower molecular weight HPC was used, indicating the more efficient wetting, nucleation and growth effects dominates.

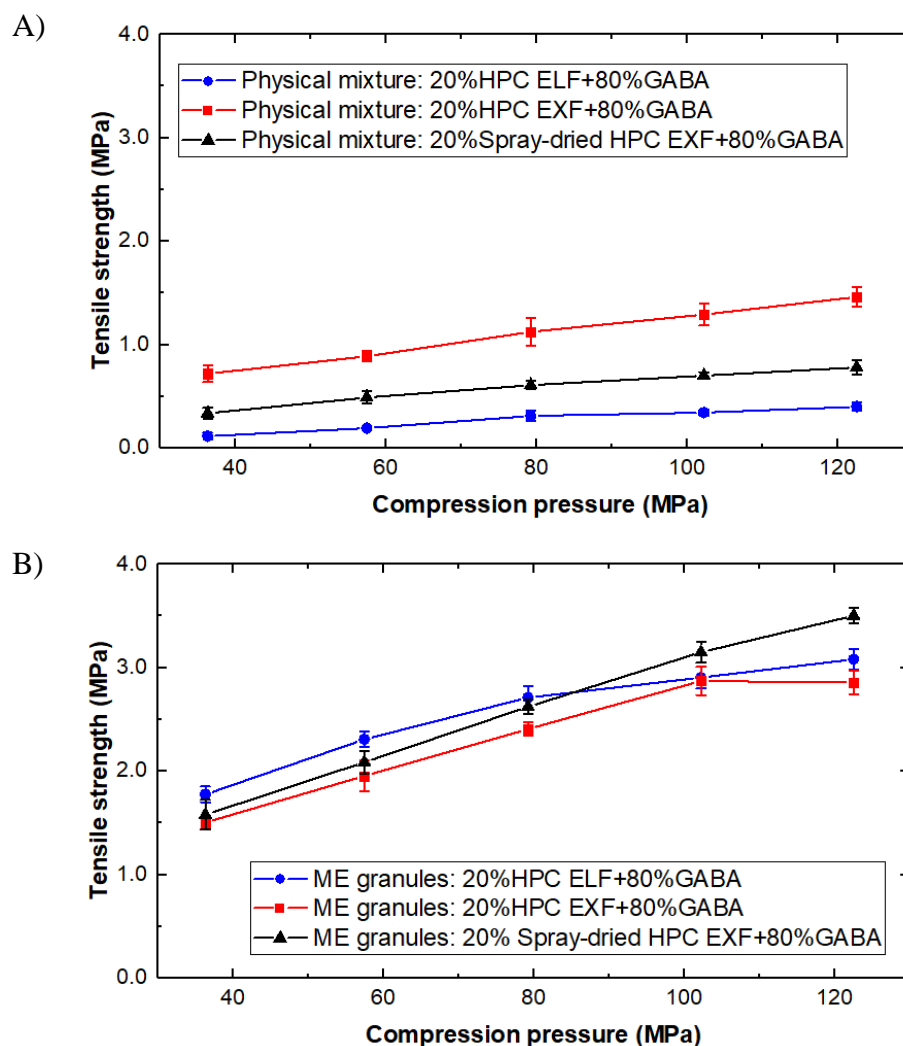


Figure 3.15 Compression profiles of A) physical mixtures and B) melt-extruded granules based on HPC of different molecular weight and particle size. ELF (40,000, 160  $\mu\text{m}$   $D_{50}$ ); EXF (80,000, 50  $\mu\text{m}$   $D_{50}$ ), and spray-dried EXF (80,000, 10  $\mu\text{m}$   $D_{50}$ ).

While tableability of the three physical mixtures differed (Figure 3.15A), there was no significant difference in the tableability of GABA granules based on three different HPC grades (Figure 3.15B). Thus, in term of granule tableability, the TSMG process is robust against variations in particle size of HPC.

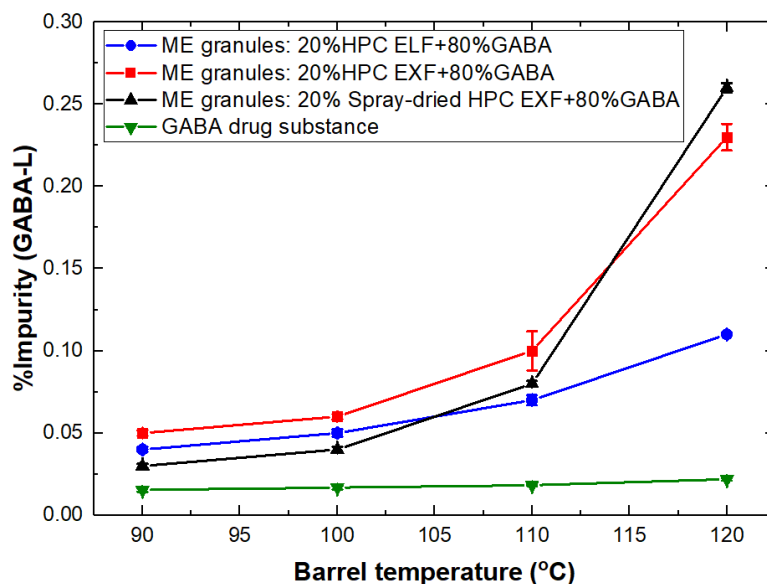


Figure 3.16 Gabapentin-lactam content of GABA drug substance and melt-extruded 80% GABA-20% HPC granules containing HPC of different particle sizes; processing conditions: 10 g/min feed rate, 100 rpm screw speed and four different barrel temperatures (90, 100, 110 and 120°C).

GABA granules with different HPC grades processed at different barrel temperatures (90-120°C, with the feed rate of 10 g/min, 100 rpm) were also examined for effects of processing temperature on chemical instability of GABA (Figure 3.16). When the barrel temperature was at 120 °C, GABA-lactam level in spray-dried HPC EXF-GABA, HPC EXF-GABA, and HPC ELF-GABA granules was 0.26, 0.23 and 0.11%, respectively.  $D_{50}$  of GABA crystals in TSMG granules was around 8-10  $\mu\text{m}$  for all three granules. There was no discernable difference among these granules when subjected to XRPD, DSC and FT-IR analyses. The higher degradation in HPC EXF based granules may be attributed to the higher melt viscosity of HPC EXF during TSMG. As a result, GABA was exposed to a higher shear stress during the granulation, resulting greater GABA crystal defect or a higher level of amorphous GABA.



### 3.4.4 Distribution of thermal binder in HPC-based GABA granules

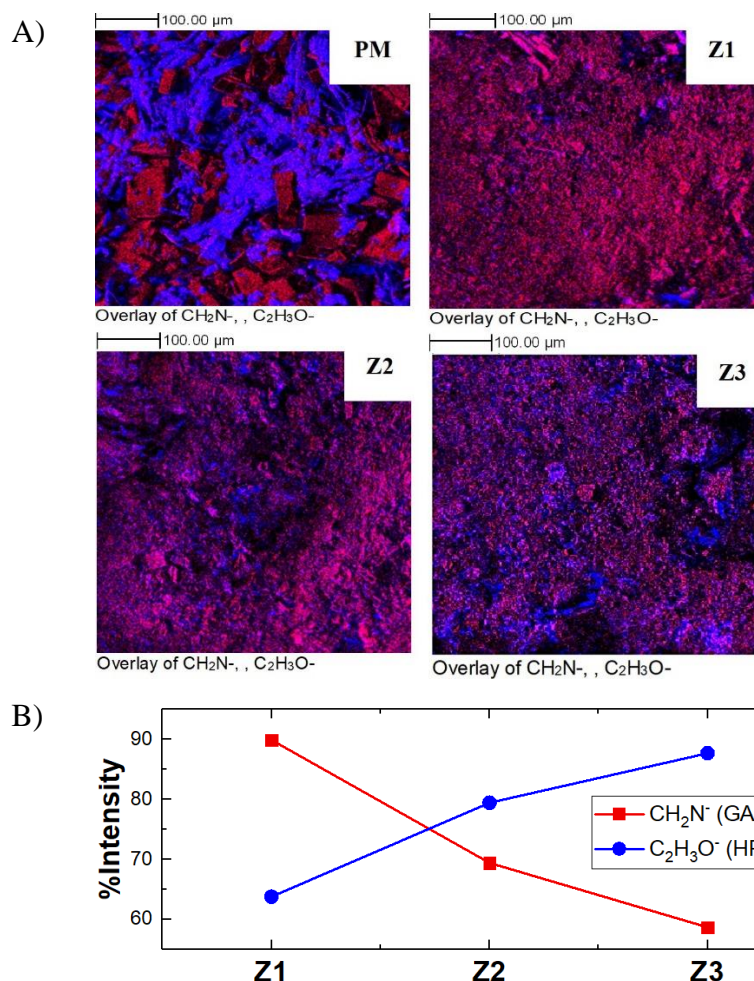


Figure 3.17 (A) ToF-SIMS image ( $500\ \mu\text{m} \times 500\ \mu\text{m}$ ) of GABA-HPC ELF granules sampled at different processing zone. Blue color is indicative of HPC and red color is indicative of GABA. (B) the signal intensity of  $\text{CH}_2\text{N}^-$  and  $\text{C}_2\text{H}_3\text{O}^-$  of HPC EXF and GABA at different processing zones.

The improved tableability of HPC EXF-based GABA granules was likely attributable to the coating of GABA surfaces by HPC as a result of the TSMG process. Surface modifications using highly bonding polymers have been shown to be highly effective in improving the compaction properties of powders (Shi, L. & Sun, C. C., 2010). Time-of-flight Secondary Ion Mass Spectrometry (ToF-SIMS) imaging of granules recovered in different processing sections along the screw axis (Figure 3.17A) shed light onto the different distribution patterns of HPC in

these granules. The HPC in the granules was significantly smaller and more uniformly distributed than that in physical mixture. In addition, the signal intensity for HPC EXF increased as powder blend proceeds further along the barrel (Figure 3.17B), indicating surface enrichment of HPC EXF with the progression of the granulation process. Both the HPC EXF size reduction and surface enrichment are consistent with the surface coating mechanism used to explain the improved tableability of the various HPC-GABA granules (Figure 3.15).

### 3.5 CONCLUSION

We have evaluated the effect of three types of thermal binders, PEG 8000, Compritol, and HPC ELF on the chemical stability and tableability of GABA granules (80% drug loading) prepared using a twin-screw melt granulation process. Polymorphic form change of GABA was not observed under the current processing conditions for all three formulations. HPC ELF was found to be the most effective binder in improving the tableability of GABA. Improvement in the tableability resulted from the size reduction and surface-enrichment of HPC ELF in the melt-extruded granules.

However, HPC ELF also led to greater levels of GABA chemical degradation and significant size reduction of GABA crystals due to higher thermal and mechanical stresses. The impurity level in HPC ELF-based granules continued to increase from 0.14 to 0.38% upon storage for 3 months at 40 °C/75% RH. For HPC ELF-based formulation,  $D_{50}$  of GABA crystals decreased from 63 to 10  $\mu\text{m}$  during TSMG. Higher thermal stress for HPC-based formulation resulted from (1) the higher barrel temperature required to achieve sufficient agglomeration and (2) greater heat dissipation due to the higher mechanical stress resulting from the higher melt viscosity of HPC ELF. Even though PEG 8000 and Compritol were not as effective as HPC ELF in improving the compaction properties of GABA, chemical degradation of GABA was not observed with PEG 8000 and Compritol-based granules. The impurity content of these granules did not increase following 3 months storage at 40 °C/75% RH. Moreover, the granule properties were affected by the molecular weight and particle size of HPC. Lower molecular weight HPC corresponds to more efficient granulation and lower level of GABA degradation. Granule growth was also enhanced when HPC of smaller particle size was used. Importantly, the tableability of the granules was robust against variations in the molecular weight and particle size of HPC.

### 3.6 REFERENCES

- Batra, A., Desai, D., & Serajuddin, A. T. (2017). Investigating the Use of Polymeric Binders in Twin Screw Melt Granulation Process for Improving Compactibility of Drugs. *J Pharm Sci*, 106(1), 140-150. doi:10.1016/j.xphs.2016.07.014
- Chen, B., Zhu, L., Zhang, F., & Qiu, Y. (2016). Process Development and Scale-Up Twin-Screw Extrusion. In Y. Qiu, Y. Chen, G. G. Z. Zhang, L. Yu, & R. V. Mantri (Eds.), *Developing Solid Oral Dosage Forms: Pharmaceutical Theory and Practice* (Second;2;2nd; ed.). US: Academic Press.
- Dombe, G., Mehilal, Bhongale, C., Singh, P. P., & Bhattacharya, B. (2015). Application of Twin Screw Extrusion for Continuous Processing of Energetic Materials. *Central European Journal of Energetic Materials*, 12(3), 507-522.
- Gamlen, M., & Eardley, C. (1986). Continuous extrusion using a Baker Perkins MP50 (multipurpose) extruder. *Drug Dev Ind Pharm*, 12, 1701-11713.
- Ghebre-Sellassie, I., Mollan, M. J., Pathak, N., Lodaya, M., & Fessehaie, M. (2002). U.S. Patent 2304392A.
- Hsu, C. H., Ke, W. T., & Lin, S. Y. (2010). Progressive steps of polymorphic transformation of gabapentin polymorphs studied by hot-stage FTIR microspectroscopy. *Journal of Pharmacy and Pharmaceutical Sciences*, 13(1), 67-77.
- Iveson, S. M., Litster, J. D., & Ennis, B. J. (1996). Fundamental studies of granule consolidation Part 1: Effects of binder content and binder viscosity. *Powder Technology*, 88(1), 15-20. doi:[https://doi.org/10.1016/0032-5910\(96\)03096-3](https://doi.org/10.1016/0032-5910(96)03096-3)
- Iveson, S. M., Litster, J. D., Hapgood, K., & Ennis, B. J. (2001). Nucleation, growth and breakage phenomena in agitated wet granulation processes: a review. *Powder Technology*, 117(1), 3-39. doi:[https://doi.org/10.1016/S0032-5910\(01\)00313-8](https://doi.org/10.1016/S0032-5910(01)00313-8)
- Keen, J. M., Foley, C. J., Hughey, J. R., Bennett, R. C., Jannin, V., Rosiaux, Y., . . . McGinity, J. W. (2015). Continuous twin screw melt granulation of glyceryl behenate: Development of controlled release tramadol hydrochloride tablets for improved safety. *Int J Pharm*, 487(1-2), 72-80. doi:10.1016/j.ijpharm.2015.03.058
- Kittikunakorn, N., DiNunzio, J. C., Martin, C., & Zhang, F. (2018). Processes, Challenges, and the Future of Twin-Screw Granulation for Manufacturing Oral Tablets and Capsules. *AAPS NewsMagazine*, Mar(Mar), 12-18.
- Kumar, A., Dhondt, J., De Leersnyder, F., Vercruysse, J., Vanhoorne, V., Vervaet, C., . . . Nopens, I. (2015b). Evaluation of an in-line particle imaging tool for monitoring twin-screw granulation performance. *Powder Technology*, 285, 80-87. doi:<https://doi.org/10.1016/j.powtec.2015.05.031>
- Lakshman, J. P., Kowalski, J., Vasanthavada, M., Tong, W. Q., Joshi, Y. M., & Serajuddin, A. T. M. (2011b). Application of Melt Granulation Technology to Enhance Tableting Properties of Poorly Compactible High-Dose Drugs. *Journal of Pharmaceutical Sciences*, 100(4), 1553-1565. doi:10.1002/jps.22369
- Lee, S. (2017). Modernizing the Way Drugs Are Made: A Transition to Continuous Manufacturing. Retrieved from <https://www.fda.gov/Drugs/NewsEvents/ucm557448.htm>
- Liu, Y., Thompson, M. R., & O'Donnell, K. P. (2018). Impact of non-binder ingredients and molecular weight of polymer binders on heat assisted twin screw dry granulation.

- International Journal of Pharmaceutics*, 536(1), 336-344. doi:10.1016/j.ijpharm.2017.11.061
- Markarian, J. (2017). Scaling up a continuous granulation process. *Pharmaceutical Technology*, 41, 30-31.
- Marsac, P. J., Li, T., & Taylor, L. S. (2009). Estimation of Drug–Polymer Miscibility and Solubility in Amorphous Solid Dispersions Using Experimentally Determined Interaction Parameters. *Pharmaceutical Research*, 26(1), 139-151. doi:10.1007/s11095-008-9721-1
- Monteyne, T., Heeze, L., Mortier, S. T., Oldorp, K., Cardinaels, R., Nopens, I., . . . De Beer, T. (2016). The use of rheology to elucidate the granulation mechanisms of a miscible and immiscible system during continuous twin-screw melt granulation. *Pharmaceutical Research*, 33(10), 2481-2494.
- Mu, B., & Thompson, M. R. (2012). Examining the mechanics of granulation with a hot melt binder in a twin-screw extruder. *Chemical Engineering Science*, 81, 46-56. doi:10.1016/j.ces.2012.06.057
- Osei-Yeboah, F., & Sun, C. C. (2015a). Tableability Modulation Through Surface Engineering. *J Pharm Sci*, 104(8), 2645-2648. doi:10.1002/jps.24532
- Osei-Yeboah, F., & Sun, C. C. (2015b). Validation and applications of an expedited tablet friability method. *Int J Pharm*, 484(1-2), 146-155. doi:10.1016/j.ijpharm.2015.02.061
- Paudel, A., Rajjada, D., & Rantanen, J. (2015). Raman spectroscopy in pharmaceutical product design. *Adv Drug Deliv Rev*, 89, 3-20. doi:<https://doi.org/10.1016/j.addr.2015.04.003>
- Rials, T. G., & Glasser, W. G. (1988). Thermal and dynamic mechanical properties of hydroxypropyl cellulose films. *Journal of Applied Polymer Science*, 36(4), 749-758. doi:10.1002/app.1988.070360402
- Shi, L., & Sun, C. C. (2010). Transforming powder mechanical properties by core/shell structure: compressible sand. *J Pharm Sci*, 99(11), 4458-4462. doi:10.1002/jps.22172
- Tan, D. C. T., Chin, W. W. L., Tan, E. H., Hong, S. Q., Gu, W., & Gokhale, R. (2014). Effect of binders on the release rates of direct molded verapamil tablets using twin-screw extruder in melt granulation. *International Journal of Pharmaceutics*, 463(1), 89-97. doi:10.1016/j.ijpharm.2013.12.053
- Van Melkebeke, B., Vermeulen, B., Vervaet, C., & Remon, J. P. (2006). Melt granulation using a twin-screw extruder: A case study. *International Journal of Pharmaceutics*, 326(1-2), 89-93. doi:10.1016/j.ijpharm.2006.07.005
- Vasanthavada, M., Wang, Y. F., Haefele, T., Lakshman, J. P., Mone, M., Tong, W. Q., . . . Serajuddin, A. T. M. (2011). Application of Melt Granulation Technology Using Twin-screw Extruder in Development of High-dose Modified-release Tablet Formulation. *Journal of Pharmaceutical Sciences*, 100(5), 1923-1934. doi:10.1002/jps.22411
- Weatherley, S., Mu, B., Thompson, M. R., Sheskey, P. J., & O'Donnell, K. P. (2013). Hot-melt granulation in a twin screw extruder: effects of processing on formulations with caffeine and Ibuprofen. *J Pharm Sci*, 102(12), 4330-4336. doi:10.1002/jps.23739
- White, J. L., & Bumm, S. H. (2010). Perspectives on the Transition from Batch to Continuous Mixing Technologies in the Compounding Industry. *International Polymer Processing*, 25(5), 322-326. doi:10.3139/217.2293
- Zong, Z. X., Desai, S. D., Kaushal, A. M., Barich, D. H., Huang, H. S., Munson, E. J., . . . Kirsch, L. E. (2011). The Stabilizing Effect of Moisture on the Solid-State Degradation of Gabapentin. *AAPS PharmSciTech*, 12(3), 924-931. doi:10.1208/s12249-011-9652-8

## **Chapter 4: Effect of Screw Profile and Processing Conditions on Physical Transformation and Chemical Degradation of Gabapentin during Twin-Screw Melt Granulation<sup>3</sup>**

### **4.1 ABSTRACT**

Twin-screw melt granulation (TSMG) was applied to process a powder blend consisting of 80% gabapentin (GABA) and 20% hydroxypropyl cellulose. The effect of screw profile and processing conditions on the process-induced transformation and chemical degradation of gabapentin was studied. When a neutral kneading block was used, gabapentin underwent polymorphic transformation. A forward kneading block in combination with processing under torque conditions was required to minimize chemical degradation and to inhibit polymorphic transformation of gabapentin. Both the size of the extruded granules and gabapentin degradant level correlated positively with the specific rate, the ratio between feed rate and screw speed. At higher specific rate, the barrel was filled to a greater extent. The material packing and compressive forces were enhanced, as proven by the increased rupturing of CAMES® sensor beads and GABA crystal size reduction. This resulted in more interaction between the powder particles and facilitated granule growth. Simultaneously, this also resulted in higher degradant level. To attain adequate tableability, the specific rate must reach a threshold value. The development of an optimum TSMG process requires balancing processing parameters based on the physical and chemical stability of GABA as well as its tableability.

---

<sup>3</sup> Kittikunakorn, N., Sun, C. C., & Zhang, F. (2019). Effect of screw profile and processing conditions on physical transformation and chemical degradation of gabapentin during twin-screw melt granulation. *European Journal of Pharmaceutical Sciences*, 131, 243-253.

I am the primary author of this work.

## 4.2 INTRODUCTION

In pharmaceutical manufacturing, powder blends are commonly granulated in order to (1) prevent material segregation, (2) improve flow properties, and (3) improve tabletability. Melt granulation is a water and solvent-free process where a molten binder at an elevated temperature enables granulation under shear followed by solidification when cooled to room temperature (Royce, Suryawanshi, Shah, & Vishnupad, 1996). Even though less commonly used than other granulation technologies, melt granulation offers unique advantages. In comparison to high-shear wet granulation and fluid-bed granulation, one major advantage of melt granulation is that solvent mediated chemical degradation (e.g., hydrolysis) and solid state changes (e.g., salt disproportionation) are avoided since no water or solvent is used (Kowalski, Kalb, Joshi, & Serajuddin, 2009) (Nie, Byrn, & Zhou, 2017). Another major advantage of melt granulation is that the tabletability of granules is generally improved, which is in contrast to the usual deterioration in tabletability of granules prepared by dry granulation or high-shear wet granulation (Shi, Feng, & Sun, 2011; Sun, C. C. & Kleinebudde, 2016).

Traditionally, melt granulation process is carried out in jacketed batch mixers, such as high-shear and fluid-bed granulators. During batch melt granulation, only low melting point binders, e.g., PEG 8000 and waxes, can be used because of the low mixing intensity and efficiency. At the same time, potential thermal degradation of drugs by the exposure to an elevated temperature during twin-screw extrusion is a major drawback, especially if the drug is thermal labile (Haser & Zhang, 2018). These low melting point binders, however, exhibit a limited ability to improve granule tabletability. Some thermoplastic binders, such as hydroxypropyl cellulose (HPC), can profoundly improve granule tabletability when coated on particle surfaces; however, they cannot be used in batch melt granulation because very high temperatures are required for successful granulation in the batch mode (Batra, A., Desai, D., & Serajuddin, A. T. M., 2017). However, they can be used in twin screw melt granulation (TSMG) because, in addition to heating by the barrel, frictional and viscous heat dissipation occurs at the particle-particle or particle-screw/barrel contact surfaces driven by the rotating screws (Kittikunakorn, N., DiNunzio, Martin, et al., 2018). Consequently, the elevated temperature from frictional and viscous heat dissipation happens at local contact points instead of the whole powder bed. This makes it possible to granulate powders without exposing bulk powder to an

excessively high temperature. In addition, the short residence time (usually < 30 seconds) during TSMG further reduces any possible thermal degradation (Mu & Thompson, 2012). One commercial product that involves TSMG in its manufacturing is Eucreas™ where TSMG of metformin-hydroxypropyl cellulose (HPC) granule was used for making immediate-release tablets (Lakshman et al., 2011b). In this case, TSMG was used because it is more effective than wet granulation and roller compaction in improving the flowability and tableability of metformin.

As an inherently continuous process, TSMG can be readily integrated into the continuous manufacturing of pharmaceutical dosage forms. With the recent surge of interest in continuous manufacturing (Lee, 2017), TSMG has attracted much attention. The commercial successes discussed earlier highlight the potential of TSMG in pharmaceutical manufacturing. However, clearer understanding of TSMG through systematic studies is needed for the pharmaceutical industry to fully embrace this granulation process (Monteyne, Vancoillie, Remon, Vervaet, & De Beer, 2016a).

Despite the clear advantages TSMG offers, one major concern that slows its adaption by the pharmaceutical industry is the potential chemical and physical instability of drug substances during TSMG. Chemical stability of drug substance has not been extensively studied in the context of TSMG. Polymorphic changes during TSMG have been reported but have not been systematically correlated with processing conditions (Monteyne, Tinne et al., 2016). Hence, there is a need for systematic understanding of the level of risks in chemical degradation and solid form change to facilitate a broader adoption of TSMG by the pharmaceutical industry.

During TSMG, drug substance could undergo process-induced form transformation via kinetic trapping and relaxation mechanisms (Morris et al., 2001). A metastable form of drug becomes stable inside the barrel under the conditions induced by the mechanical and thermal stresses. Upon exiting the extruder barrel, this metastable form should “relax” to a stable form at ambient conditions, thermodynamically speaking. However, the time course of this relaxation depends on the characteristics of the process at the molecular level. If the cooling of the granules is fast, drug might be kinetically trapped as metastable form following TSMG. Processing-induced transformations of drug crystals during pharmaceutical manufacturing are well known but difficult to predict or control.

This study is aimed at mechanistically understanding the effect of screw profile and processing conditions on polymorph transformation and chemical degradation during TSMG, using gabapentin (GABA)–hydroxypropyl cellulose (HPC) as a model formulation (Figure 4.1). GABA is used here because it undergoes both chemical degradation and solid form changes at elevated temperatures (Hsu, C. H. et al., 2010; Zong, Z. X. et al., 2011). The selection of HPC as a thermoplastic binder is based on its effectiveness in improving tabletability (Picker-Freyer, K. & Dürig, T., 2007). HPC is an amorphous thermoplastic polymer with a glass transition temperature of about 20 °C (Rials & Glasser, 1988).

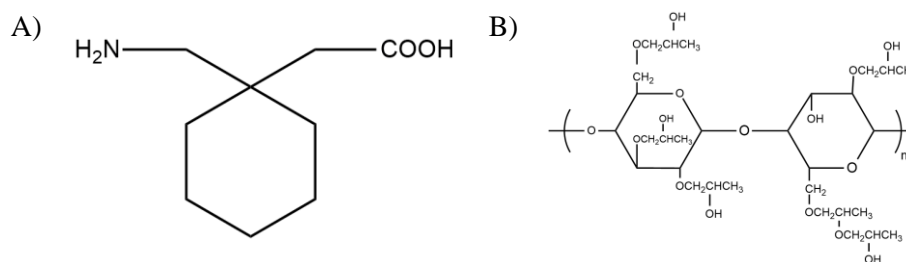


Figure 4.1 Chemical structure of (A) gabapentin (GABA) and (B) hydroxypropyl cellulose (HPC).

## 4.3 MATERIALS AND METHODS

### 4.3.1 Materials

Gabapentin (GABA, Form II) was purchased from ShenZhen Nexconn Pharmatechs (Shenzhen, China). GABA has water solubility of 100 mg/mL at 25 °C and a melting point of 174°C. Hydroxypropyl cellulose (HPC, Klucel® EXF) was a gift from Ashland Inc. (Wilmington, DE). All other chemicals were of ACS grade or higher. Calibrated Microencapsulated Sensor (CAMES) beads (Mach 1 Inc., King of Prussia, PA) were used to measure the mechanical stress inflicted onto formulation during melt granulation. The CAMES beads in the size range of 54-63  $\mu\text{m}$  and rupture shear stress of 300 kPa were used in this work. A powder consisting of 80% (w/w) GABA and 20% (w/w) HPC was prepared by mixing with 25 rpm for 10 min using a Turbula® Shaker-Mixer (Glen Mills, Clifton, NJ).



Table 4.1 A list of extrusion runs and their processing conditions

	Screw profile	Feed Rate (kg/hr)	Screw Speed (RPM)	Torque (G.m)	Comments
1	A	0.60	100	1250	Runs 1 and 2 are used to evaluate the effect of screw profile, specifically kneading elements.
2	B	0.60	100	750	
3	B	0.30	100	300	Runs 3 through 14 are used to evaluate the effect of processing conditions, specifically feed rate and screw speed, on the physicochemical properties of GABA granules.
4	B	0.30	150	220	
5	B	0.30	200	222	
6	B	0.30	300	120	
7	B	0.45	100	460	
8	B	0.45	150	375	
9	B	0.45	200	345	
10	B	0.45	300	220	
11	B	0.60	100	750	Containing CAMES beads at 1% to evaluate the mechanical stress at two extremes of the specific rate.
12	B	0.60	150	415	
13	B	0.60	200	370	
14	B	0.60	300	315	
15	B	0.30	300	120	
16	B	0.60	100	750	

The barrel temperatures at zones 1, 2, and 3 were set at 70°C, 110°C and 110°C, respectively.

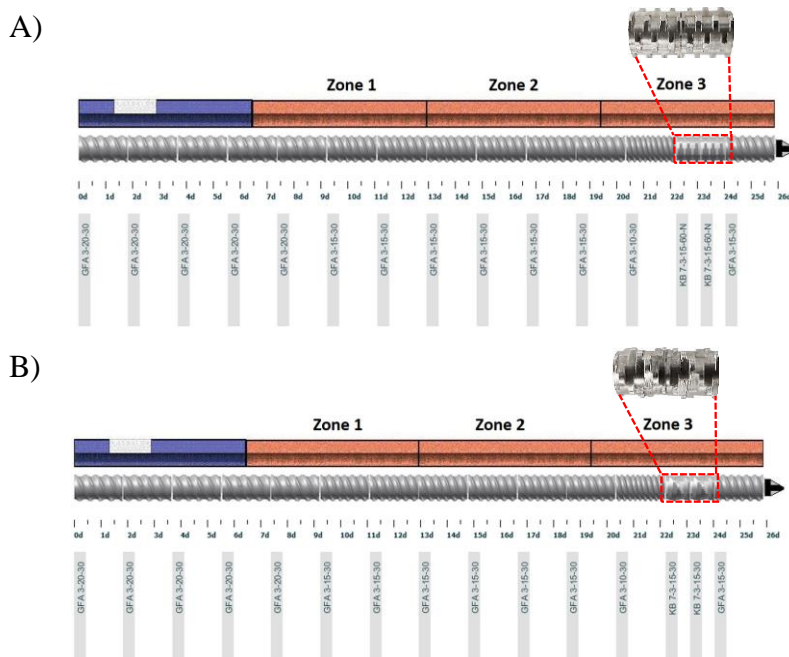


Figure 4.2 Barrel configuration and screw profile with open-end discharge (A) two 60° offset neutral kneading blocks, (B) two 30° offset forward kneading blocks.

GFA X-XX-XX Co-rotating conveying screw-trilobal screw-pitch length (mm)-screw length (mm).

KB X-X-XX-XX Kneading block-number of kneading segment-screw length (mm)-the angle (°).0d to 26d Length to diameter ratio (total barrel length is 420 mm; barrel diameter is 16 mm).

## **4.3.2 Methods**

### **4.3.2.1 Twin-screw melt granulation**

All extrusion experiments were performed on a co-rotating twin screw extruder (Nano-16, American Leistritz Extruder Corp., Somerville, NJ), where tri-lobal screw elements were used. A twin-screw volumetric feeder (Brabender Technologie, Ontario, Canada) was used to control the powder feed rate. The barrel was divided into four zones. The feeding zone was maintained at room temperature with water circulation. The barrel temperatures at zones 1, 2, and 3 were set at 70°C, 110°C and 110°C, respectively. The barrel temperature was selected based on the soften temperature of HPC at 100-120°C. The extruder was operated without a die using screw designs detailed in Figure 4.2. The feed rate and screw speed were systematically varied as needed (Table 4.1). Both barrel temperature and torque were monitored throughout the study. Each sample was collected when steady torque and barrel temperature were attained (usually around 5 min after parameters were adjusted). As granules were exiting the barrel, their temperature was measured using a visual infrared thermometer (Fluke®, VT04A, FLUKE, Everett, WA) that blends a visual image with infrared heat map overlay. The distance between the thermometer and granules was kept at 5 cm.

### **4.3.2.2 Granule size distribution**

Granule size distribution was characterized using a Dynamic Image Analyzer (Retsch Camsizer® P4, V.4.2.1., Haan, Germany). Approximately 10 g of granules was poured into the feeder of the instrument. Images of the falling granule were captured by a camera (CCD-Basic and CCD-Zoom) with an image rate of 100% (60 images per second). The covered area of the image at which the measurement was included was 2%. The feeder control level for advancing the material from the funnel to the shaft prior to image acquisition and feeder start value for the measurement were set at 65 and 55, respectively.

### **4.3.2.3 Tableability of melt-extruded granules**

The size of granules collected following granulated in twin screw extruder were reduced with a co-mill (Quadro comil, U5-0516, Ontario, Canada). A screen with round holes (0.032 inch) and an impeller speed of 1000 rpm were used for all formulations. Granules between 250

μm to 850 μm (60-20 mesh) were collected and mixed with 0.5% magnesium stearate in a Turbula® Shaker-Mixer (Glen Mills, Clifton, NJ) at 25 rpm for 3 minutes. The tablets (350 ± 5 mg) were compressed with a manual tablet compression machine (MTCM-I, Globe pharma, NJ, USA) using flat-faced, round (11 mm diameter) tooling. Tablet hardness, thickness, and diameter were recorded, and the tensile strength (MPa) of the tablets from each formulation was calculated using the equation:

$$TS = \frac{2F}{\pi DH} \quad \text{Equation 4.1}$$

where F, D and H denote the tablet hardness (N), tablet diameter (mm) and tablet thickness (mm), respectively. The compression force ranged from 3 to 12 KN. A total of 5 tablets were prepared and tested under each set of conditions.

#### 4.3.2.4 HPLC analysis of GABA and its degradant

GABA granules were stored in a desiccator at ambient conditions prior to analysis. GABA and GABA-L contents were analyzed with a Thermo Scientific Dionex Ultimate 3000 HPLC system (Thermo Scientific, Sunnyvale, CA, USA). An Ultimate 3000 autosampler was utilized to inject 20-μl samples. The HPLC system also included dual Ultimate pumps and an Ultimate RS variable wavelength detector operating at 210 nm. The mobile phase consisted of 60% (v/v) water, 30% (v/v) methanol and 10% (v/v) acetonitrile. An isocratic flow at 0.8 mL/min was used. Injections were passed through an Inertsil® ODS-2, C18 reverse phase column, 4.6 x 150 mm, with 5 μm packing, (GL Sciences Inc, Japan) kept at room temperature. The retention times of GABA and GABA-L were approximately 3.2 min and 12.8 min, respectively. The standard and sample solutions were diluted using highly purified water to achieve GABA concentrations in the linear range of the calibration curve (0-10 mg/ml). Diluted solutions were sonicated and filtered through a 0.45 μm Nylon membrane prior to HPLC analysis. Chromeleon Version 6.80 software (Thermo Scientific, Sunnyvale, CA, USA) was used to process all chromatography data. The LOD and LOQ of GABA-L were 0.03 and 0.08 μg/mL, respectively.

#### **4.3.2.5 Particle size of gabapentin in melt-extruded granules**

To determine the particle size of GABA in the TSMG granules, granules were dispersed in acetone, which does not dissolve GABA but readily dissolves HPC. GABA particles were then recovered by filtration and analyzed on a laser diffraction sizer (Sympatec Helos, Sympatec GmbH, Germany), equipped with a dispersing cuvette and an R3 lens. A background measurement was taken with the blank acetone medium in the cuvette. Each GABA dispersion in acetone was added to the cuvette drop-wise until the light obscuration was in the range of 10-25%. Light diffraction data was then collected for 100 ms.

#### **4.3.2.6 FT-IR analysis**

FT-IR analysis was performed to determine the polymorphic form of GABA in the physical mixture and granules using a Thermo Nicolet iS50 spectrometer (ThermoFisher Scientific, Waltham, MA) equipped with an attenuated total reflection accessory. Each sample was placed on the germanium crystal surface compressed using the built-in pressure tower to achieve uniform contact between the solid and the crystal. The samples were analyzed at room temperature with the following settings: 4000–600  $\text{cm}^{-1}$ , 64 scans, and a resolution of 4  $\text{cm}^{-1}$ . The peak positions were determined using OMNIC software peak picking function (ThermoFisher Scientific, Waltham, MA).

#### **4.3.2.7 Powder X-ray diffraction (PXRD)**

The polymorphic form of GABA in the physical mixture and granules was determined by using a Rigaku Miniflex 600 (Rigaku Americas, The Woodlands, Texas, USA) instrument equipped with a Cu-K $\alpha$  radiation source generated at 40 kV and 15 mA. Samples were scanned in continuous mode with a step size of 0.025° over a 2 $\theta$  range of 5° to 45° at a rate of 2.5° min<sup>-1</sup>. Data was analyzed by MDI Jade 9 software.

### **4.4 RESULTS AND DISCUSSION**

The effect of screw profile, specifically the geometry of kneading block, on process-induced transformation of GABA was investigated initially. Upon the selection of an optimal screw profile, the effects of processing conditions, including screw speed and feed rate, on

GABA granule size, polymorphic form, chemical stability, crystal defect, and tabletability were studied.

#### **4.4.1 Effect of screw profile (kneading block)**

All four known GABA polymorphs have extensive networks of hydrogen bonding between  $\text{NH}_3^+$  and  $\text{COO}^-$  groups of neighboring zwitterionic GABA in crystals. Form I is a monohydrate and forms II through IV are anhydrous. GABA Form II used in this study is the most stable form at ambient condition. GABA Form II is known to undergo a form change and chemical degradation simultaneously under heating (Hsu, C. H. et al., 2010). Since GABA was subjected to elevated thermal and mechanical stresses during TSMG, it was pertinent to assess potential processing-induced physical and chemical changes of GABA.

To study the effect of screw profile, we focused on the kneading-block screw geometry, since kneading blocks impose the most intense mixing, thermal stresses, and mechanical stresses on the materials. At kneading blocks, pressure traps are formed to squeeze, shear, and elongate the powder blend, leading to powder agglomeration (Thiele, 2018). It was observed in our previous study that granulation, chemical degradation, and size reduction of drug crystals for GABA-HPC formulations took place predominately at the kneading block (Kittikunakorn, N., Koleng, Listro, Sun, & Zhang, 2019). Figure 4.2 illustrates two screw profiles. The processing parameters for these two runs (runs 1 and 2) can be found in Table 4.1. Both screw profiles consist of forward-conveying and kneading elements. The design of the screw profile was based on the results from our prior study (Kittikunakorn, N., Koleng, J.J., et al., 2019) and it was intended to minimize GABA degradation. Large-pitch conveying elements were used in this study since small-pitch conveying element resulted in higher degree of fill and greater GABA degradation in our prior study. Kneading elements were positioned at zone 3 so that granules exit the barrel immediately following the granules formation. The only difference between these two screw profiles is the geometry of the kneading elements ( $60^\circ$  neutral KB7-3-15-60-N for profile A vs.  $30^\circ$  forward KB7-3-15-30 for profile B). These two types of kneading elements have different stacking angles between adjacent discs. A  $60^\circ$  stacking angle functions as a neutral element which conveys material neither forward nor reverse, while a  $30^\circ$  stacking angle indicates a forward conveying element. Therefore, a  $60^\circ$  kneading block provides more dispersive and

distributive mixing than a 30° kneading block. As shown in Table 4.1, the extrusion torques were 650 and 1,300 G.m for screw profiles containing 30° and 60° kneading blocks, respectively. Correspondingly, higher thermal and mechanical stresses were anticipated with a 60° kneading block.

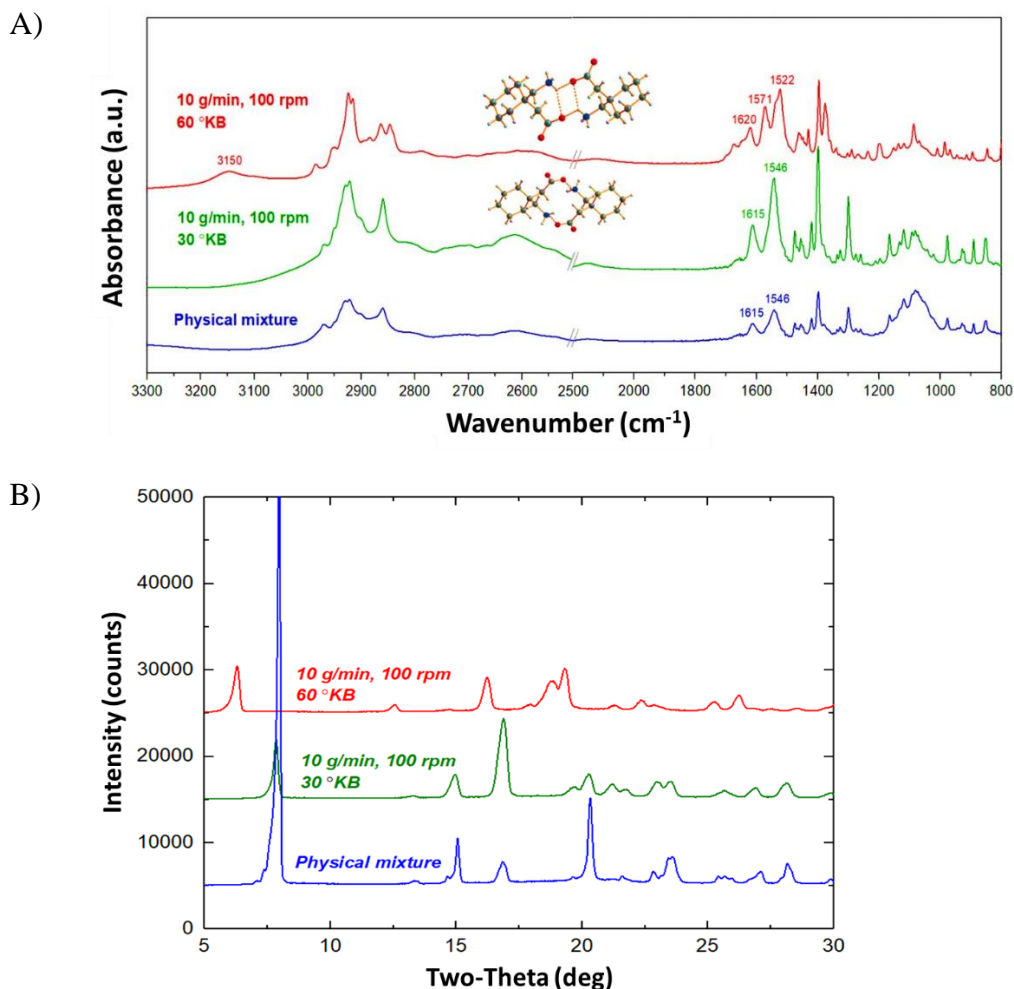


Figure 4.3 Polymorphic transformation of GABA determined by (A) XRPD, and (B) FT-IR. Processed at 10 g/min and 100 rpm with 30° forward or 60° neutral kneading block.

GABA polymorphs differ in the region of 1700 - 1500  $\text{cm}^{-1}$  in their FT-IR spectra. The peak at 1615  $\text{cm}^{-1}$  is the characteristic band of C=O stretching vibration of  $\text{COO}^-$  group and the peak at 1546  $\text{cm}^{-1}$  is from N-H scissoring vibration of  $\text{NH}_3^+$  group. In the spectrum for the melt-extruded GABA granules using 60° kneading block (Figure 4.3A), C=O peak shifted to a higher

wave number (from 1615 to 1620  $\text{cm}^{-1}$ ), N-H peak shifted to a lower wave number (from 1546 to 1522  $\text{cm}^{-1}$ ), and a new strong peak appeared at 1571  $\text{cm}^{-1}$ . These FTIR peaks correspond to the characteristic peaks of GABA form IV. Thus, conversion of Form II to Form IV took place during TSMG when a 60° kneading block was used. The results from FT-IR analysis were supported with those from XRPD analysis (Figure 4.3B). With 60° kneading blocks, the characteristic diffraction peak of Form II at 7.3 degree 2 $\theta$  angle was absent in the XRPD pattern of melt-extruded granules, while the characteristic diffraction peak of Form IV at 6.3 degree was observed (Hsu, C. H. et al., 2010). In comparison, these changes were absent in FT-IR spectra and XRPD patterns of granules prepared using the 30° kneading blocks. We attributed the solid form change associated with the use of 60° kneading blocks to the higher thermal and mechanical stresses arising from higher frictional and viscous heat dissipation. Based on these findings, the screw profile 30° containing kneading blocks (Figure 4.2B) was used for the remainder of the study (runs 3 through 16, Table 4.1).

GABA form IV becomes stable inside the barrel under the conditions induced by the mechanical and thermal stresses. Upon exiting the extruder barrel, form IV should “relax” to form II at ambient conditions, thermodynamically speaking. However, the cooling of the granules was so fast that GABA was kinetically trapped as metastable form IV following TSMG.

#### **4.4.2 Effect of processing condition on the physicochemical properties of GABA granules**

The effects of processing condition on the granule attributes, such as size, shape, and strength have been studied (Liu, Y., Thompson, & O'Donnell, 2018; Monteyne, T., Vancoillie, J., et al., 2016a). However, the effect of processing conditions on the chemical stability and polymorphic transformation has not been systematically investigated.

To evaluate the effect of processing conditions on the properties of GABA granules, twin-screw melt granulation was carried out using screw profile B (Figure 4.2). The highest torque used in this part of the study was 750 G.m because greater than 0.4% GABA-L impurity content accepted by USP and process-induced transformation were observed when the torque exceeded 1,200 G.m.

One of our objectives is to identify a correlation between physicochemical properties of GABA granules and processing parameters. A twin-screw process can be defined using machine

parameters and system parameters. Machine parameters, e.g., feed rate, screw speed, and screw profiles, can be controlled directly. System parameters, such as specific mechanical energy, shear rate, and specific rate, are functions of both the machine parameters and material properties. System parameters are machine independent. Certain system parameters should be kept the same during process scale-up in order to achieve the same quality attributes (Haser et al., 2018)

#### **4.4.2.1 Effect of screw speed and feed rate on GABA granule size**

Full factorial designs of experiment were performed by three feed rates (5, 7.5 and 10 g/min) and four screw speeds (100, 150, 200 and 300 rpm) as shown in (Table 4.1). When other things are equal, granule size increased with an increase in feed rate or a decrease in screw speed (Figure 4.4). This may be explained by considering the specific rate, the ratio between feed rate and screw speed. As a very useful system parameter to describe twin-screw extrusion, specific rate indicates the degree of the available barrel volume filled by the powder. It strongly influences compressive/shear stresses applied to the formulation. At a higher specific rate, the material packing and compressive forces between the screws were higher. As a result, the more extensive interactions between the powder particles, or the yet developed granules, led to greater extend of granule growth. A sigmoidal correlation between the granule size and the specific rate is observed in this work (Figure 4.5). Similar effects of screw speed and feed rate were reported for metformin-HPC granules prepared using TSMG (Lakshman et al., 2011b).



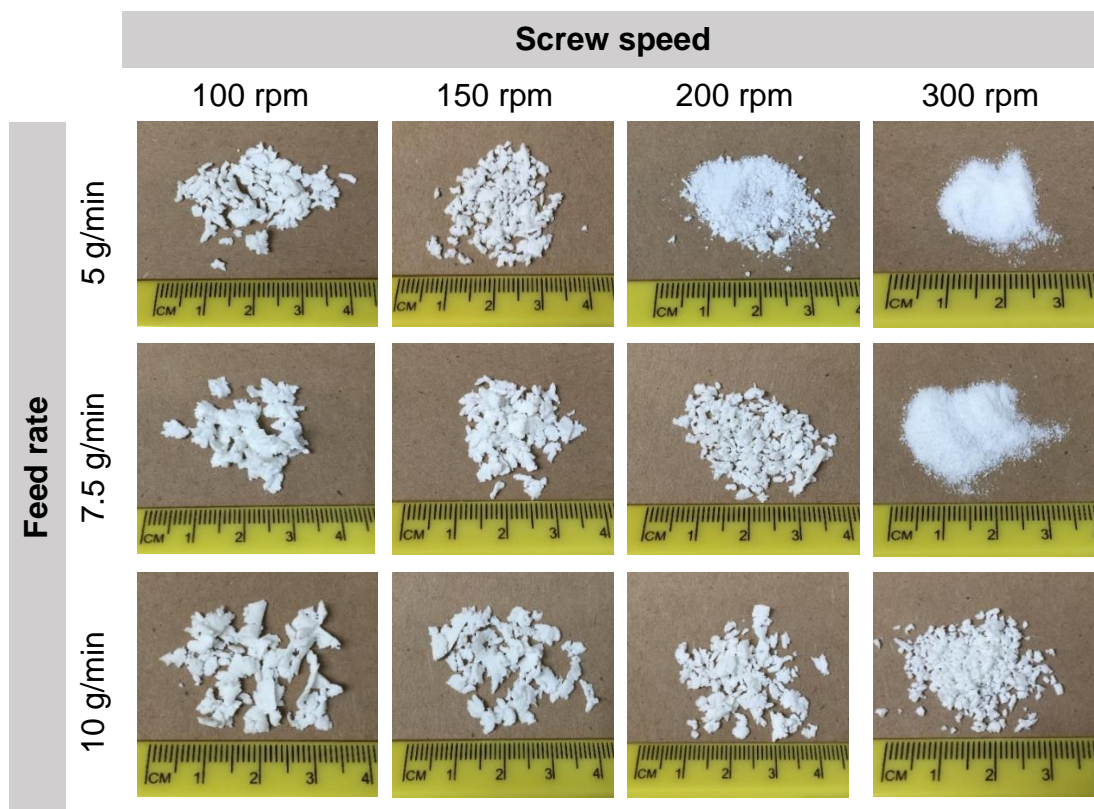


Figure 4.4 Images of melt-extruded granules processed at various processing conditions; feed rate: 5 g/min, 7.5 g/min, or 10 g/min; screw speed: 100 rpm, 150 rpm, 200 rpm, or 300 rpm.

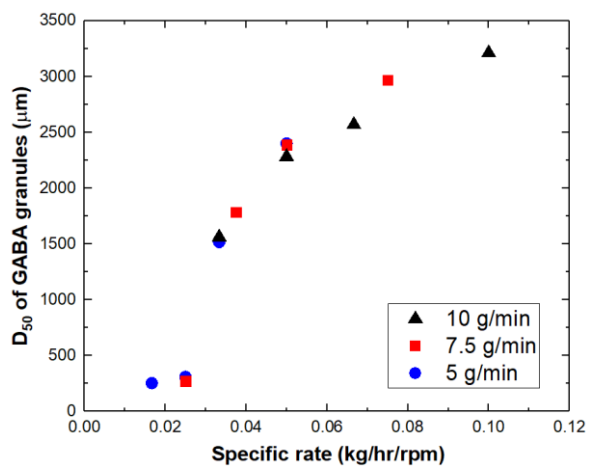


Figure 4.5 Correlation between granules size ( $D_{50}$ ) and specific rate of melt granulation process ( $n=3$ , means are reported).

#### 4.4.2.2 Effect of screw speed and feed rate on both polymorphic form stability and disorder of GABA crystals

When compared to the physical mixture, no changes in GABA solid form were detected in TSMG granules prepared using different feed rates and screw speeds by both FTIR and XRPD techniques. Representative FT-IR spectra and XRPD profiles of granules prepared at the lowest and highest specific rates are shown in Figure 4.6 and Figure 4.7, respectively.

As the result of thermal and mechanical stresses during TSMG, amorphous GABA and disordered GABA crystal lattice in GABA granules may have a significantly negative impact on the physical and chemical stability of GABA (Adrianowicz et al., 2011) (Fukuoka, Makita, & Yamamura, 1986). Greater molecular mobility in amorphous materials and disordered crystals allows for greater and faster chemical degradation (Makoto & Nobuyoshi, 1990).

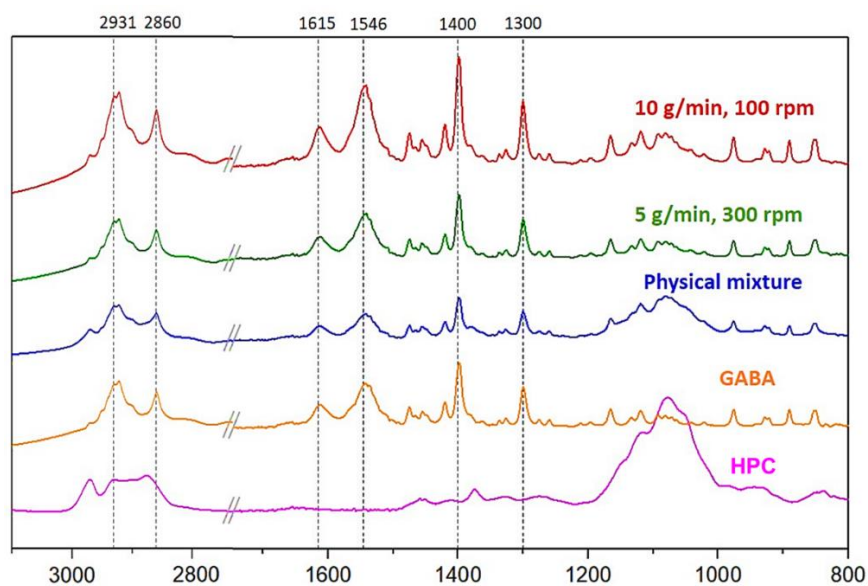


Figure 4.6 ATR-FTIR spectra of GABA and HPC raw materials, their physical mixtures, and melt-extruded granules processed at different conditions.

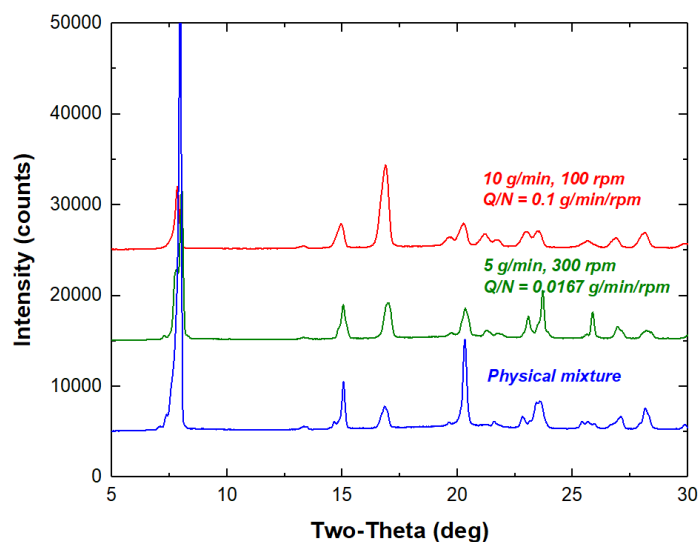


Figure 4.7 XRD pattern of GABA-HPC physical mixture and melt-extruded granules processed at highest (0.10 g/min/rpm – 10 g/min at 100 rpm) and lowest (0.0167 g/min/rpm – 5 g/min at 300 rpm) specific rates (Q/N).

#### 4.4.2.3 Effect of screw speed and feed rate on GABA chemical stability

GABA undergoes intramolecular cyclization to form beta-lactam (GABA-L) at elevated temperatures. GABA-L is a genotoxic impurity with a USP specification of less or equal to 0.4%. The thermal stress during melt granulation could lead to GABA degradation. Even though heat did conduct from the barrel to granules, the primary source of thermal stress in TSMG is from the dispersive and distributive mixing of the rotating screws, which generates thermal stress via viscous and frictional heat dissipation. As a result, the temperature of GABA granules ranged from 120 to 130°C, 10 to 20°C higher than the barrel temperature of 110°C.

GABA-L content in the melt-extruded granules was affected by both machine parameters, i.e., screw speed and feed rate, and was higher at a higher feed rate and lower screw speed (Figure 4.8). Another process parameter, specific mechanical energy (SME), may be potentially used to correlate with GABA-L level. SME represents the amount of power generated by the motor that input into each kg of the material processed. SME can be calculated using Equation 4.2.

$$\text{SME} = \frac{\text{KW (motor rating)} \times \% \text{ Torque} \times \frac{\text{RPM running}}{\text{RPM max}} \times 0.97 \text{ (gear efficiency)}}{\text{Feed Rate} \left( \frac{\text{kg}}{\text{hr}} \right)} \quad \text{Equation 4.2}$$

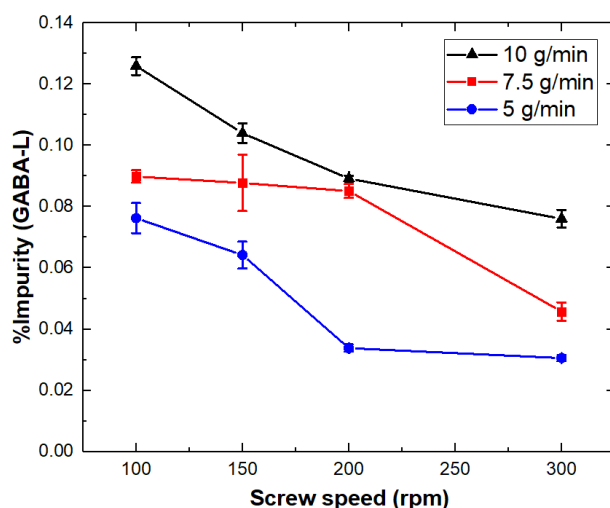


Figure 4.8 GABA-L content of melt-extruded GABA granules processed at various combination of screw speeds and feed rates (error bar represents the standard deviation of triplicate analyses).

For amorphous solid dispersions, higher levels of degradation generally correlate with higher SME, as in the meloxicam and copovidone formulation (Haser, A., Huang, S., Listro, T., White, D., & Zhang, F., 2017). However, there was no clear correlation between GABA-L level and SME (Figure 4.9A). Instead, a positive roughly linear correlation between GABA-L level and specific rate is observed (Figure 4.9B). This correlation may be explained in the same way as the observed correlation between granule size and specific rate (Figure 4.5). In Figure 4.10, GABA-L level was plotted as a function of granule size to further illustrate that the same mixing mechanisms contributed to both the granule growth and GABA degradation. Heating of the formulation is required for both granule growth and GABA degradation. Both frictional heat dissipation and heat conducted from the barrel contributed to the heating of the formulation. At a higher specific rate, the degree of fill was higher. As a result, the heat transfer from the barrel to the formulation became more efficient. Our hypothesis is that heat conducted from the barrel played a very significant role in the current melt granulation process.

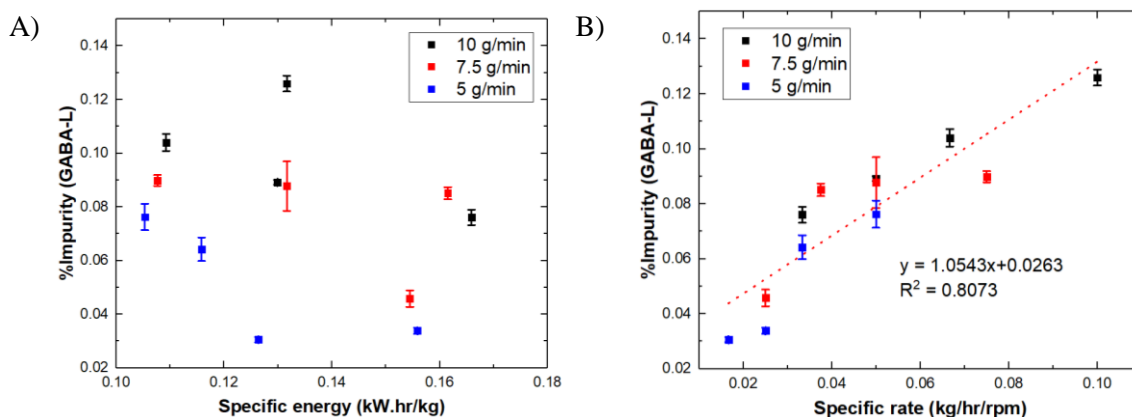


Figure 4.9 Relation between GABA-L content of melt-extruded GABA granules and system parameters of melt extrusion. (A) Specific mechanical energy, and (B) Specific rate.

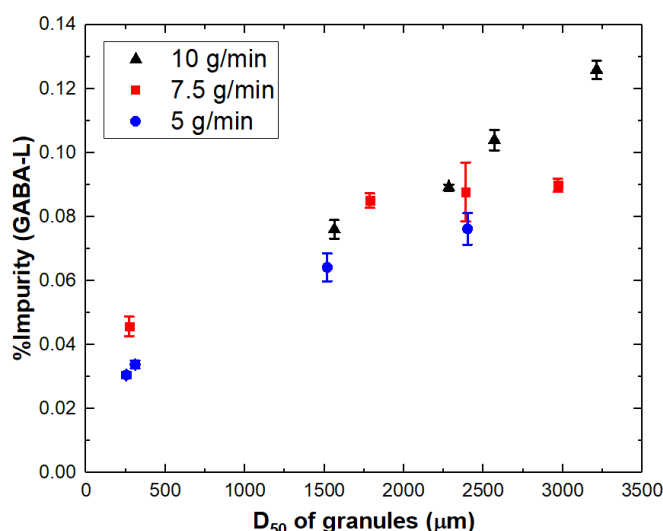


Figure 4.10 Correlation between GABA-L content and the size of melt-extruded GABA granules.

Particle sizes of GABA crystals in the melt-extruded granules may be used to probe the mechanical stresses during TSMG, as higher mechanical stresses likely cause more GABA crystal fracture and size reduction. Particle size distribution profiles of extracted GABA crystals in melt-extruded granules prepared at the lowest (5 g/min and 300 rpm) specific rates were the same as GABA drug substance (Figure 4.11), indicating minimal mechanical stress during TSMG. In contrast,  $D_{50}$  of GABA dropped from 64  $\mu\text{m}$  to 18  $\mu\text{m}$  at the highest specific rate at 10 g/min and 100 rpm (Figure 4.11), which clearly indicated that GABA was subjected to higher

mechanical stress. Following a significant drop initially, GABA  $D_{50}$  did not significantly decrease once the specific rate reached 0.03 g/min/rpm (Figure 4.12). This implies that the critical brittle-ductile transition size of GABA is 10 – 20  $\mu\text{m}$  under the conditions employed in this work (Kendall, 1978). At or below the critical size, reduction of GABA by crack propagation is impossible.

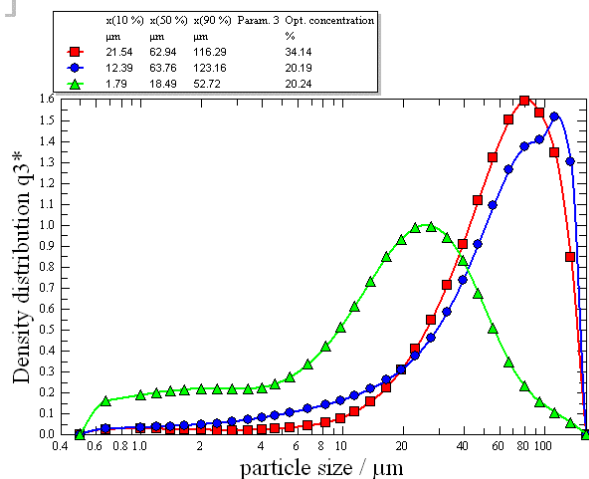


Figure 4.11 Particle size distribution of gabapentin (GABA) drug substance and GABA crystals in the melt-extruded granules at highest (0.10 g/min/rpm – 10 g/min at 100 rpm) and lowest (0.0167 g/min/rpm – 5 g/min at 300 rpm) specific rates.

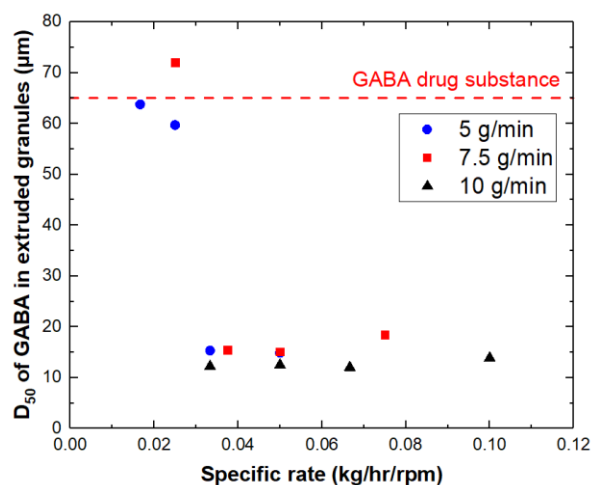


Figure 4.12 Correlation between  $D_{50}$  of GABA crystals in the melt-extruded granules and specific rate (Initial GABA crystal size has  $D_{50}$  of 65  $\mu\text{m}$ ) (n=3, mean values are reported).

The effect of specific rate on the mechanical stress during TSMG was confirmed using CAMES beads. CAMES beads are microcapsules consisting of a cross-linked polymeric shells with dye-containing cores manufactured using a coacervation process. Calibrated shear stress levels of CAMES beads are provided by the manufacturer. When mechanical stresses during TSMG exceed the strength of the shell, CAMES beads rupture to release the encapsulated AUTOMATE blue 8A dye. CAMES beads have been used to measure stress distribution during twin-screw polymer compounding (Balakrishnan, Dryer, & Bigio, 2017). CAMES beads (54-63  $\mu\text{m}$  in diameter, 330 kPa strength) were incorporated into GABA-HPC blend at 1% level. Once the extrusion reached a steady state, the extruder was stopped, and the screws were pulled out immediately. GABA granules were sampled at different axial positions and the concentration of the released dye in GABA granules was measured using LC-MS. As mentioned before, GABA degradation occurred predominately over the kneading blocks. CAMES beads rupture continuously along the axial direction of the screw under both the lowest (5 g/min and 300 rpm) and highest (10 g/min and 100 rpm) specific rates. 80% of beads ruptured even prior to entering the kneading block at the highest specific rate, while a maximum of 40% of beads ruptured at the lowest specific rate (Figure 4.13). Thus, mechanical stresses are on average greater at higher specific rate. However, the impurity profile (Figure 4.13A) increased exponentially as compared to the linear increase of the percentage of rupture for CAMES sensor (Figure 4.13B). It was hypothesized that the degradation of GABA might not occur until the shear stress reached a threshold.

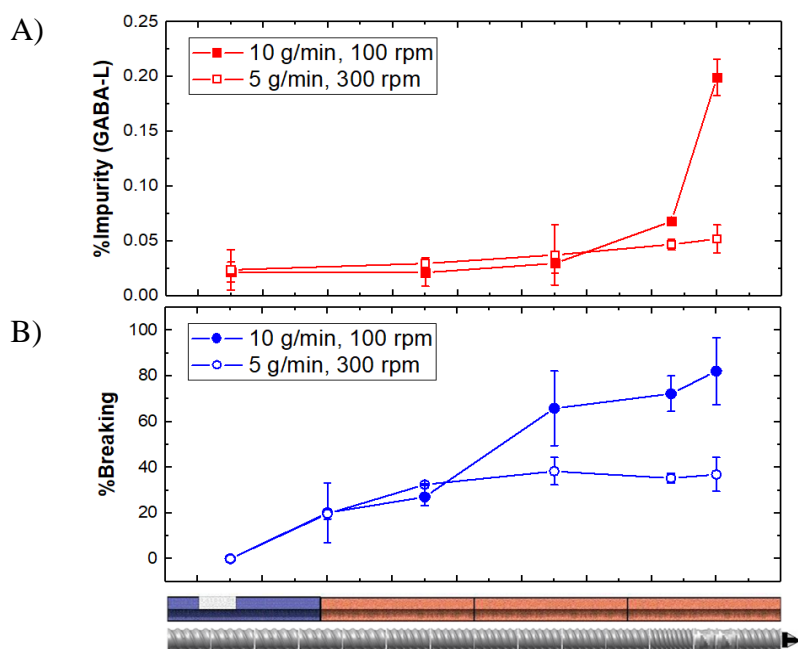


Figure 4.13 (A) The percentage of GABA degradant and (B) CAMES beads breakage along the axial direction at the highest (0.10 g/min/rpm – 10 g/min at 100 rpm) and lowest (0.0167 g/min/rpm – 5 g/min at 300 rpm) specific rates. (n=3, mean value and standard deviation are reported)

#### 4.4.2.4 Effect of processing condition on the tabletability of GABA granules

The primary motivation of GABA TSMG is to improve its tabletability since GABA exhibits poor tabletability and is a high dose drug (Jagdale, Kuchekar, Satapathy, & Chabukswar, 2010a). We had previously shown that the surface of TSMG GABA-HPC granules is enriched by HPC (Kittikunakorn, N., Koleng, J.J., et al., 2019). This spatial arrangement of HPC is expected to significantly improve tabletability of GABA granules as surface modification is extremely effective in improving powder compaction properties (Shi, L. & Sun, C. C., 2010).



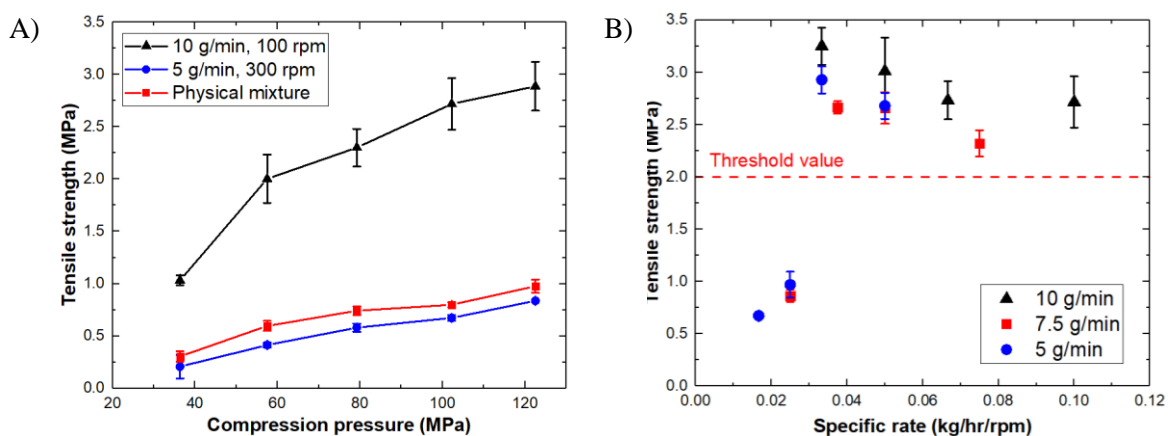


Figure 4.14 (A) Compression profiles of physical mixture and melt-extruded granules processed at high and low degree of fill and (B) correlation between tensile strength of the tablets prepared at 100 MPa compression pressure and the tensile strength of tablet. (n=5, mean value and standard deviation are reported)

The tableability, i.e., tablet tensile strength as a function of compression pressure, of the TSMG granulates (20-60 mesh) prepared at the highest specific rate is significantly higher than those of the physical mixture and the granule prepared at the lowest specific rate (Figure 4.14A). Tablets with tensile strength of equal to or greater than 2 MPa are considered to have sufficient mechanical strength (Osei-Yeboah, F. & Sun, C. C., 2015b). By this measure, the tableability of GABA granules processed at the lowest specific rate (5 g/min and 300 rpm) physical blend is deficient, since tensile strength barely reached 1 MPa at the highest pressure of 120 MPa used in this study (Figure 4.14A). Granules processed at the highest specific rate (10 g/min and 100 rpm) could reach 2 MPa tensile strength even at 60 MPa. The significantly improved tableability of the granules prepared at the highest specific rate is attributed to the efficient spreading and coating of HPC on the GABA surface, which was inadequate at the lowest specific rate. In Figure 4.14B, when plotted against specific rate, the tensile strength of tablets at 100 MPa compaction pressure for all granules jumped to above 2 MPa when the specific rate reached 0.03 g/min/rpm. This corresponds to change in GABA crystal reduction (Figure 4.12). Therefore, the smaller GABA size likely also contributed to the improved tableability at the highest specific rate. With further increase in the specific rate, the tensile strength of tablets

distributed in a range of 2.2 to 3.3 MPa. Therefore, the tableability enhancement was robust once the threshold specific rate was reached.

#### **4.5 CONCLUSIONS**

Process-induced transformation and chemical degradation of gabapentin during TSMG have been investigated using a formulation containing 20% HPC Klucel EXF. The 60° neutral kneading block led to significantly higher thermal and mechanical stresses, which caused more significant GABA conversion from form II to form IV. The usage of a 30° forward kneading block in combination with a low extrusion torque was required in order to prepare GABA granules with no polymorphic transformation and good chemical stabilities (GABA-L level below 0.15%). Under these machine parameters, a higher specific rate was found to lead to larger extruded granules, smaller GABA crystals, and higher tableability, but also higher degradant content in GABA granules. This was attributed to the higher mechanical stresses at higher specific rate, which was proven using CAMES sensors. Thus, a successful TSMG process requires a balance between achieving sufficient granule growth to improve tableability, process-induced form change, and chemical degradation of GABA.

## 4.6 REFERENCES

- Adrijanowicz, K., Kaminski, K., Grzybowska, K., Hawelek, L., Paluch, M., Gruszka, I., . . . Guzik, L. (2011). Effect of cryogrinding on chemical stability of the sparingly water-soluble drug furosemide. *Pharm Res*, 28(12), 3220-3236. doi:10.1007/s11095-011-0496-4
- Balakrishnan, N., Dryer, B., & Bigio, D. (2017). *Validation of residence stress distribution approach using 1-D computer simulations*. Paper presented at the SPE ANTEC, Anaheim.
- Batra, A., Desai, D., & Serajuddin, A. T. M. (2017). Investigating the Use of Polymeric Binders in Twin Screw Melt Granulation Process for Improving Compactibility of Drugs. *Journal of Pharmaceutical Sciences*, 106(1), 140-150. doi:10.1016/j.xphs.2016.07.014
- Fukuoka, E., Makita, M., & Yamamura, S. (1986). Some physicochemical properties of glassy indomethacin. *Chem Pharm Bull (Tokyo)*, 34(10), 4314-4321.
- Haser, A., Haight, B., Berghaus, A., Machado, A., Martin, C., & Zhang, F. (2018). Scale-Up and In-line Monitoring During Continuous Melt Extrusion of an Amorphous Solid Dispersion. *AAPS PharmSciTech*, 19(7), 2818-2827. doi:10.1208/s12249-018-1162-5
- Haser, A., Huang, S., Listro, T., White, D., & Zhang, F. (2017). An approach for chemical stability during melt extrusion of a drug substance with a high melting point. *Int J Pharm*, 524(1-2), 55-64. doi:10.1016/j.ijpharm.2017.03.070
- Haser, A., & Zhang, F. (2018). New Strategies for Improving the Development and Performance of Amorphous Solid Dispersions. *AAPS PharmSciTech*, 19(3), 978-990. doi:10.1208/s12249-018-0953-z
- Hsu, C. H., Ke, W. T., & Lin, S. Y. (2010). Progressive steps of polymorphic transformation of gabapentin polymorphs studied by hot-stage FTIR microspectroscopy. *Journal of Pharmacy and Pharmaceutical Sciences*, 13(1), 67-77.
- Jagdale, S., Kuchekar, B., Satapathy, J., & Chabukswar, A. (2010a). Pharmaceutical equivalence of gabapentin tablets with various extragranular binders. *Revista de Ciências Farmacêuticas Básica e Aplicada*, 31(1), 25-31.
- Kendall, K. (1978). The impossibility of comminuting small particles by compression. *Nature*, 272, 710. doi:10.1038/272710a0
- Kittikunakorn, N., DiNunzio, J. C., Martin, C., & Zhang, F. (2018). Processes, Challenges, and the Future of Twin-Screw Granulation for Manufacturing Oral Tablets and Capsules. *AAPS NewsMagazine*, Mar(Mar), 12-18.
- Kittikunakorn, N., Koleng, J. J., Listro, T., Sun, C. Q., & Zhang, F. (2019). Effects of Thermal Binders on Chemical Stabilities and Tabletability of Gabapentin Granules Prepared by Twin-Screw Melt Granulation. *International Journal of Pharmaceutics*, 559, 37-47.
- Kowalski, J., Kalb, O., Joshi, Y. M., & Serajuddin, A. T. M. (2009). Application of melt granulation technology to enhance stability of a moisture sensitive immediate-release drug product. *International Journal of Pharmaceutics*, 381(1), 56-61. doi:<http://dx.doi.org/10.1016/j.ijpharm.2009.05.043>
- Lakshman, J. P., Kowalski, J., Vasanthavada, M., Tong, W. Q., Joshi, Y. M., & Serajuddin, A. T. M. (2011b). Application of Melt Granulation Technology to Enhance Tableting Properties of Poorly Compactible High-Dose Drugs. *Journal of Pharmaceutical Sciences*, 100(4), 1553-1565. doi:10.1002/jps.22369

- Lee, S. (2017). Modernizing the Way Drugs Are Made: A Transition to Continuous Manufacturing. Retrieved from <https://www.fda.gov/Drugs/NewsEvents/ucm557448.htm>
- Liu, Y., Thompson, M. R., & O'Donnell, K. P. (2018). Impact of non-binder ingredients and molecular weight of polymer binders on heat assisted twin screw dry granulation. *International Journal of Pharmaceutics*, 536(1), 336-344. doi:10.1016/j.ijpharm.2017.11.061
- Makoto, O., & Nobuyoshi, K. (1990). Effect of grinding on the crystallinity and chemical stability in the solid state of cephalothin sodium. *International Journal of Pharmaceutics*, 62(1), 65-73. doi:[https://doi.org/10.1016/0378-5173\(90\)90031-X](https://doi.org/10.1016/0378-5173(90)90031-X)
- Monteyne, T., Heeze, L., Oldörp, K., Vervaet, C., Remon, J.-P., & De Beer, T. (2016). Vibrational spectroscopy to support the link between rheology and continuous twin-screw melt granulation on molecular level: A case study. *European Journal of Pharmaceutics and Biopharmaceutics*, 103, 127-135. doi:10.1016/j.ejpb.2016.03.030
- Monteyne, T., Vancoillie, J., Remon, J. P., Vervaet, C., & De Beer, T. (2016a). Continuous melt granulation: Influence of process and formulation parameters upon granule and tablet properties. *European Journal of Pharmaceutics and Biopharmaceutics*, 107, 249-262. doi:10.1016/j.ejpb.2016.07.021
- Morris, K. R., Griesser, U. J., Eckhardt, C. J., & Stowell, J. G. (2001). Theoretical approaches to physical transformations of active pharmaceutical ingredients during manufacturing processes. *Advanced Drug Delivery Reviews*, 48(1), 91-114. doi:[https://doi.org/10.1016/S0169-409X\(01\)00100-4](https://doi.org/10.1016/S0169-409X(01)00100-4)
- Mu, B., & Thompson, M. R. (2012). Examining the mechanics of granulation with a hot melt binder in a twin-screw extruder. *Chemical Engineering Science*, 81, 46-56. doi:10.1016/j.ces.2012.06.057
- Nie, H., Byrn, S. R., & Zhou, Q. (2017). Stability of pharmaceutical salts in solid oral dosage forms. *Drug Development and Industrial Pharmacy*, 43(8), 1215-1228. doi:10.1080/03639045.2017.1304960
- Osei-Yeboah, F., & Sun, C. C. (2015b). Validation and applications of an expedited tablet friability method. *Int J Pharm*, 484(1-2), 146-155. doi:10.1016/j.ijpharm.2015.02.061
- Picker-Freyer, K., & Dürig, T. (2007). Physical mechanical and tablet formation properties of hydroxypropylcellulose: In pure form and in mixtures. *AAPS PharmSciTech*, 8, E1-E9. doi:10.1208/pt0804092
- Rials, T. G., & Glasser, W. G. (1988). Thermal and dynamic mechanical properties of hydroxypropyl cellulose films. *Journal of Applied Polymer Science*, 36(4), 749-758. doi:10.1002/app.1988.070360402
- Royce, A., Suryawanshi, J., Shah, U., & Vishnupad, K. (1996). Alternative Granulation Technique: Melt Granulation. *Drug Development and Industrial Pharmacy*, 22(9-10), 917-924. doi:10.3109/03639049609065921
- Shi, L., Feng, Y., & Sun, C. C. (2011). Massing in high shear wet granulation can simultaneously improve powder flow and deteriorate powder compaction: a double-edged sword. *European Journal of Pharmaceutical Sciences*, 43(1-2), 50-56. doi:10.1016/j.ejps.2011.03.009
- Shi, L., & Sun, C. C. (2010). Transforming powder mechanical properties by core/shell structure: compressible sand. *J Pharm Sci*, 99(11), 4458-4462. doi:10.1002/jps.22172

- Sun, C. C., & Kleinebudde, P. (2016). Mini review: Mechanisms to the loss of tabletability by dry granulation. *European Journal of Pharmaceutics and Biopharmaceutics*, 106, 9-14. doi:10.1016/j.ejpb.2016.04.003
- Thiele, W. (2018). Twin-Screw Extrusion and Screw Design. In I. Ghebre-Sellassie & C. Martin (Eds.), *Pharmaceutical Extrusion Technology* (2nd ed., pp. 71-93). New York: CRC Press.
- Zong, Z. X., Desai, S. D., Kaushal, A. M., Barich, D. H., Huang, H. S., Munson, E. J., . . . Kirsch, L. E. (2011). The Stabilizing Effect of Moisture on the Solid-State Degradation of Gabapentin. *AAPS PharmSciTech*, 12(3), 924-931. doi:10.1208/s12249-011-9652-8

## **Chapter 5: Is the Melt Granulation Behavior Same between Leistritz Nano-16 and Micro-18 Extruders?**

### **5.1 ABSTRACT**

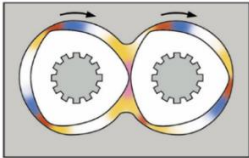
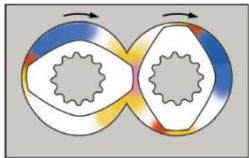
Using 80% Gabapentin and 20% hydroxypropyl cellulose (Klucel) blend as a model formulation, we investigated how differences in mixing elements geometry between the Leistritz Nano-16 and Micro-18 extruders affect granulation mechanisms and granule properties. Because of their thinner discs (2.5 mm wide), kneading blocks in Nano-16 are less efficient in dispersive mixing than kneading blocks in the Micro-18. Therefore, the formulation could only be granulated under a higher degree of fill (DF) by enhancing axial compaction and heating by the barrel. In contrast, efficient dispersive mixing by the kneading blocks (5 mm wide) in the Micro-18 enabled granulation without axial compaction and barrel heating. Higher specific mechanical energy (SME) achieved at higher screw speeds and lower feed rates (lower DF) led to a greater degree of granulation. Because of the difference in granulation mechanisms between the two extruders, correlations between granule properties and processing parameters is different between the two extruders. Tabletability and degradant content of granules correlated positively with DF for the Nano-16 and with SME for the Micro-18.

### **5.2 INTRODUCTION**

Granulation processes are commonly used in pharmaceutical manufacturing to (1) prevent segregation, (2) ensure uniformity (Pandey & Badawy, 2019), (3) improve flow, and (4) enhance the tabletability of powder blends (Batra, A. et al., 2017). Various granulation technique such as wet, melt, and dry granulation can be used to granulate powders (Parikh, 2005). Granulation is traditionally carried out in batch process. In order to achieve better process control and consistency in product quality, the transition of wet and melt granulation from batch to continuous process using twin-screw extruders has recently drawn significant interest in the pharmaceutical industry.

Twin-screw melt granulation (TSMG) is a continuous and solvent-free process which is suitable for both water and solvent-sensitive drug substances (Ghebre-Sellassie, I. et al., 2002). TSMG can effectively improve the tableability of a drug substance by modifying the surface of drug crystal with molten binder, which solidifies upon cooling after exiting the extruder (Kittikunakorn, N., Sun, C. C., et al., 2019). The successful application of TSMG to the manufacture of Eucrase™ tablets (TSMG of metformin with hydroxypropyl cellulose) has drawn the pharmaceutical industry's interest to this process (Lakshman et al., 2011a). However, one of the major limitations of TSMG is the undesired physicochemical changes it can induce in drug substances during processing. The granule temperature is elevated as a result of the heat conducted from the barrel and of the viscous heat dissipation by the rotating screws (Rauwendaal, 2016). Elevated thermal and mechanical stresses cause undesired process-induced transformations of drug substances. Polymorphic changes and chemical degradation of drug substances during TSMG have been reported (Kittikunakorn, N., Sun, C. C., et al., 2019; Lakshman et al., 2011a). Therefore, a systematic study of the process-induced physicochemical changes of drug substances in TSMG is needed to facilitate broader adoption and better process design for TSMG by the pharmaceutical industry.

Table 5.1 Differences of machine and screw geometry at kneading zone between Leistritz Nano-16 and Micro-18 extruders

Parameter	Nano-16 extruder	Micro-18 extruder
Screw configuration		
Screw diameter (mm)	16	18
Overflight gap (mm)	0.05	0.1
Maximum channel depth (mm)	1.2	3.1
Free volume (cc./dia)	1	3.2
Disc width of kneading element (mm)	2.5	5
Disc stacking angle of kneading element*	30	30

\* tri-lobal kneading element for Nano-16 vs. bi-lobal kneading element for Micro-18. Neutral position would be 60° and 90° for Nano-16 and Micro-19. Therefore, from stacking angle perspective, the kneading elements used in Nano-16 provides more dispersive mixing.

The Leistritz Nano-16 and Micro-18 are co-rotating twin-screw extruders commonly used at different stages of product development. As shown in Table 5.1, the Nano-16 extruder (trilobal screw element) is designed with a minimal free volume to enable preclinical development with a small amount of material (< 50 g). The ratio between barrel length and inner diameter of the barrel is 26:1 for the Nano-16. Trilobal screw elements in the Nano-16 have 15.9 mm outer diameters. In comparison, the Micro-18 extruder has a higher free volume and is used to support phases 1 through 3 clinical trials (0.5 to 4 kg per hour production rate). Bilobal screw elements in the Micro-18 have 17.8 mm outer diameters. The ratio between barrel length and inner diameter of the barrel is 25:1 for the Micro-18. The Micro-18 offers several advantages, such as ability to scale-up and flexible process design and control (e.g., side stuffing, downstream feeding, and vacuum) (Martin, 2013a).

TSMG of Gabapentin (GABA) and hydroxypropyl cellulose (Klucel) using the Nano-16 extruder was investigated in our prior study (Kittikunakorn, N., Sun, C. C., et al., 2019). As a high-dose drug (up to 800 mg per tablet) with poor compaction properties, GABA requires tabletability improvement via granulation (Jagdale, Kuchekar, Satapathy, & Chabukswar, 2010b). Klucel is a highly effective polymeric binder in tabletability enhancement (Picker-Freyer, K. M. & Dürig, T., 2007). A low glass transition temperature of 20°C and a softening temperature between 100 and 120°C (Rials & Glasser, 1988) make Klucel an ideal thermal binder for TSMG. GABA was selected as a model drug because of its poor thermal stability. It undergoes intramolecular cyclization followed by dehydration to yield gabapentin-lactam (GABA-L) at elevated temperatures (Zong, Z., Qiu, Tinmanee, & Kirsch, 2012). GABA consists of four polymorphic forms, of which Form II is the most stable. Form I is the monohydrate form and Form II-IV is the anhydrous form (Reece & Levendis, 2008). Under mechanical stress such as milling, GABA was reported to undergo process-induced polymorphic transformation (Lin, Hsu, & Ke, 2010; Tinmanee, Stamatis, Ueyama, Morris, & Kirsch, 2018). In our prior study of GABA TSMG using the Nano-16, the degree of fill (DF) was identified to be the critical processing parameter controlling the physicochemical properties of granules (Kittikunakorn, N., Sun, C. C., et al., 2019). However, in order to achieve higher throughput and more flexible process design, we need to transfer the granulation process to Micro-18.



Transition of TSMG from the Nano-16 to the Micro-18 extruder is complex due to differences in machine parameters such as screw geometry and free volume. Djuric et al. reported that differences in granule formation were observed between two twin-screw extruders (APV Baker and Leistritz), leading to the differences in granule properties such as flowability, porosity, and tensile strength. They concluded that these two extruders cannot be simply interchanged without further geometric optimization (Djuric, D., Van Melkebeke, Kleinebudde, Remon, & Vervaet, 2009).

Therefore, the aims of our study are (1) to investigate the differences in granulation mechanisms, and (2) to determine the differences in the granulation process-granule properties correlation between the Nano-16 and the Mico-18. Granule properties focus on GABA physicochemical stability and tabletability.

### **5.3 MATERIAL AND METHODS**

#### **5.3.1 Material**

Gabapentin (GABA, Form II) was purchased from ShenZhen Nexconn Pharmatechs (Shenzhen, China). GABA has a melting point of 174°C and water solubility of 100 mg/ml at 25°C. Hydroxypropyl cellulose (Klucel™ EF) was kindly donated from Ashland Inc. (Wilmington, DE). All other chemicals were ACS grade or higher.

#### **5.3.2 Methods**

##### **5.3.2.1 Twin-screw melt granulation**

A powder consisting of 80% (w/w) GABA and 20% (w/w) Klucel was prepared by mixing in a V-shape blender (MaxiBlend, GlobePharma, New Brunswick, NJ) at 25 rpm for 10 min. All experiments were carried out using a Leistritz Nano-16 or Micro-18 co-rotating twin-screw extruder (American Leistritz Extruder Corp., Somerville, NJ). A twin-screw volumetric feeder (Brabender Technologies, Ontario, Canada) was used to control the feed rate. For the Nano-16, the barrel was divided into four zones. The barrel temperatures at zones 1 through 4 were maintained at 25°C, 70°C, 110°C, and 110°C, respectively. The temperatures were chosen based on the softening temperature of Klucel at 100-120°C. For the Micro-18, the barrel was divided into five zones. The first zone was maintained at room temperature with water

circulation. The barrel temperature from zone 2 to zone 5 was set at 60°C. Both the Nano-16 and the Micro-18 were operated with an open-end discharge configuration. The screw design used in each extruder is presented in Figure 5.1. Steady state torque was recorded throughout the study. Granule temperature was measured with a non-contact infrared thermometer (Fluke, VT04A, Everett, WA). Screw speed and feed rate were systematically varied as listed in Table 5.2.

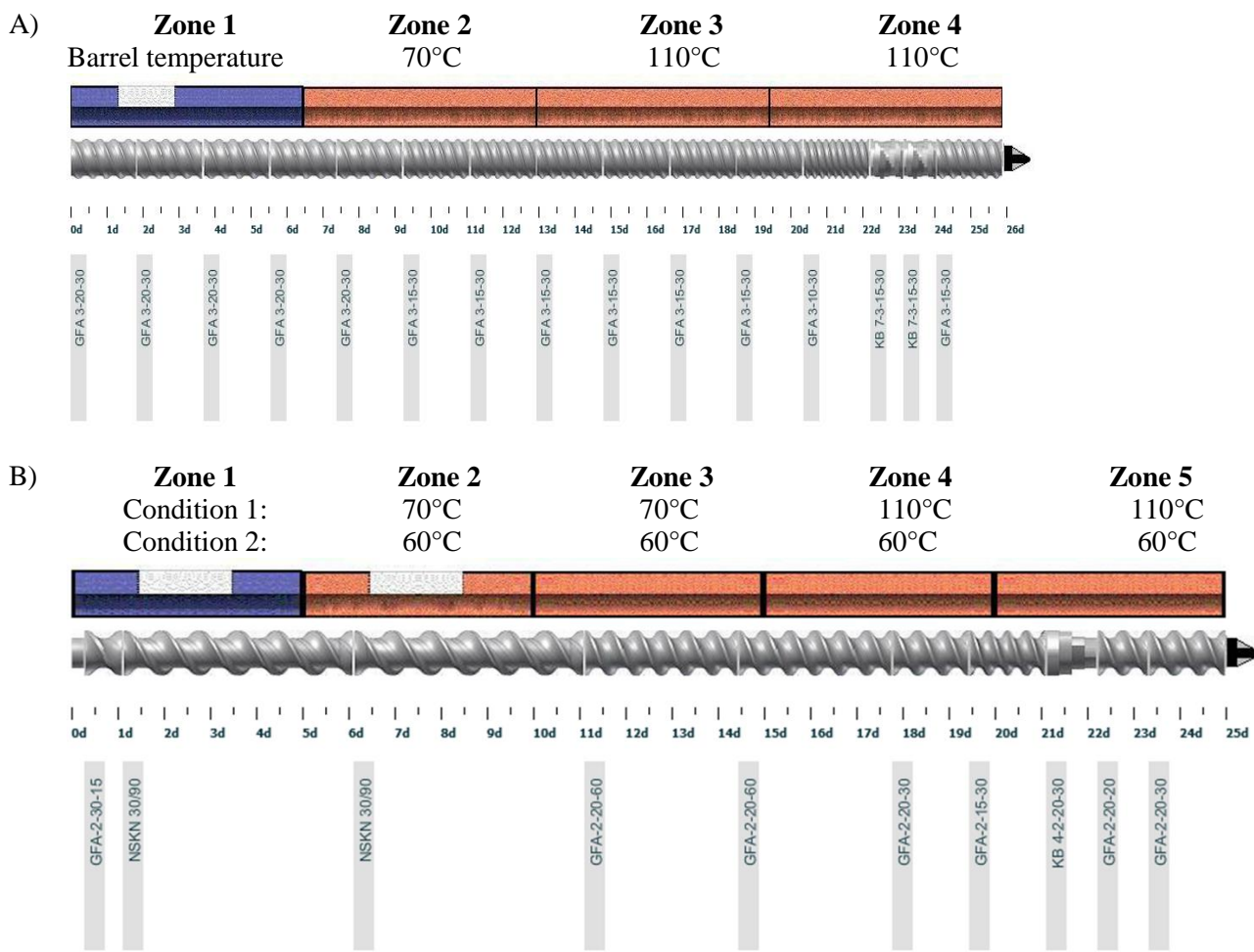


Figure 5.1 Barrel configuration, screw profile with open-end discharge, and barrel temperature of (A) Nano-16 (B) Micro-18 twin-screw extruder.

GFA X-XX-XX Co-rotating conveying screw-trilobal screw-pitch length (mm)-screw length (mm).  
KB X-X-XX-XX Kneading block-number of kneading segment-screw length (mm)-the angle (°).  
0d to 26d Length to diameter ratio (total barrel length is 420 mm; barrel diameter is 16 mm).

Table 5.2 A list of extrusion runs and their processing condition.

Extruder	Run	Feed rate (g/min)	Screw speed (rpm)	Degree of fill (%)	Torque (%)	Granule temperature (°C)	Comments
Nano-16 Twin-screw extruder	F1	10.0	100	25.0	13.8	129	Barrel temperature of zone 1-3 was set at 70-110-110°C, respectively.  No granule formation for Runs no. F3 and F6
	F2	10.0	150	16.7	7.2	130	
	F3	10.0	200	12.5	2.7	117	
	F4	12.5	100	31.3	17.0	133	
	F5	12.5	150	20.8	11.1	135	
	F6	12.5	200	15.6	2.9	122	
	F7	15.0	100	37.5	20.0	136	
	F8	15.0	150	25.0	12.9	138	
	F9	15.0	200	18.8	10.3	140	
	F10	20.0	100	50.0	24.3	140	
	F11	20.0	150	33.3	15.7	145	
	F12	20.0	200	25.0	12.7	146	
Micro-18 Twin-screw extruder	F13	21.3	100	12.5	31	90	Barrel temperature of zone 1-4 was set at 60°C.
	F14	21.3	150	8.3	25	92	
	F15	21.3	200	6.2	22	112	
	F16	21.3	300	4.2	19	123	
	F17	42.7	100	25.0	40	86	
	F18	42.7	150	16.7	33	92	
	F19	42.7	200	12.5	27	99	
	F20	42.7	300	8.3	23	108	
	F21	64.0	100	37.5	51	92	
	F22	64.0	150	25.0	43	97	
	F23	64.0	200	18.8	38	103	
	F24	64.0	300	12.5	28	110	
	F25	85.3	100	50.0	70	96	
	F26	85.3	150	33.3	51	102	
	F27	85.3	200	25.0	43	104	
	F28	85.3	300	16.7	33	112	

### 5.3.2.2 Assay and impurity content

Gabapentin and degradant (GABA-L) content were analyzed using a Thermo Scientific Dionex Ultimate 3000 HPLC system (Thermo Scientific, Sunnyvale, CA) equipped with dual Ultimate pumps and an RS variable wavelength UV detector. The mobile phase consisted of 60% (v/v) water, 30% (v/v) methanol, and 10% (v/v) acetonitrile with an isocratic flow rate of 0.8 mL/min. The standard and sample solutions were prepared to be within the linear concentration range of 0-10 mg/mL. Prior to injection, the solutions were filtered through a 0.45 µm Nylon membrane. 20-µl samples were injected onto an Inertsil™ ODS-2 C18 reversed phase

column (4.6 x 150 mm, with 5  $\mu\text{m}$  packing, GL Sciences Inc., Japan) at room temperature. The chromatography data were processed and analyzed using Chromeleon software (Version 6.8, Thermo Scientific, Sunnyvale, CA). The retention times of GABA and GABA-L were 3.2 and 12.8 min, respectively. The LOD and LOQ of GABA-L were 0.03 and 0.08  $\mu\text{g/mL}$ , respectively.

### 5.3.2.3 Enthalpy change during twin-screw melt granulation

Based on Hess's law, the enthalpy change of any reaction is independent of the number of ways the product can be obtained, as long as the initial and final product are the same. Therefore, the enthalpy difference ( $\Delta H$ ) between the physical mixture and granules exiting the extruder can be calculated by dividing the granulation process into the following two steps shown in Figure 5.2A.

Step 1:  $\Delta H$  between physical mixture and granules at 25°C, and

Step 2:  $\Delta H$  between granules at 25°C and granule exiting extruder at elevated temperature.

$\Delta H$  in Step 1 and Step 2 can be measured and calculated using a solution isothermal micro-calorimeter and a differential scanning calorimeter, respectively.

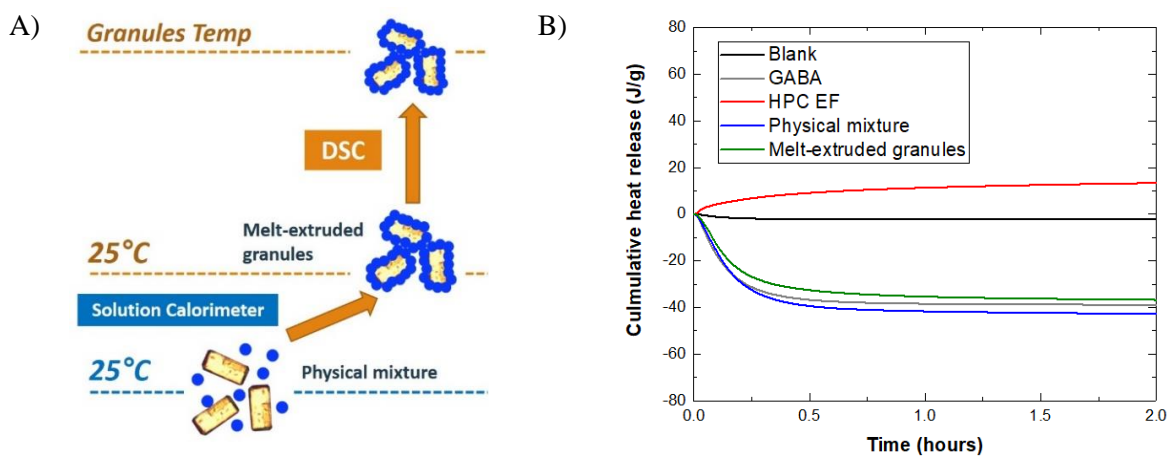


Figure 5.2 (A) Schematic diagram demonstrating enthalpy measurement using thermodynamic method and (B) Measured cumulative heat release of each material from isothermal microcalorimetry analyses.

#### **a) Solution isothermal micro-calorimetry**

$\Delta H$  values between physical mixture and granules at 25°C were obtained using isothermal micro-calorimeter (TAM IV, TA instrument, New Castle, DE). Experiments were performed at 25°C, using 0.1 g of each sample and 4 mL of deionized (DI) water at 25°C  $\pm$  0.2°C. Each sample was placed within the calorimeter using the titration cell. Once the measured heat signal was moderately stable, the initial baseline for each experiment was initiated. After completion of the initial baseline, the sample was stirred at 150 rev/min for 2.5 min as 4 mL of DI water was directly injected. The stirring rate was shown to minimally affect the heat evolution in relation to the effects of the addition of water and dissolution. The heat evolution of a blank sample, that is a sample system containing no powder material before DI water was injected, was also monitored, with identical conditions to all other samples analyzed. Each sample was monitored for a minimum of 5 hr following water injection.

#### **b) Differential scanning calorimetry (DSC)**

The heat capacity of granules at various temperature was determined using a differential scanning calorimeter (DSC Q20, TA instruments, New Castle, DE). A pair of pans and lids that were to be used for the reference and sample were selected so as to have similar weights ( $\pm 5$  mg). Prior to the heat capacity measurement, the DSC was calibrated using indium, ramping from 100 to 180°C at a heating rate of 10°C/min. The onset melting point of indium should be in the range at  $156.6 \pm 0.3^\circ\text{C}$ . Then MDSC heat capacity calibration was performed using sapphire to determine the calibration factor. The sample was heated from 25 to 250°C with a heating rate of 3°C/min and an amplitude of 1°C every 120 seconds. The enthalpy change of the sample was then calculated using the equation:

$$\Delta H = \int_{T_2}^{T_1} C_p dT \quad \text{Equation 5.1}$$

where  $\Delta H$  is enthalpy change,  $C_p$  is the heat capacity, and  $T$  is temperature.

#### **5.3.2.4 Tabletability of melt-extruded granules**

GABA-Klucel granules were milled using a co-mill (Quadro comil, U5-0516, Ontario, Canada) with a round-hole screen (0.032 inches.) and an impeller speed of 1000 rpm. Granules

between 250  $\mu\text{m}$  to 850  $\mu\text{m}$  (60-20 mesh) were collected. The collected granules were mixed with 0.5% (w/w) magnesium stearate in a Turbula® Shaker-Mixer (Glen Mills, Clifton, NJ) at 25 rpm for 3 min. Tableability of the granules was characterized using a compaction simulator (Presster®, Metropolitan Computing Corporation, NJ, USA). 300 mg of granules were compressed with flat-faced round tooling with a 10 mm diameter over a range of compression pressures between 25 and 300 MPa. The dwell time and tablet production rate were set at 10 ms and 103,000 tablets/hr, respectively. Tablets were kept in the sealed container for two hours to allow stress relaxation. The breaking force of the tablets was then measured using a texture analyzer (Texture Technologies Corp., Surrey, UK). The speed of the probe was set at 0.01 mm/s. The tensile strength of the tablets was calculated based on the following equation (Fell & Newton, 1970):

$$TS = \frac{2F}{\pi \cdot D \cdot H} \quad \text{Equation 5.2}$$

where F, D, H represents the breaking force (N), tablet diameter (mm), and tablet thickness (mm), respectively.

### 5.3.2.5 Granule density

A multipycnometer (Quantachrome Instruments, Boynton Beach, FL) was used to measure the density of the granules along the axial direction of the screw. Immediately after the extruder was stopped, the screws were pulled out and granules were sample at various locations. Helium controlled at 20 psi was used as the displacement gas in the system. Granules were placed in the micro cell to at least 75% of the cell volume, and the sample weight was recorded. The sample volume was calculated based on the equation:

$$V_p = V_c - V_r \left( \left( \frac{P_1}{P_2} \right) - 1 \right) \quad \text{Equation 3}$$

where  $V_p$  is the sample volume ( $\text{cm}^3$ ),  $V_c$  is the cell volume ( $\text{cm}^3$ ),  $V_r$  is the reference volume ( $\text{cm}^3$ ),  $P_1$  is the pressure reading after pressurizing the reference volume (kPa), and  $P_2$  is the pressure reading after including the cell volume (kPa). The granule density was then calculated by dividing the sample weight (g) with  $V_p$  ( $\text{cm}^3$ ). The measurement was carried out at room temperature and repeated three times. It should be noted that as helium gas cannot penetrate though the granules, the sample volume ( $V_p$ ) represents the volume of granules including the

volume of closed pore inside the granules but excluding the volume of open pore and the void between the granules. Therefore, the measured granules density in this study is not true density of the material. It can be called apparent density or skeleton density (Webb, 2001)

#### **5.3.2.6 Binder distribution**

Granules were dispersed in a 20% sodium chloride solution in which GABA can be freely dissolved but Klucel is not soluble. Blue dye (Paragon stain) was added in the solution to stain Klucel. Samples were kept at ambient conditions for at least 5 hr to allow GABA to dissolve and Klucel to be stained. The remaining scaffold of Klucel was analyzed using a compound light microscope in the phase-contrast mode (Nikon Eclipse Ni, Nikon Instruments Inc., Japan) at 40x magnification. Images were captured using the NIS-Elements software. The resolution and size of captured images were set at 3x8 bit and 4908x3264, respectively. The captured images were further processed using ImageJ. The color distribution represents the amount of Klucel based on the distribution of dye intensity.

#### **5.3.2.7 Particle size of GABA in melt-extruded granules**

Particle size of GABA in melt-extruded granules was measured using a laser diffraction analyzer with a cuvette dispersing system (Sympatec Helos (R3 lens), Sympatec GmbH, Germany). The melt-extruded granules were initially dispersed in acetone for at least 3 hr under gentle stirring. Acetone was selected as a dispersing solvent as it readily dissolves Klucel but cannot dissolve GABA. During measurement with laser diffraction analyzer, the dispersion of GABA in acetone was added dropwise to the cuvette filled with acetone until the light obscuration was between 10-25%. The data was collected every 100 ms for 10 sec.

### **5.4 RESULTS AND DISCUSSIONS**

#### **5.4.1 Scale-up from Nano-16 to Micro-18**

Scale-up of twin-screw process is generally based on system parameters including degree of fill, specific mechanical energy, shear rate, and residence time. In our previous study of TSMG of GABA-Klucel using a Leistritz Nano-16, feed rate and screw speed were varied to determine the correlation between processing parameters and granule quality attributes. It was

concluded that the degree of fill (DF) is the system parameter that correlated well with the properties of granules (Kittikunakorn, N., Sun, C. C., et al., 2019). Therefore, in our initial attempt to scale-up from the Nano-16 to the Micro-18, DF was kept the same. The DF is calculated based on the conveying elements leading to the kneading elements with the following equation (Todd, 1998a):

$$\%Fill = \frac{Feed\ rate}{(Cross\ section\ area \times Pitch\ length \times rpm \times Density)/2} \times 100 \quad \text{Equation 5.4}$$

The screw designs used in the Nano-16 and the Micro-18 are shown in Figure 5.1. Because polymorphic transformation of GABA was observed with the more aggressive 60° kneading element in our previous Nano-16 study (Kittikunakorn, N., Sun, C. C., et al., 2019), a 30° kneading element was selected for granulation for both the Nano-16 and the Micro-18. The barrel temperatures of zone 2 through zone 4 in the Nano-16 were set at 70, 110, and 110°C, respectively. At a temperature below 110°C, a powder blend could not be granulated without the heat conducted from the barrel. The degradant level ranged from 0.01 to 0.1% in the Nano-16. When the same temperature profile was used in the Micro-18, significant degradation (> 0.4%, w/w) was observed in the Micro-18. Therefore, a lower barrel temperature (60°C), which was the minimum temperature that GABA formulation could be granulated, was used in zones 2 through 5 to minimize GABA degradation in the Micro-18. The mean residence times of granules processed by the Nano-16 and the Micro-18 were between 17-45 seconds and 13-20 seconds, respectively.



### 5.4.2 Correlation between processing parameters and chemical stability of GABA granules. Nano-16 vs. Micro-18

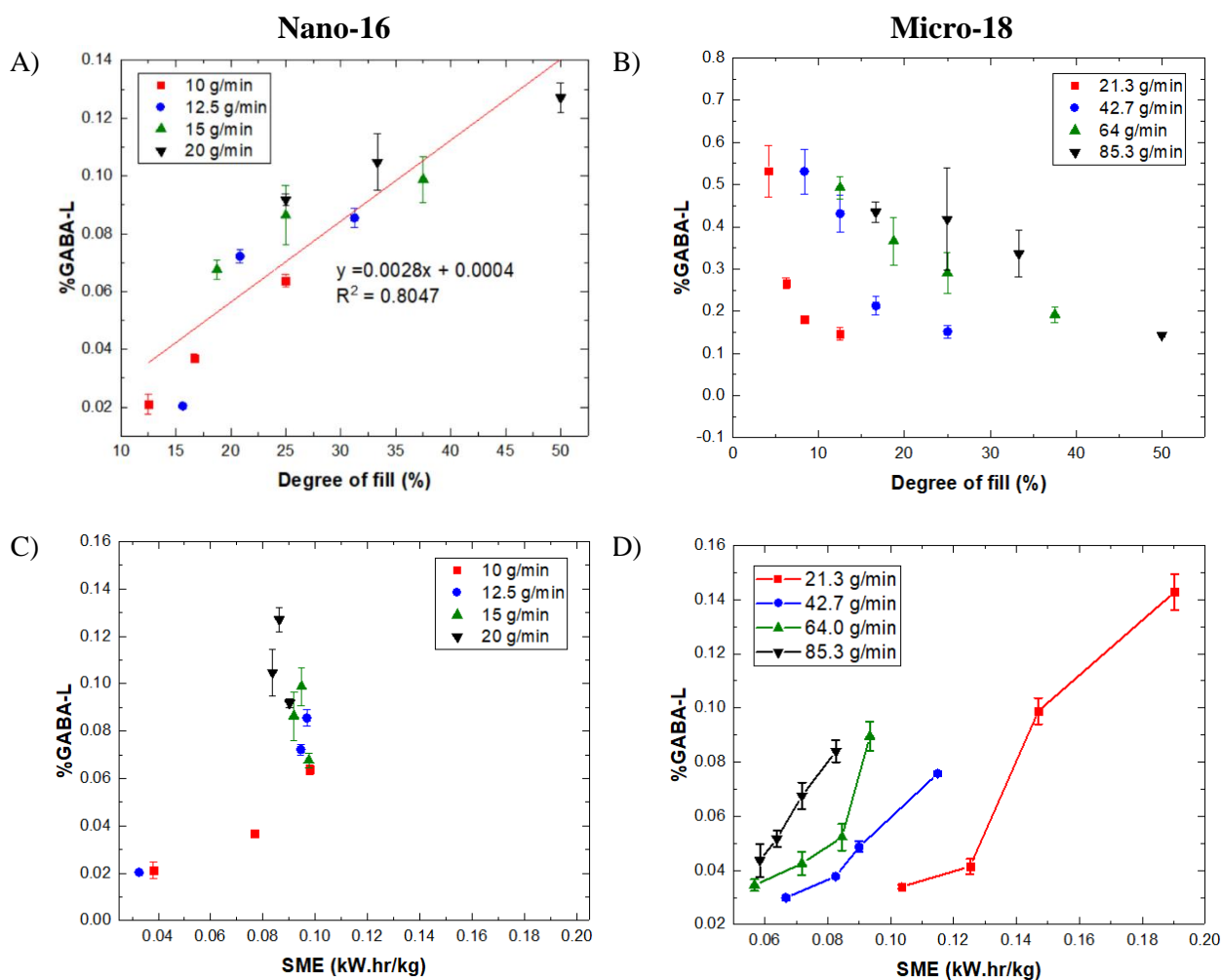


Figure 5.3 Correlation between (A and C) %GABA-L and Degree of fill, (B and D) %GABA-L and SME of GABA granules processed using Nano-16 and Micro-18.

Granulation of 80% GABA and 20% Klucel mixture in the Nano-16 could only occur at DF higher than 18% and high barrel temperatures ( $\geq 110^\circ\text{C}$ ), while granulation in the Micro-18 occurred at all DFs ranging from 4.2 to 50% and low barrel temperatures ( $60^\circ\text{C}$ ). One of the primary granule properties we focused on is GABA chemical stability. Gabapentin lactam (GABA-L) is the primary degradant of GABA. As illustrated in Figure 5.3A and Figure 5.3B, the correlation between GABA-L content and DF is opposite between the Nano-16 (positive) and

the Micro-18 (negative). Instead, GABA-L content of GABA granules prepared using the Micro-18 correlated positively with SME (Figure 5.3D) and granule temperature (Figure 5.4). There was no clear trend between GABA-L content and SME in Nano-16 (Figure 5.3C).

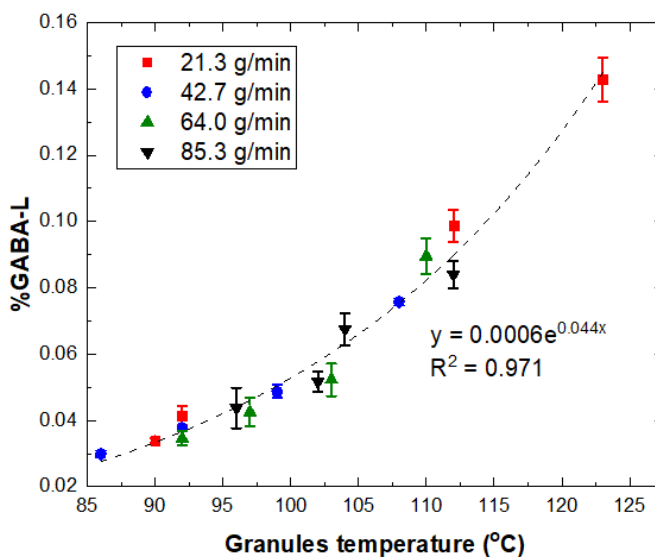


Figure 5.4 Correlation between degradant content and the temperature of GABA granules prepared using the Micro-18.

It was hypothesized that the observed difference in granulation behavior arises from differences in screw geometry (Table 5.1) between the Nano-16 and the Micro-18. The intensity of the mixing of kneading elements depends on screw geometry. A narrow overflight gap, a shallower channel, and a more aggressive stacking angle should all result in more intense dispersive mixing in the Nano-16. However, disc width plays a more dominant role in mixing. As the kneading disc becomes thicker, the more dispersive mixing it provides (Andersen, 2018). The width of the kneading disc in the Nano-16 (2.5 mm) is only half of that in Micro-18 (5 mm), leading to less-intensive dispersive mixing. As a result, a higher barrel temperature was required in the Nano-16 extruder to melt Klucel. Heat transfer between the barrel and processed material is needed to facilitate the melting of Klucel in Nano-16.

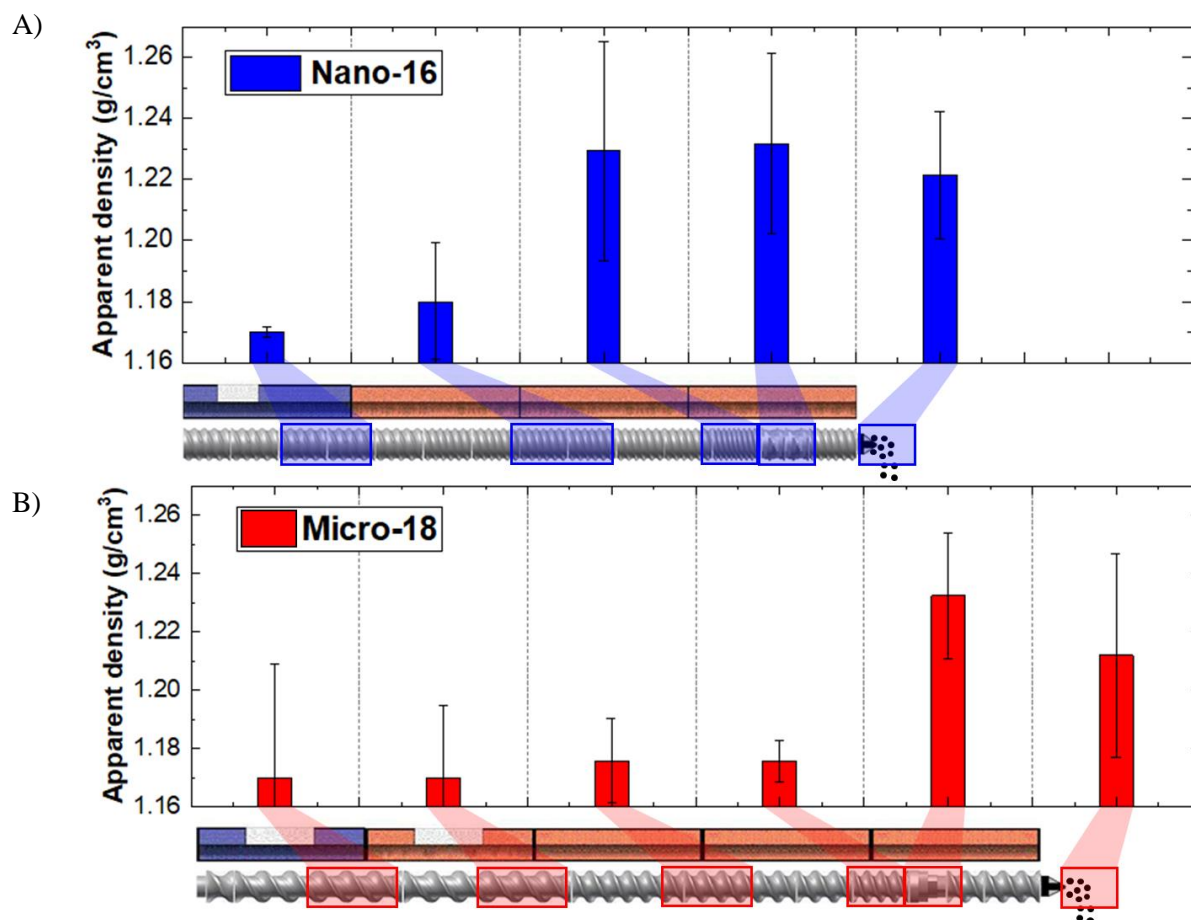


Figure 5.5 Apparent density of granules sampled along the barrel (A) Nano-16 (operated at the feed rate of 15 g/min, screw speed of 100 rpm) (B) Micro-18 (operated at the feed rate 64 g/min, screw speed of 100 rpm).

Additionally, higher DF was required in the Nano-16 to promote granulation by increasing the axial mixing and compression. The apparent density of formulation along the barrel is shown in Figure 5.5. The formulation density increased prior to kneading zone, indicating pre-granulation in the Nano-16. It was concluded that granule formation in the Nano-16 was largely due to axial compaction and heat conducted from the barrel. However, the higher the DF was, the greater the extent of shear stresses the material was exposed to. This led to breakage and amorphization of GABA crystals (Kittikunakorn, N., Sun, C. C., et al., 2019). As a result, the degradation of gabapentin correlated positively to DF.

In comparison, granulation in the Micro-18 only occurred at the kneading element. As shown in Figure 5.5, the formulation remained in powder form and was heated to 52-57°C prior to entering the kneading element. The melting of Klucel and granulation were all attributed to the viscous heat dissipation at the kneading element. The energy input by the kneading element is defined by SME. SME represents the amount of power generated by the screw and transferred into each unit of mass of the material (Repka, Langley, & DiNunzio, 2013). SME is calculated using the equation (Martin, 2013a):

$$SME = \frac{kW (motor\ rating) \times \%Torque \times \frac{RPM\ running}{max\ RPM} \times 0.97 (gear\ efficiency)}{Feed\ rate\ (\frac{kg}{hr})} \quad \text{Equation 5.5}$$

The higher the SME and granule temperature were, the higher the GABA-L content was. The correlation between degradant level and SME in the Micro-18 is similar to that for hot-melt extrusion of amorphous solid dispersion (Haser, Abbe, Huang, Siyuan, Listro, Tony, White, David, & Zhang, Feng, 2017b). The positive correlation between GABA-L content and SME in Micro-18 was observed at all powder feed rates (Figure 5.3D). As screw speed increased from 100 to 300 rpm, the GABA-L content increased. However, an offset between four feed rates was apparent. As a result, the granules processed at the same SME but different feed rate exhibited different degradation content. This phenomenon was investigated, and the results are presented in the following section.

#### 5.4.3 Offset between Degradant Content-SME Profiles at Different Feed Rates for the Micro-18

The offset in the degradant content-SME profiles was hypothesized to be due to the different heat loss to the barrel as the result of the different residence times. Energy transfer during the extrusion process relates to the physicochemical transformation of the material (Godavarti & Karwe, 1997). The schematic diagram of the energy flows in a melt granulation process is illustrated in Figure 5.6 and the energy balance can be written as follows:

$$SME = Q + \Delta H \quad \text{Equation 5.6}$$

where SME is specific mechanical energy,  $Q$  is the amount of heat transfer between formulation and barrel, and  $\Delta H$  is the enthalpy difference between the material entering and exiting the zone 5 of the barrel.

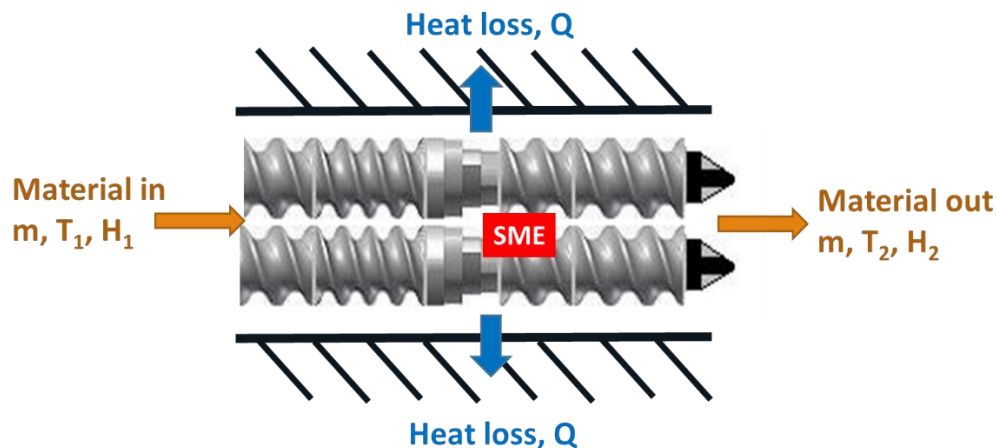


Figure 5.6 Schematic diagram showing the energy balance at zone 5 (kneading zone).

$Q$  is a function of the temperature differential between the material and barrel and the residence time of the material. The barrel temperature was set at 60 °C to minimize the degradation during melt granulation. Due to the dispersive mixing of kneading element, the temperature of GABA granules ranged from 86 to 123°C, significantly higher than the barrel temperature. Therefore, heat transfer from the granules to the barrel was anticipated. Varying the feed rate affects the residence time of material in the filled region where the kneading elements were located.

To further assess our hypothesis, the amount of heat loss during the melt granulation process was determined using two different methods: (1) a thermodynamic method and (2) a heat transfer method.

In the thermodynamic method, the heat loss was calculated based on an energy balance of the TSMG process. The energy input is equivalent to specific mechanical energy (SME) The energy outflow is equivalent to the sum of the heat transferred to the barrel and the enthalpy difference between the granules and feed powder (Godavarti & Karwe, 1997).  $\Delta H$  was measured using solution calorimetry (Figure 5.2B) and DSC (Alin et al., 2018). Therefore, the amount of heat loss ( $Q$ ) can be calculated from the difference between SME and  $\Delta H$ .

In the heat transfer method, Q was measured directly from barrel heating following the shut off of the cooling water. Initially, the TSMG was run at the barrel temperature of 60°C with cooling water turned on. After the system reached steady state, the water cooling system was shut off. With the extruder still running, the increase in barrel temperature at zone 5 (the where kneading element is positioned) was recorded at 5 min. The heat loss to the barrel was calculated using the following equation:

$$\text{Heat loss (J/g)} = \frac{\Delta T \times C_p \text{ (J/}^\circ\text{C} \cdot \text{kg)} \times M \text{ (kg)}}{\text{Feed rate (g/min)} \times \text{time (min)}} \quad \text{Equation 5.6}$$

where  $\Delta T$  is the temperature difference,  $C_p$  is the heat capacity of the barrel (440C stainless steel), and M is mass of the barrel.

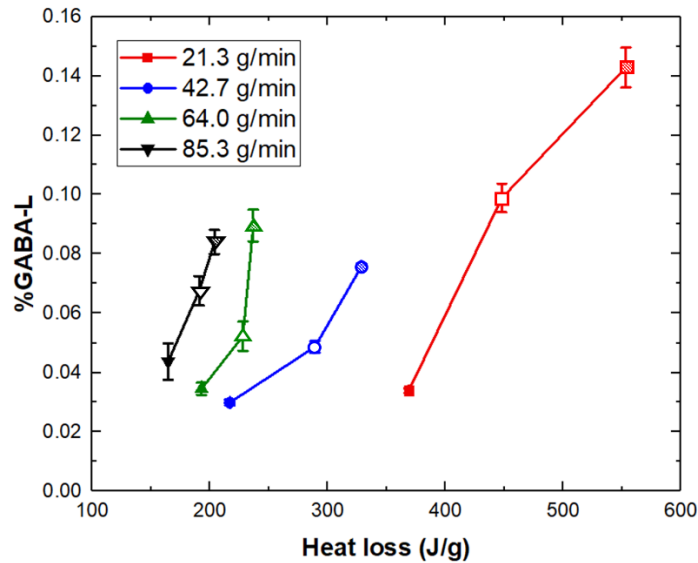


Figure 5.7 Amount of heat loss to the barrel during granulation process at various feed rates calculated by heat transfer method. Each line represents each feed rate operated at screw speed of 100 rpm (■), 200 rpm (□), and 300 rpm (▣).

Figure 5.7 shows the measured heat loss at various feed rates calculated from the energy required to increase barrel temperature after turning off the cooling system (heat transfer method). Higher amounts of heat loss observed at low feed rates were due to a longer residence time in the kneading section, promoting the heat loss from the granules to the barrel. Once the heat loss to the barrel is accounted for, GABA-L content correlated positively to SME-Q or  $\Delta H$

across all processing conditions. SME-Q or  $\Delta H$  represents the total energy absorbed by the material (Figure 5.8). This result confirmed our hypothesis that the offset between SME and GABA-L content was due to the different amount of heat loss transferred to the barrel during TSMG process at different feed rate.

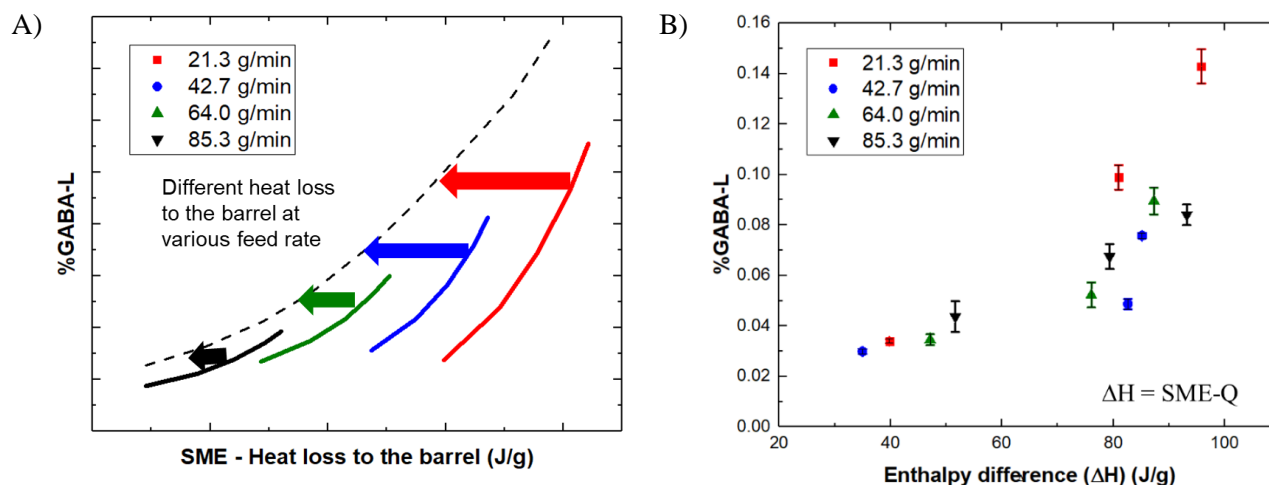


Figure 5.8 (A) The correlation between %GABA-L and specific mechanical energy (B) the correlation between %GABA-L and enthalpy difference between the material entering and exiting the barrel zone 5.

#### 5.4.4 Crystal form changes and particle size reduction of GABA

GABA consists of four polymorphic forms (Form I-IV). Its molecule contains an extensive H-bond between  $-\text{NH}_3^+$  and  $-\text{COO}^-$  groups and can easily form GABA-L via intramolecular cyclization (Braga et al., 2008). It was reported in our previous study that GABA underwent polymorphic transformation from the stable Form II to Form IV during TSMG with  $60^\circ$  kneading elements due to intensive high shear stress. (Kittikunakorn, N., Sun, C. C., et al., 2019). In this study, the polymorph transformation of GABA was investigated using FTIR (Hsu, C.-H., Ke, W.-T., & Lin, S.-Y., 2010). Polymorphic transformation of GABA was not observed for all melt-extruded granules prepared in this study (data was not presented).

However, due to high mechanical stresses during TSMG, the size reduction of GABA crystal was observed. In the Nano-16, the particle size reduction of GABA was dependent on DF. The higher DF was, the greater the reduction of GABA particle size was due to the compaction force generated from the material packing at high DF. The initial particle size ( $D_{50}$ )

of GABA is around 70  $\mu\text{m}$ . At low DF (less than 20%),  $D_{50}$  of GABA did not change. However, at higher DF,  $D_{50}$  of GABA decreased to 10-20  $\mu\text{m}$ . Above 20% DF, the threshold of crystal strength was reached, and there was no further decrease in GABA particle size. On the other hand, the reduction of GABA  $D_{50}$  was observed ( $D_{50}$  is between 10-20  $\mu\text{m}$ ) in all granules produced from the Micro-18 regardless of DF or SME. This indicated the high mixing efficiency of the kneading element in Micro-18, as compared to Nano-16 which relied on the high compaction force at high DF for granulation formation. The size reduction of GABA crystals generated the crystal defect or amorphous content in the melt-extruded granules, which subsequently accelerated the degradation of GABA.

#### **5.4.5 Physical properties of granules, Nano-16 vs. Micro-18**

The difference of granule formation mechanism between the Nano-16 and the Micro-18 also affected the shape and tabletability of GABA granules.

##### **5.4.5.1 Granule shape**

As discussed in the previous section, the granulation mechanisms between the Nano-16 and the Micro-18 are different. Granulation in the Nano-16 is dependent on the heating by the barrel and axial compaction. High DF is required to facilitate granule growth by improving Klucel melting and interactions between GABA and Klucel. As shown in Figure 5.9, enlargement of granules was observed when operated at low screw speed (high DF) in the Nano-16. Fragmentation of granules occurred at higher screw speeds. Higher screw speeds led to lower DF as there is not enough material to be compacted to form granules. Therefore, smaller granules and fines were generated.

In contrast, elongated granule shapes were observed in the Micro-18. With the increase in screw speed from 100 to 300 rpm, the granules became even more elongated, as indicated by the decrease of aspect ratio from 0.570 to 0.245. Unlike Nano-16, granule formation in the Micro-18 occurred predominately via dispersive mixing of the kneading block, due to the restricted heat transfer from the barrel and the high efficiency of the dispersive mixing of kneading element. At higher screw speeds, the material was subjected to higher shear rate and higher SME. As a result, the formation of elongated granules was observed following the granulation. Similar results were observed by Thompson and O'Donnell in which the noodle-like extended shape of lactose



granules were produced with increasing screw speeds. They hypothesized that this noodle-like shape of granules occurred by the rolling effect when the material was rolled at the interface between screw flight and the barrel surface which often arose after the material came out of the kneading element (Thompson & O'Donnell, 2015).

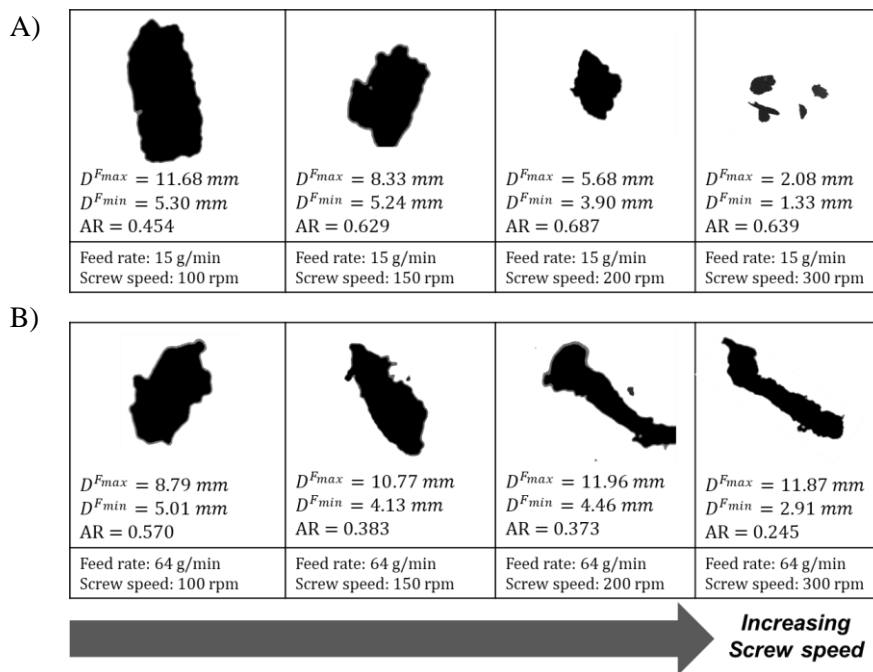


Figure 5.9 Images of melt-extruded granules processed with (A) Nano-16 extruder at given feed rate of 15 g/min and (B) Micro-18 extruder at the feed rate of 64 g/min with increasing screw speed (100, 150, 200, 300 rpm). \*AR is aspect ratio,  $D^{Fmax}$  is maximum diameter, and  $D^{Fmin}$  is minimum diameter.

#### 5.4.5.2 Tableability of GABA granules

One of the primary objectives of granulation is to improve the tableability of GABA by surface modification (Steffens & Wagner, 2019b). In our previous study, it was demonstrated that the improved tableability of GABA was due to the enrichment of Klucel on GABA surface using Time-of-flight secondary ion mass spectrometry (ToF-SIMS) (Kittikunakorn, Nada et al., 2019).

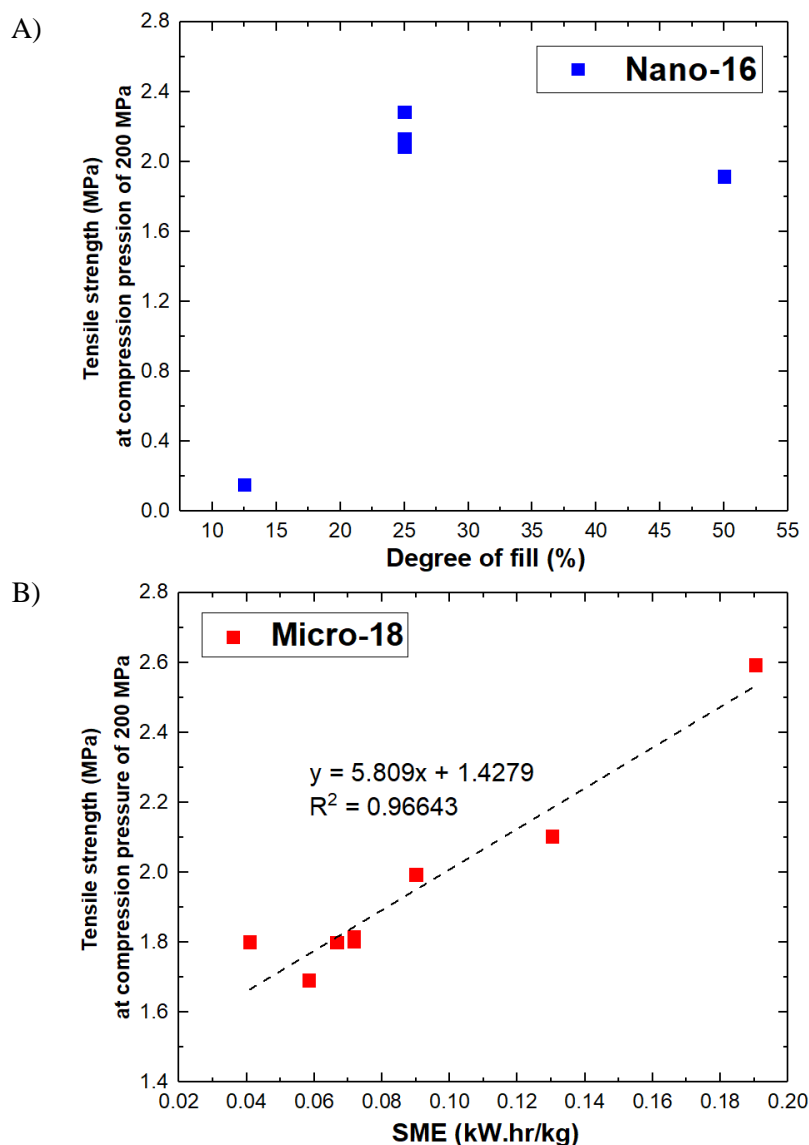


Figure 5.10 Correlation between process parameter and tensile strength of melt-extruded GABA tablets containing granules processed with (A) Nano-16 (B) Micro-18.

Differences in screw geometry between the Nano-16 and the Micro-18 also affected the correlation between processing parameters and the tabletability. In the Nano-16, DF is the critical parameter affecting the granules' tabletability. A minimal 15% DF was required to achieve 2MPa tensile strength, which is considered to be the target value for tableting (Osei-Yeboah, Frederick & Sun, Changquan Calvin, 2015). Further increase in DF up to 50% did not

significantly improve the tabletability (Figure 5.10A). The improved tabletability of granules can be explained by the granule formation mechanism. In the Nano-16, pre-granulation occurs even before the kneading section which is due to efficient heat transfer from the barrel that results in softening the Klucel. Consequently, high compaction force, which was a result of high DF, facilitates the spreading of Klucel on the GABA crystal surface, leading to improved tabletability. However, once the threshold DF was reached, the tabletability improvement was quite robust.

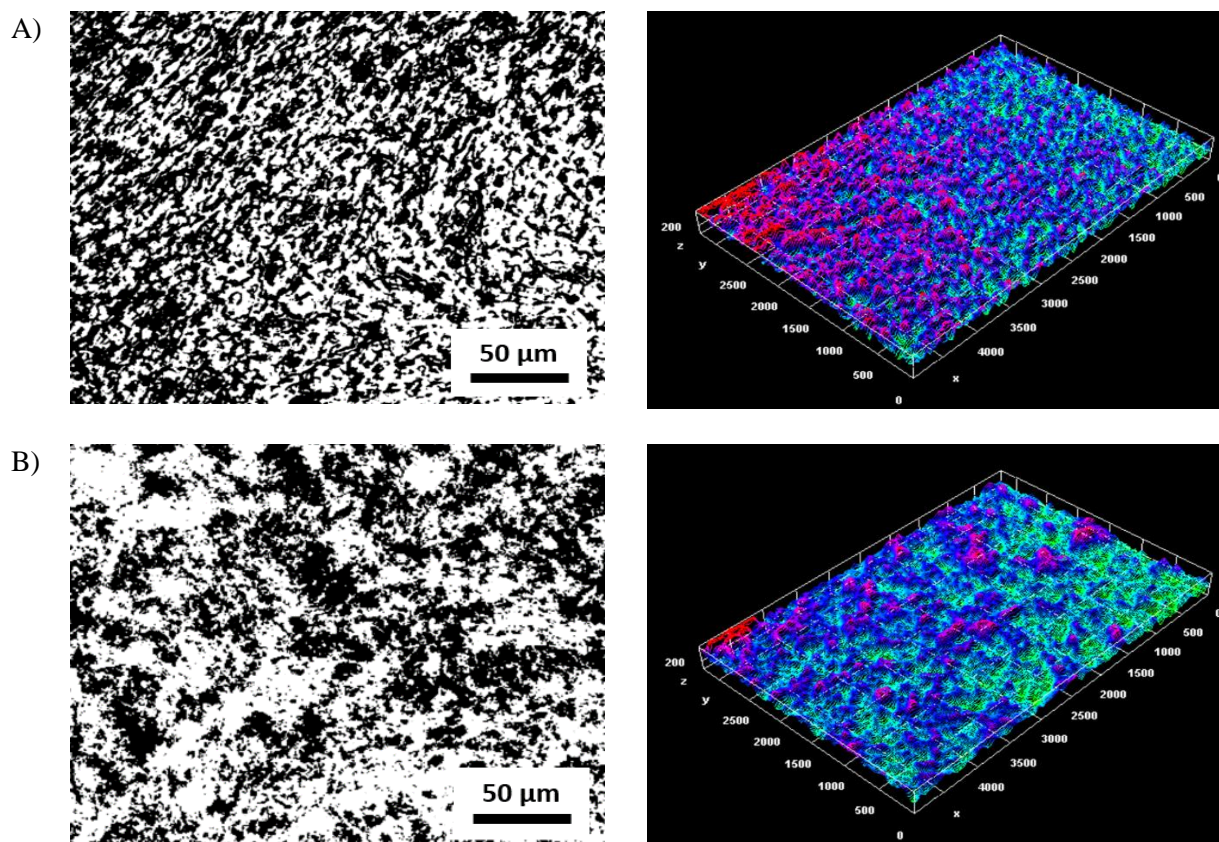


Figure 5.11 Binder distribution of melt-extruded GABA granules processed with Micro-18 at (A) high SME (0.18 kW.hr/kg, Run F16 in Table 5.2) and (B) low SME (0.06 kW.hr/kg, Run F25 in Table 5.2).

Improvement in the tabletability of GABA granules prepared using the Micro-18 was achieved under all conditions. Higher SME corresponded to better tabletability (Figure 5.10B). This was attributed to the granulation mechanism dominated by the dispersive mixing of

kneading blocks. Higher SME generated more mechanical energy to facilitate the Klucel spreading on the surface of GABA crystals. Distribution patterns of Klucel in GABA granules processed at the highest (F16) and the lowest (F25) SME are presented in Figure 5.11. Granules were dispersed into the 20% sodium chloride solution in which GABA can be freely dissolved but Klucel cannot be dissolved. The remaining scaffold of Klucel was analyzed using phase-contrast mode microscopy, and the data were processed and plotted using Image J. The Klucel scaffold in GABA granule F16 illustrated the continuous connection of Klucel spreading which attributed to the better improvement of tabletability. In contrast, the scaffold in GABA granule F25 showed discrete Klucel-rich and Klucel-poor phases, resulting in poor tabletability.

## **5.5 CONCLUSION**

The effect of the different screw geometries on the physicochemical properties of granules was investigated using Leistritz Nano-16 and Micro-18 extruders. The dissimilarity of these two extruders exhibits the different granulation mechanisms and different correlations between process parameters and granule properties. For Nano-16, DF was a critical parameter, where higher DF led to higher degradant levels and more compressible granules. For granules prepared using the Micro-18, SME was a critical parameter, where a higher SME led to higher degradant level and more compressible granules. The distinct behaviors call for close monitoring of both DF and SME to attain successful scale-up of TSMG from the Nano-16 to the Micro-18.

## 5.6 REFERENCES

- Alin, J., Setiawan, N., Defrese, M., DiNunzio, J., Lau, H., Lupton, L., . . . Marsac, P. J. (2018). A novel approach for measuring room temperature enthalpy of mixing and associated solubility estimation of a drug in a polymer matrix. *Polymer*, 135, 50-60. doi:<https://doi.org/10.1016/j.polymer.2017.11.056>
- Andersen, P. G. (2018). *Fundamentals Of Twin-Screw Compounding: Kneading Block Performance Characteristics*. Paper presented at the SPE International Conference.
- Batra, A., Desai, D., & Serajuddin, A. T. (2017). Investigating the Use of Polymeric Binders in Twin Screw Melt Granulation Process for Improving Compactibility of Drugs. *J Pharm Sci*, 106(1), 140-150. doi:10.1016/j.xphs.2016.07.014
- Braga, D., Grepioni, F., Maini, L., Rubini, K., Polito, M., Brescello, R., . . . Piedade, M. F. M. (2008). Polymorphic gabapentin: thermal behaviour, reactivity and interconversion of forms in solution and solid-state. *New Journal of Chemistry*, 32(10), 1788-1795. doi:10.1039/b809662g
- Djuric, D., Van Melkebeke, B., Kleinebudde, P., Remon, J. P., & Vervaet, C. (2009). Comparison of two twin-screw extruders for continuous granulation. *European Journal of Pharmaceutics and Biopharmaceutics*, 71(1), 155-160. doi:10.1016/j.ejpb.2008.06.033
- Fell, J. T., & Newton, J. M. (1970). Determination of Tablet Strength by the Diametral-Compression Test. *Journal of Pharmaceutical Sciences*, 59(5), 688-691. doi:<https://doi.org/10.1002/jps.2600590523>
- Ghebre-Sellassie, I., Mollan, M. J., Pathak, N., Lodaya, M., & Fessehaie, M. (2002). U.S. Patent 2304392A.
- Godavarti, S., & Karwe, M. V. (1997). Determination of Specific Mechanical Energy Distribution on a Twin-Screw Extruder. *Journal of Agricultural Engineering Research*, 67(4), 277-287. doi:<https://doi.org/10.1006/jaer.1997.0172>
- Haser, A., Huang, S., Listro, T., White, D., & Zhang, F. (2017b). An approach for chemical stability during melt extrusion of a drug substance with a high melting point. *International Journal of Pharmaceutics*, 524(1), 55-64. doi:<https://doi.org/10.1016/j.ijpharm.2017.03.070>
- Hsu, C.-H., Ke, W.-T., & Lin, S.-Y. (2010). Progressive Steps of Polymorphic Transformation of Gabapentin Polymorphs Studied by Hot-stage FTIR Microspectroscopy. 13(1). doi:10.18433/J3FS32
- Jagdale, S., Kuchekar, B., Satapathy, J., & Chabukswar, A. (2010b). Pharmaceutical equivalence of gabapentin tablets with various extragranular binders. *Journal of Basic and Applied Pharmaceutical Sciences Rev Ciênc Farm Básica Apl*, 31.
- Kittikunakorn, N., Koleng, J. J., Listro, T., Calvin Sun, C., & Zhang, F. (2019). Effects of thermal binders on chemical stabilities and tabletability of gabapentin granules prepared by twin-screw melt granulation. *International Journal of Pharmaceutics*, 559, 37-47. doi:<https://doi.org/10.1016/j.ijpharm.2019.01.014>
- Kittikunakorn, N., Sun, C. C., & Zhang, F. (2019). Effect of screw profile and processing conditions on physical transformation and chemical degradation of gabapentin during twin-screw melt granulation. *European Journal of Pharmaceutical Sciences*, 131, 243-253. doi:<https://doi.org/10.1016/j.ejps.2019.02.024>

- Lakshman, J. P., Kowalski, J., Vasanthavada, M., Tong, W. Q., Joshi, Y. M., & Serajuddin, A. T. (2011a). Application of melt granulation technology to enhance tableting properties of poorly compactible high-dose drugs. *J Pharm Sci*, 100(4), 1553-1565. doi:10.1002/jps.22369
- Lin, S.-Y., Hsu, C.-H., & Ke, W.-T. (2010). Solid-state transformation of different gabapentin polymorphs upon milling and co-milling. *International Journal of Pharmaceutics*, 396(1-2), 83-90. doi:10.1016/j.ijpharm.2010.06.014
- Martin, C. (2013a). Twin Screw Extrusion for Pharmaceutical Processes. 47-79. doi:10.1007/978-1-4614-8432-5\_2
- Osei-Yeboah, F., & Sun, C. C. (2015). Validation and applications of an expedited tablet friability method. *International Journal of Pharmaceutics*, 484(1), 146-155. doi:<https://doi.org/10.1016/j.ijpharm.2015.02.061>
- Pandey, P., & Badawy, S. I. F. (2019). Chapter 18 - A Quality By Design Approach to Scale-Up of High Shear Wet Granulation Process. In A. S. Narang & S. I. F. Badawy (Eds.), *Handbook of Pharmaceutical Wet Granulation* (pp. 615-650): Academic Press.
- Parikh, D. M. (2005). *Handbook of Pharmaceutical Granulation Technology* (Vol. 154). Hoboken: Informa Healthcare.
- Picker-Freyer, K. M., & Dürig, T. (2007). Physical mechanical and tablet formation properties of hydroxypropylcellulose: In pure form and in mixtures. *AAPS PharmSciTech*, 8(4), 82. doi:10.1208/pt0804092
- Rauwendaal, C. (2016). Heat transfer in twin screw compounding extruders. *AIP Conference Proceedings*, 1779(1), 030014. doi:10.1063/1.4965484
- Reece, H. A., & Levendis, D. C. (2008). Polymorphs of gabapentin. *Acta Crystallographica Section C*, 64(3), o105-o108. doi:10.1107/S0108270107066279
- Repka, M. A., Langley, N., & DiNunzio, J. (2013). *Melt Extrusion: Materials, Technology and Drug Product Design* (1;2013; ed. Vol. 9). Dordrecht: Springer.
- Rials, T. G., & Glasser, W. G. (1988). Thermal and dynamic mechanical properties of hydroxypropyl cellulose films. *Journal of Applied Polymer Science*, 36(4), 749-758. doi:10.1002/app.1988.070360402
- Steffens, K. E., & Wagner, K. G. (2019b). Improvement of tabletability via twin-screw melt granulation: Focus on binder distribution. *International Journal of Pharmaceutics*, 570, 118649. doi:<https://doi.org/10.1016/j.ijpharm.2019.118649>
- Thompson, M. R., & O'Donnell, K. P. (2015). "Rolling" phenomenon in twin screw granulation with controlled-release excipients. *Drug Development and Industrial Pharmacy*, 41(3), 482-492. doi:10.3109/03639045.2013.879723
- Tinmanee, R., Stamatis, S., Ueyama, E., Morris, K., & Kirsch, L. (2018). Polymorphic and Covalent Transformations of Gabapentin in Binary Excipient Mixtures after Milling-Induced Stress. *Pharmaceutical Research*, 35(2), 1-12. doi:10.1007/s11095-017-2285-1
- Todd, D. B. (1998a). *Plastics compounding : equipment and processing*: Hanser Publishers.
- Webb, P. A. (2001). Volume and Density Determinations for Particle Technologists *Micromeritics Instrument Corp.*
- Zong, Z., Qiu, J., Tinmanee, R., & Kirsch, L. E. (2012). Kinetic model for solid-state degradation of gabapentin. *Journal of Pharmaceutical Sciences*, 101(6), 2123-2133. doi:10.1002/jps.23115



## Bibliography

- Adrjanowicz, K., Kaminski, K., Grzybowska, K., Hawelek, L., Paluch, M., Gruszka, I., . . . Guzik, L. (2011). Effect of cryogrinding on chemical stability of the sparingly water-soluble drug furosemide. *Pharm Res*, 28(12), 3220-3236. doi:10.1007/s11095-011-0496-4
- Alexis, F. (2005). Factors affecting the degradation and drug-release mechanism of poly(lactic acid) and poly[(lactic acid)-co-(glycolic acid)]. *Polymer International*, 54, 36-46. doi:10.1002/pi.1697
- Alin, J., Setiawan, N., Defrese, M., DiNunzio, J., Lau, H., Lupton, L., . . . Marsac, P. J. (2018). A novel approach for measuring room temperature enthalpy of mixing and associated solubility estimation of a drug in a polymer matrix. *Polymer*, 135, 50-60. doi:<https://doi.org/10.1016/j.polymer.2017.11.056>
- Andersen, P. G. (2018). *Fundamentals Of Twin-Screw Compounding: Kneading Block Performance Characteristics*. Paper presented at the SPE International Conference.
- Balakrishnan, N., Dryer, B., & Bigio, D. (2017). *Validation of residence stress distribution approach using 1-D computer simulations*. Paper presented at the SPE ANTEC, Anaheim.
- Batra, A., Desai, D., & Serajuddin, A. T. (2017). Investigating the Use of Polymeric Binders in Twin Screw Melt Granulation Process for Improving Compactibility of Drugs. *J Pharm Sci*, 106(1), 140-150. doi:10.1016/j.xphs.2016.07.014
- Braga, D., Grepioni, F., Maini, L., Rubini, K., Polito, M., Brescello, R., . . . Piedade, M. F. M. (2008). Polymorphic gabapentin: thermal behaviour, reactivity and interconversion of forms in solution and solid-state. *New Journal of Chemistry*, 32(10), 1788-1795. doi:10.1039/b809662g
- Burggraef, A., Van Den Kerkhof, T., Hellings, M., Remon, J. P., Vervaet, C., & De Beer, T. (2010). Evaluation of in-line spatial filter velocimetry as PAT monitoring tool for particle growth during fluid bed granulation. *European Journal of Pharmaceutics and Biopharmaceutics*, 76(1). doi:10.1016/j.ejpb.2010.06.001
- Cartwright, J. J., Robertson, J., D'Haene, D., Burke, M. D., & Hennenkamp, J. R. (2013). Twin screw wet granulation: Loss in weight feeding of a poorly flowing active pharmaceutical ingredient. *Powder Technology*, 238, 116-121. doi:<https://doi.org/10.1016/j.powtec.2012.04.034>
- Chen, B., Zhu, L., Zhang, F., & Qiu, Y. (2016). Process Development and Scale-Up Twin-Screw Extrusion. In Y. Qiu, Y. Chen, G. G. Z. Zhang, L. Yu, & R. V. Mantri (Eds.), *Developing Solid Oral Dosage Forms: Pharmaceutical Theory and Practice* (Second;2;2nd; ed.). US: Academic Press.
- Dhenge, R. M., Cartwright, J. J., Hounslow, M. J., & Salman, A. D. (2012a). Twin screw granulation: Steps in granule growth. *International Journal of Pharmaceutics*, 438(1), 20-32. doi:<https://doi.org/10.1016/j.ijpharm.2012.08.049>

- Dhenge, R. M., Cartwright, J. J., Hounslow, M. J., & Salman, A. D. (2012b). Twin screw wet granulation: Effects of properties of granulation liquid. *Powder Technology*, 229(Supplement C), 126-136. doi:<https://doi.org/10.1016/j.powtec.2012.06.019>
- Dhenge, R. M., Fyles, R. S., Cartwright, J. J., Doughty, D. G., Hounslow, M. J., & Salman, A. D. (2010). Twin screw wet granulation: Granule properties. *Chemical Engineering Journal*, 164(2), 322-329. doi:<https://doi.org/10.1016/j.cej.2010.05.023>
- DiNunzio, J. C., Zhang, F., Martin, C., & McGinity, J. W. (2012). Melt extrusion. In R. O. Williams Iii, A. B. Watts, & D. A. Miller (Eds.), *Formulating Poorly Water Soluble Drugs* (1. ed.). New York, NY: AAPS Advances in the Pharmaceutical Sciences, Springer New York.
- Djuric, D. (2008). *Continuous Granulation with a Twin-Screw Extruder* (Vol. 1): Cuvillier Verlag.
- Djuric, D., & Kleinebudde, P. (2008). Impact of screw elements on continuous granulation with a twin-screw extruder. *Journal of Pharmaceutical Sciences*, 97(11), 4934-4942. doi:10.1002/jps.21339
- Djuric, D., Van Melkebeke, B., Kleinebudde, P., Remon, J. P., & Vervaet, C. (2009). Comparison of two twin-screw extruders for continuous granulation. *European Journal of Pharmaceutics and Biopharmaceutics*, 71(1), 155-160. doi:10.1016/j.ejpb.2008.06.033
- Dombe, G., Mehilal, Bhongale, C., Singh, P. P., & Bhattacharya, B. (2015). Application of Twin Screw Extrusion for Continuous Processing of Energetic Materials. *Central European Journal of Energetic Materials*, 12(3), 507-522.
- Douroumis, D. (2012). *Hot-melt extrusion pharmaceutical applications*. Chichester, West Sussex, U.K: Wiley.
- Ennis, B. J. (2010). Theory of Granulation: An Engineering Perspective. In D. M. Parikh. (Ed.), *Handbook of pharmaceutical granulation technology* (Vol. 3): New York : Informa Healthcare USA.
- Fell, J. T., & Newton, J. M. (1970). Determination of Tablet Strength by the Diametral-Compression Test. *Journal of Pharmaceutical Sciences*, 59(5), 688-691. doi:<https://doi.org/10.1002/jps.2600590523>
- Fonteyne, M., Soares, S., Vercruysse, J., Peeters, E., Burggraeve, A., Vervaet, C., . . . De Beer, T. (2012). Prediction of quality attributes of continuously produced granules using complementary pat tools. *European Journal of Pharmaceutics and Biopharmaceutics*, 82(2), 429-436. doi:10.1016/j.ejpb.2012.07.017
- Fonteyne, M., Vercruysse, J., De Leersnyder, F., Besseling, R., Gerich, A., Oostra, W., . . . De Beer, T. (2016). Blend uniformity evaluation during continuous mixing in a twin screw granulator by in-line NIR using a moving F-test. *Analytica Chimica Acta*, 935, 213-223. doi:<https://doi.org/10.1016/j.aca.2016.07.020>
- Fukuoka, E., Makita, M., & Yamamura, S. (1986). Some physicochemical properties of glassy indomethacin. *Chem Pharm Bull (Tokyo)*, 34(10), 4314-4321.
- Furudate, T., Kurasako, Y., Takata, E., Morishita, T., Miwa, A., Suzuki, R., & Terada, K. (2015). Possibility of monitoring granulation by analyzing the amount of hydroxypropylcellulose, a binder on the surface of granules, using ToF-SIMS.



- International Journal of Pharmaceutics*, 495(2), 642-650. doi:10.1016/j.ijpharm.2015.09.060
- Gamlen, M. J., & Eardley, C. (1986). Continuous Extrusion Using a Raker Perkins MP50 (Multipurpose) Extruder. *Drug Development and Industrial Pharmacy*, 12(11-13), 1701-1713. doi:10.3109/03639048609042604
- Ghebre-Sellassie, I., Martin, C. E., Zhang, F., & Dinunzio, J. (2018). *Pharmaceutical extrusion technology* (2 ed. Vol. 217). Boca Raton, Florida :: CRC Press.
- Ghebre-Sellassie, I., Matthew J. Mollan, J., Pathak, N., Lodaya, M., & Fessehaie, M. (2002). U.S. Patent 2304392A.
- Ghebre-Sellassie, I., Mollan, M. J., Pathak, N., Lodaya, M., & Fessehaie, M. (2002). U.S. Patent 2304392A.
- Giles, H. F. (2005). *Extrusion : the definitive processing guide and handbook / by Harold F. Giles, Jr., John R. Wagner, Jr., Eldridge M. Mount, III*. Norwich, NY: William Andrew Pub.
- Godavarti, S., & Karwe, M. V. (1997). Determination of Specific Mechanical Energy Distribution on a Twin-Screw Extruder. *Journal of Agricultural Engineering Research*, 67(4), 277-287. doi:<https://doi.org/10.1006/jaer.1997.0172>
- Grymonpré, W., De Jaeghere, W., Peeters, E., Adriaenssens, P., Remon, J. P., & Vervaet, C. (2016). The impact of hot-melt extrusion on the tableting behaviour of polyvinyl alcohol. *International Journal of Pharmaceutics*, 498(1-2). doi:10.1016/j.ijpharm.2015.12.020
- Grymonpré, W., Verstraete, G., Vanhoorne, V., Remon, J. P., De Beer, T., & Vervaet, C. (2017). Downstream processing from melt granulation towards tablets : in-depth analysis of a continuous twin-screw melt granulation process using polymeric binders. *European Journal of Pharmaceutics and Biopharmaceutics*, 124. doi:10.1016/j.ejpb.2017.12.005
- Harting, J., & Kleinebudde, P. (2018). Development of an in-line Raman spectroscopic method for continuous API quantification during twin-screw wet granulation. *European Journal of Pharmaceutics and Biopharmaceutics*, 125, 169-181. doi:<https://doi.org/10.1016/j.ejpb.2018.01.015>
- Haser, A., Haight, B., Berghaus, A., Machado, A., Martin, C., & Zhang, F. (2018). Scale-Up and In-line Monitoring During Continuous Melt Extrusion of an Amorphous Solid Dispersion. *AAPS PharmSciTech*, 19(7), 2818-2827. doi:10.1208/s12249-018-1162-5
- Haser, A., Huang, S., Listro, T., White, D., & Zhang, F. (2017). An approach for chemical stability during melt extrusion of a drug substance with a high melting point. *Int J Pharm*, 524(1-2), 55-64. doi:10.1016/j.ijpharm.2017.03.070
- Haser, A., & Zhang, F. (2018). New Strategies for Improving the Development and Performance of Amorphous Solid Dispersions. *AAPS PharmSciTech*, 19(3), 978-990. doi:10.1208/s12249-018-0953-z
- Hou, H. H., Rajesh, A., Pandya, K. M., Lubach, J. W., Muliadi, A., Yost, E., . . . Nagapudi, K. (2019). Impact of Method of Preparation of Amorphous Solid Dispersions on Mechanical Properties: Comparison of Coprecipitation and Spray

- Drying. *Journal of Pharmaceutical Sciences*, 108(2), 870-879. doi:<https://doi.org/10.1016/j.xphs.2018.09.008>
- Hsu, C. H., Ke, W. T., & Lin, S. Y. (2010). Progressive steps of polymorphic transformation of gabapentin polymorphs studied by hot-stage FTIR microspectroscopy. *Journal of Pharmacy and Pharmaceutical Sciences*, 13(1), 67-77.
- Huang, S., Mao, C., Williams, R. O., & Yang, C.-Y. (2016). Solubility Advantage (and Disadvantage) of Pharmaceutical Amorphous Solid Dispersions. *Journal of Pharmaceutical Sciences*, 105(12), 3549-3561. doi:10.1016/j.xphs.2016.08.017
- Iveson, S. M., Litster, J. D., & Ennis, B. J. (1996). Fundamental studies of granule consolidation Part 1: Effects of binder content and binder viscosity. *Powder Technology*, 88(1), 15-20. doi:[https://doi.org/10.1016/0032-5910\(96\)03096-3](https://doi.org/10.1016/0032-5910(96)03096-3)
- Iveson, S. M., Litster, J. D., Hapgood, K., & Ennis, B. J. (2001). Nucleation, growth and breakage phenomena in agitated wet granulation processes: a review. *Powder Technology*, 117(1), 3-39. doi:[https://doi.org/10.1016/S0032-5910\(01\)00313-8](https://doi.org/10.1016/S0032-5910(01)00313-8)
- Jagdale, S., Kuchekar, B., Satapathy, J., & Chabukswar, A. (2010a). Pharmaceutical equivalence of gabapentin tablets with various extragranular binders. *Revista de Ciências Farmacêuticas Básica e Aplicada*, 31(1), 25-31.
- Jagdale, S., Kuchekar, B., Satapathy, J., & Chabukswar, A. (2010b). Pharmaceutical equivalence of gabapentin tablets with various extragranular binders. *Journal of Basic and Applied Pharmaceutical Sciences Rev Ciênc Farm Básica Apl*, 31.
- Keen, J. M., Foley, C. J., Hughey, J. R., Bennett, R. C., Jannin, V., Rosiaux, Y., . . . McGinity, J. W. (2015). Continuous twin screw melt granulation of glyceryl behenate: Development of controlled release tramadol hydrochloride tablets for improved safety. *Int J Pharm*, 487(1-2), 72-80. doi:10.1016/j.ijpharm.2015.03.058
- Keleb, E. I., Vermeire, A., Vervaet, C., & Remon, J. P. (2004). Extrusion Granulation and High Shear Granulation of Different Grades of Lactose and Highly Dosed Drugs: A Comparative Study. *Drug Development and Industrial Pharmacy*, 30(6), 679-691. doi:10.1081/DDC-120039338
- Kendall, K. (1978). The impossibility of comminuting small particles by compression. *Nature*, 272, 710. doi:10.1038/272710a0
- Kittikunakorn, N., DiNunzio, J., Martin, C., & Zhang, F. (2018). Processes, Challenges and Futures in Twin-screw Continuous Granulation for Manufacturing Oral Tablets and Capsules. *Cover article AAPS Newsmagazine*. 12-18, Mar 2018, 12-18.
- Kittikunakorn, N., DiNunzio, J. C., Martin, C., & Zhang, F. (2018). Processes, Challenges, and the Future of Twin-Screw Granulation for Manufacturing Oral Tablets and Capsules. *AAPS NewsMagazine*, Mar(Mar), 12-18.
- Kittikunakorn, N., Koleng, J. J., Listro, T., Calvin Sun, C., & Zhang, F. (2019). Effects of thermal binders on chemical stabilities and tabletability of gabapentin granules prepared by twin-screw melt granulation. *International Journal of Pharmaceutics*, 559, 37-47. doi:<https://doi.org/10.1016/j.ijpharm.2019.01.014>

- Kittikunakorn, N., Sun, C. C., & Zhang, F. (2019). Effect of screw profile and processing conditions on physical transformation and chemical degradation of gabapentin during twin-screw melt granulation. *European Journal of Pharmaceutical Sciences*, 131, 243-253. doi:<https://doi.org/10.1016/j.ejps.2019.02.024>
- Kowalski, J., Kalb, O., Joshi, Y. M., & Serajuddin, A. T. M. (2009). Application of melt granulation technology to enhance stability of a moisture sensitive immediate-release drug product. *International Journal of Pharmaceutics*, 381(1), 56-61. doi:<http://dx.doi.org/10.1016/j.ijpharm.2009.05.043>
- Kumar, A., Dhondt, J., De Leersnyder, F., Vercruyse, J., Vanhoorne, V., Vervae, C., . . . Nopens, I. (2015a). Evaluation of an in-line particle imaging tool for monitoring twin-screw granulation performance. *Powder Technology*, 285(Supplement C), 80-87. doi:<https://doi.org/10.1016/j.powtec.2015.05.031>
- Lakshman, J. P., Kowalski, J., Vasanthavada, M., Tong, W. Q., Joshi, Y. M., & Serajuddin, A. T. (2011a). Application of melt granulation technology to enhance tableting properties of poorly compactible high-dose drugs. *J Pharm Sci*, 100(4), 1553-1565. doi:10.1002/jps.22369
- Lee, S. (2017). Modernizing the Way Drugs Are Made: A Transition to Continuous Manufacturing. Retrieved from <https://www.fda.gov/Drugs/NewsEvents/ucm557448.htm>
- Lin, S.-Y., Hsu, C.-H., & Ke, W.-T. (2010). Solid-state transformation of different gabapentin polymorphs upon milling and co-milling. *International Journal of Pharmaceutics*, 396(1-2), 83-90. doi:10.1016/j.ijpharm.2010.06.014
- Lindberg, N. O., Tufvesson, C., Holm, P., & Olbjer, L. (1988). Extrusion of an Effervescent Granulation with a Twin Screw Extruder, Baker Perkins MPF 50 D. Influence on Intragranular Porosity and Liquid Saturation. *Drug Development and Industrial Pharmacy*, 14(13), 1791-1798. doi:10.3109/03639048809151987
- Liu, H., Ricart, B., Stanton, C., Smith-Goettler, B., Verdi, L., O'Connor, T., . . . Yoon, S. (2019). Design space determination and process optimization in at-scale continuous twin screw wet granulation. *Computers & Chemical Engineering*, 125. doi:10.1016/j.compchemeng.2019.03.026
- Liu, Y., Thompson, M. R., & O'Donnell, K. P. (2018). Impact of non-binder ingredients and molecular weight of polymer binders on heat assisted twin screw dry granulation. *International Journal of Pharmaceutics*, 536(1), 336-344. doi:10.1016/j.ijpharm.2017.11.061
- Lodaya, M., Mollan, M., & Ghebre-Sellassie, I. (2003). Twin-screw wet granulation. In I. Ghebre-Sellassie & C. Martin (Eds.), *Pharmaceutical Extrusion Technology* (pp. 323-344): CRC Press.
- Lodaya, M., & Thompson, M. (2018). Continuous Oral Solid Dose Manufacture. In I. Ghebre-Sellassie, C. Martin, F. Zhang, & J. DiNunzio (Eds.), *Pharmaceutical Extrusion Technology* (2 ed.): CRC Press.
- Madarász, L., Nagy, Z. K., Hoffer, I., Szabó, B., Csontos, I., Pataki, H., . . . Marosi, G. (2018). Real-time feedback control of twin-screw wet granulation based on image analysis. *International Journal of Pharmaceutics*, 547(1), 360-367. doi:<https://doi.org/10.1016/j.ijpharm.2018.06.003>

- Makoto, O., & Nobuyoshi, K. (1990). Effect of grinding on the crystallinity and chemical stability in the solid state of cephalothin sodium. *International Journal of Pharmaceutics*, 62(1), 65-73. doi:[https://doi.org/10.1016/0378-5173\(90\)90031-X](https://doi.org/10.1016/0378-5173(90)90031-X)
- Maniruzzaman, M., Islam, M. T., Moradiya, H. G., Halsey, S. A., Slipper, I. J., Chowdhry, B., . . . Douroumis, D. (2014). Prediction of Polymorphic Transformations of Paracetamol in Solid Dispersions. *Journal of Pharmaceutical Sciences*, 103(6), 1819-1828. doi:10.1002/jps.23992
- Markarian, J. (2017). Scaling up a continuous granulation process. *Pharmaceutical Technology*, 41, 30-31.
- Marsac, P. J., Li, T., & Taylor, L. S. (2009). Estimation of Drug–Polymer Miscibility and Solubility in Amorphous Solid Dispersions Using Experimentally Determined Interaction Parameters. *Pharmaceutical Research*, 26(1), 139-151. doi:10.1007/s11095-008-9721-1
- Martin, C. (2013b). Twin Screw Extrusion for Pharmaceutical Processes. In M. A. Repka, N. Langley, & J. DiNunzio (Eds.), *Melt Extrusion Materials, Technology and Drug Product Design*, AAPS Advances in the Pharmaceutical Sciences Series, 9 (1st ed. 2013. ed., pp. 47-79). New York, NY: Springer New York.
- Martin, C. (2016). Twin Screw Extruders as Continuous Mixers for Thermal Processing: a Technical and Historical Perspective. *AAPS PharmSciTech*, 17(1), 3-19. doi:10.1208/s12249-016-0485-3
- Miller, R. W. (2005). Roller Compaction Technology. In D. M. Parikh (Ed.), *Handbook of Pharmaceutical Granulation Technology* (2 ed., pp. 159-190): CRC Press.
- Monteyne, T., Adriaenssens, P., Brouckaert, D., Remon, J. P., Vervaet, C., & De Beer, T. (2016). Stearic acid and high molecular weight PEO as matrix for the highly water soluble metoprolol tartrate in continuous twin-screw melt granulation. *Int J Pharm*, 512(1), 158-167. doi:10.1016/j.ijpharm.2016.07.035
- Monteyne, T., Heeze, L., Mortier, S. T., Oldorp, K., Cardinaels, R., Nopens, I., . . . De Beer, T. (2016). The use of rheology to elucidate the granulation mechanisms of a miscible and immiscible system during continuous twin-screw melt granulation. *Pharmaceutical Research*, 33(10), 2481-2494.
- Monteyne, T., Heeze, L., Mortier, S. T. F. C., Oldörp, K., Cardinaels, R., Nopens, I., . . . De Beer, T. (2016). The use of Rheology Combined with Differential Scanning Calorimetry to Elucidate the Granulation Mechanism of an Immiscible Formulation During Continuous Twin-Screw Melt Granulation. *Pharmaceutical Research*, 33(10), 2481-2494. doi:10.1007/s11095-016-1973-6
- Monteyne, T., Heeze, L., Oldörp, K., Vervaet, C., Remon, J.-P., & De Beer, T. (2016). Vibrational spectroscopy to support the link between rheology and continuous twin-screw melt granulation on molecular level: A case study. *European Journal of Pharmaceutics and Biopharmaceutics*, 103, 127-135. doi:10.1016/j.ejpb.2016.03.030
- Monteyne, T., Vancoillie, J., Remon, J. P., Vervaet, C., & De Beer, T. (2016a). Continuous melt granulation: Influence of process and formulation parameters upon granule and tablet properties. *European Journal of Pharmaceutics and Biopharmaceutics*, 107, 249-262. doi:10.1016/j.ejpb.2016.07.021

- Morris, K. R., Griesser, U. J., Eckhardt, C. J., & Stowell, J. G. (2001). Theoretical approaches to physical transformations of active pharmaceutical ingredients during manufacturing processes. *Advanced Drug Delivery Reviews*, 48(1), 91-114. doi:[https://doi.org/10.1016/S0169-409X\(01\)00100-4](https://doi.org/10.1016/S0169-409X(01)00100-4)
- Mu, B., & Thompson, M. R. (2012). Examining the mechanics of granulation with a hot melt binder in a twin-screw extruder. *Chemical Engineering Science*, 81, 46-56. doi:10.1016/j.ces.2012.06.057
- N. Kittikunakorn, D. White, T. Listro, C. Martin, X. Feng, & F. Zhang. (2017). Granulation mechanisms and the effect of processing conditions on physicochemical properties of gabapentin granules prepared by continuous twin-screw extrusion. *AAPS PharmSciTech* (Abstract AM-17-1742).
- Newman, A., & Zografi, G. (2014). Critical Considerations for the Qualitative and Quantitative Determination of Process-Induced Disorder in Crystalline Solids. *Journal of Pharmaceutical Sciences*, 103(9), 2595-2604. doi:10.1002/jps.23930
- Nie, H., Byrn, S. R., & Zhou, Q. (2017). Stability of pharmaceutical salts in solid oral dosage forms. *Drug Development and Industrial Pharmacy*, 43(8), 1215-1228. doi:10.1080/03639045.2017.1304960
- Osei-Yeboah, F., & Sun, C. C. (2015a). Tabletability Modulation Through Surface Engineering. *J Pharm Sci*, 104(8), 2645-2648. doi:10.1002/jps.24532
- Osei-Yeboah, F., & Sun, C. C. (2015). Validation and applications of an expedited tablet friability method. *International Journal of Pharmaceutics*, 484(1), 146-155. doi:<https://doi.org/10.1016/j.ijpharm.2015.02.061>
- Osei-Yeboah, F., & Sun, C. C. (2015b). Validation and applications of an expedited tablet friability method. *Int J Pharm*, 484(1-2), 146-155. doi:10.1016/j.ijpharm.2015.02.061
- Otsuka, M., Mouri, Y., & Matsuda, Y. (2003). Chemometric evaluation of pharmaceutical properties of antipyrine granules by near-infrared spectroscopy. *AAPS PharmSciTech*, 4(3), 142-148. doi:10.1208/pt040347
- Otsuka, M., Otsuka, K., & Kaneniwa, N. (1994). Relation Between Polymorphic Transformation Pathway During Grinding and the Physicochemical Properties of Bulk Powders for Pharmaceutical Preparations. *Drug Development and Industrial Pharmacy*, 20(9), 1649-1660. doi:10.3109/03639049409050205
- Pandey, P., & Badawy, S. I. F. (2019). Chapter 18 - A Quality By Design Approach to Scale-Up of High Shear Wet Granulation Process. In A. S. Narang & S. I. F. Badawy (Eds.), *Handbook of Pharmaceutical Wet Granulation* (pp. 615-650): Academic Press.
- Parikh, D. M. (2005). *Handbook of Pharmaceutical Granulation Technology* (Vol. 154). Hoboken: Informa Healthcare.
- Patil, H., Tiwari, R. V., Upadhye, S. B., Vladyka, R. S., & Repka, M. A. (2015). Formulation and development of pH-independent/dependent sustained release matrix tablets of ondansetron HCl by a continuous twin-screw melt granulation process. *Int J Pharm*, 496(1), 33-41. doi:10.1016/j.ijpharm.2015.04.009



- Paudel, A., Rajjada, D., & Rantanen, J. (2015). Raman spectroscopy in pharmaceutical product design. *Adv Drug Deliv Rev*, 89, 3-20. doi:<https://doi.org/10.1016/j.addr.2015.04.003>
- Picker-Freyer, K., & Dürig, T. (2007). Physical mechanical and tablet formation properties of hydroxypropylcellulose: In pure form and in mixtures. *AAPS PharmSciTech*, 8, E1-E9. doi:10.1208/pt0804092
- Rauwendaal, C. (2016). Heat transfer in twin screw compounding extruders. *AIP Conference Proceedings*, 1779(1), 030014. doi:10.1063/1.4965484
- Reece, H. A., & Levendis, D. C. (2008). Polymorphs of gabapentin. *Acta Crystallographica Section C*, 64(3), o105-o108. doi:10.1107/S0108270107066279
- Repka, M. A., Battu, S. K., Upadhye, S. B., Thumma, S., Crowley, M. M., Zhang, F., . . . McGinity, J. W. (2007). Pharmaceutical Applications of Hot-Melt Extrusion: Part II. *Drug Development and Industrial Pharmacy*, 33(10), 1043-1057. doi:10.1080/03639040701525627
- Repka, M. A., Langley, N., & DiNunzio, J. (2013). *Melt Extrusion: Materials, Technology and Drug Product Design* (1;2013; ed. Vol. 9). Dordrecht: Springer.
- Rials, T. G., & Glasser, W. G. (1988). Thermal and dynamic mechanical properties of hydroxypropyl cellulose films. *Journal of Applied Polymer Science*, 36(4), 749-758. doi:10.1002/app.1988.070360402
- Royce, A., Suryawanshi, J., Shah, U., & Vishnupad, K. (1996). Alternative Granulation Technique: Melt Granulation. *Drug Development and Industrial Pharmacy*, 22(9-10), 917-924. doi:10.3109/03639049609065921
- Schäfer, T. (2001). Growth mechanisms in melt agglomeration in high shear mixers. *Powder Technology*, 117(1), 68-82. doi:10.1016/S0032-5910(01)00315-1
- Schäfer, T., & Mathiesen, C. (1996a). Melt pelletization in a high shear mixer. IX. Effects of binder particle size. *International Journal of Pharmaceutics*, 139(1), 139-148. doi:[http://dx.doi.org/10.1016/0378-5173\(96\)04548-6](http://dx.doi.org/10.1016/0378-5173(96)04548-6)
- Schäfer, T., & Mathiesen, C. (1996b). Melt pelletization in a high shear mixer. VII. Effects of product temperature. *International Journal of Pharmaceutics*, 134(1-2), 105-117. doi:10.1016/0378-5173(95)04455-8
- Seem, T. C., Rowson, N. A., Ingram, A., Huang, Z., Yu, S., de Matas, M., . . . Reynolds, G. K. (2015). Twin screw granulation — A literature review. *Powder Technology*, 276(C), 89-102. doi:10.1016/j.powtec.2015.01.075
- Shanmugam, S. (2015). Granulation techniques and technologies: recent progresses. *BioImpacts : BI*, 5(1), 55-63. doi:10.15171/bi.2015.04
- Sheskey, P., Keary, C., Clark, D., & Bahwinski, K. (2007). Scale-up trials of foam-granulation technology : high shear. *Pharmaceutical Technology Europe*, 19(9), 37-46.
- Shi, L., Feng, Y., & Sun, C. C. (2011). Massing in high shear wet granulation can simultaneously improve powder flow and deteriorate powder compaction: a double-edged sword. *European Journal of Pharmaceutical Sciences*, 43(1-2), 50-56. doi:10.1016/j.ejps.2011.03.009

- Shi, L., & Sun, C. C. (2010). Transforming Powder Mechanical Properties by Core/Shell Structure: Compressible Sand. *Journal of Pharmaceutical Sciences*, 99(11), 4458-4462. doi:<https://doi.org/10.1002/jps.22172>
- Shi, L., & Sun, C. C. (2010). Transforming powder mechanical properties by core/shell structure: compressible sand. *J Pharm Sci*, 99(11), 4458-4462. doi:10.1002/jps.22172
- Steffens, K. E., & Wagner, K. G. (2019a). Improvement of tabletability via twin-screw melt granulation: Focus on binder distribution. *International Journal of Pharmaceutics*, 570. doi:10.1016/j.ijpharm.2019.118649
- Steffens, K. E., & Wagner, K. G. (2019b). Improvement of tabletability via twin-screw melt granulation: Focus on binder distribution. *International Journal of Pharmaceutics*, 570, 118649. doi:<https://doi.org/10.1016/j.ijpharm.2019.118649>
- Sun, C., & Himmelsbach, M. W. (2006). Reduced tabletability of roller compacted granules as a result of granule size enlargement. *Journal of Pharmaceutical Sciences*, 95(1), 200-206. doi:10.1002/jps.20531
- Sun, C. C., & Kleinebudde, P. (2016). Mini review: Mechanisms to the loss of tabletability by dry granulation. *European Journal of Pharmaceutics and Biopharmaceutics*, 106, 9-14. doi:10.1016/j.ejpb.2016.04.003
- Tan, D. C. T., Chin, W. W. L., Tan, E. H., Hong, S., Gu, W., & Gokhale, R. (2014). Effect of binders on the release rates of direct molded verapamil tablets using twin-screw extruder in melt granulation. *International Journal of Pharmaceutics*, 463(1), 89-97. doi:10.1016/j.ijpharm.2013.12.053
- Thiele, W. (2018). Twin-Screw Extrusion and Screw Design. In I. Ghebre-Sellassie & C. Martin (Eds.), *Pharmaceutical Extrusion Technology* (2nd ed., pp. 71-93). New York: CRC Press.
- Thompson, M. R. (2015a). Twin screw granulation - review of current progress (Vol. 41, pp. 1223-1231): Informa Healthcare.
- Thompson, M. R., & O'Donnell, K. P. (2015). "Rolling" phenomenon in twin screw granulation with controlled-release excipients. *Drug Development and Industrial Pharmacy*, 41(3), 482-492. doi:10.3109/03639045.2013.879723
- Thompson, M. R., & Sun, J. (2010). Wet granulation in a twin-screw extruder: Implications of screw design. *Journal of Pharmaceutical Sciences*, 99(4), 2090-2103. doi:10.1002/jps.21973
- Tinmanee, R., Stamatis, S., Ueyama, E., Morris, K., & Kirsch, L. (2018). Polymorphic and Covalent Transformations of Gabapentin in Binary Excipient Mixtures after Milling-Induced Stress. *Pharmaceutical Research*, 35(2), 1-12. doi:10.1007/s11095-017-2285-1
- Tiwary, A. (2007). Crystal habit changes and dosage form performance. *Encyclopedia of Pharmaceutical Technology*, 820-833.
- Todd, D. B. (1998a). *Plastics compounding : equipment and processing*: Hanser Publishers.
- Todd, D. B. (2004). Mixing of Highly Viscous Fluids, Polymers, and Pastes. In S. M. Kresta, V. A. Atiemo-Obeng, E. L. Paul, & V. Atiemo-Obeng (Eds.), *Handbook*

- of Industrial Mixing : Science and Practice* (pp. 987-1024): John Wiley & Sons, Incorporated.
- Upadhye, S. B., Vladyka, p. R. R. S., Repka, M. A., Park, J.-b., & Tiwari, R. V. (2017).
- Vaingankar, P., & Amin, P. (2017). Continuous melt granulation to develop high drug loaded sustained release tablet of Metformin HCl. *Asian Journal of Pharmaceutical Sciences*, 12(1), 37-50. doi:<https://doi.org/10.1016/j.ajps.2016.08.005>
- Van Melkebeke, B., Vermeulen, B., Vervaet, C., & Remon, J. P. (2006). Melt granulation using a twin-screw extruder: A case study. *International Journal of Pharmaceutics*, 326(1-2), 89-93. doi:10.1016/j.ijpharm.2006.07.005
- Van Melkebeke, B., Vervaet, C., & Remon, J. P. (2008). Validation of a continuous granulation process using a twin-screw extruder. *International Journal of Pharmaceutics*, 356(1-2), 224-230. doi:10.1016/j.ijpharm.2008.01.012
- Vasanthavada, M., Wang, Y., Haefele, T., Lakshman, J. P., Mone, M., Tong, W., . . . AT, M. S. (2011). Application of melt granulation technology using twin-screw extruder in development of high-dose modified-release tablet formulation. *J Pharm Sci*, 100(5), 1923-1934. doi:10.1002/jps.22411
- Veliz Moraga, S., Villa, M. P., Bertín, D. E., Cotabarren, I. M., Piña, J., Pedernera, M., & Bucalá, V. (2015). Fluidized-bed melt granulation: The effect of operating variables on process performance and granule properties. *Powder Technology*, 286, 654-667. doi:10.1016/j.powtec.2015.09.006
- Vercruysse, J., Córdoba Díaz, D., Peeters, E., Fonteyne, M., Delaet, U., Van Assche, I., . . . Vervaet, C. (2012). Continuous twin screw granulation: influence of process variables on granule and tablet quality. *European Journal of Pharmaceutics and Biopharmaceutics*, 82(1). doi:10.1016/j.ejpb.2012.05.010
- Verstraete, G., Mertens, P., Grymonpré, W., Van Bockstal, P. J., De Beer, T., Boone, M., . . . Vervaet, C. (2016). A comparative study between melt granulation/compression and hot melt extrusion/injection molding for the manufacturing of oral sustained release thermoplastic polyurethane matrices. *International Journal of Pharmaceutics*, 513(1-2). doi:10.1016/j.ijpharm.2016.09.072
- Vervaet, C., & Remon, J. P. (2010). Mlet granulation. In D. M. Parikh. (Ed.), *Handbook of pharmaceutical granulation technology* (Vol. 3): New York : Informa Healthcare USA.
- Weatherley, S., Mu, B., Thompson, M. R., Sheskey, P. J., & O' Donnell, K. P. (2013). Hot-Melt Granulation in a Twin Screw Extruder: Effects of Processing on Formulations with Caffeine and Ibuprofen. *Journal of Pharmaceutical Sciences*, 102(12), 4330-4336. doi:10.1002/jps.23739
- Webb, P. A. (2001). Volume and Density Determinations for Particle Technologists *Micromeritics Instrument Corp.*
- White, J. L., & Bumm, S. H. (2010). Perspectives on the Transition from Batch to Continuous Mixing Technologies in the Compounding Industry. *International Polymer Processing*, 25(5), 322-326. doi:10.3139/217.2293



- Xu, T., Nahar, K., Dave, R., Bates, S., & Morris, K. (2018). Polymorphic Transformation of Indomethacin during Hot Melt Extrusion Granulation: Process and Dissolution Control. *Pharmaceutical Research*, 35(7), 1-15. doi:10.1007/s11095-017-2325-x
- Yinghe He, Lian X. Liu, James D. Litster, & Kayrak-Talay, D. (2010). Scale-up Considerations in Granulation. In D. M. Parikh. (Ed.), *Handbook of pharmaceutical granulation technology* (Vol. 3): New York : Informa Healthcare USA.
- Yoshioka, S., & Aso, Y. (2007). Correlations between molecular mobility and chemical stability during storage of amorphous pharmaceuticals (Vol. 96, pp. 960-981). Hoboken: Wiley Subscription Services, Inc., A Wiley Company.
- Ziegler, G. R., & Aguilar, C. A. (2003). Residence time distribution in a co-rotating, twin-screw continuous mixer by the step change method. *Journal of Food Engineering*, 59(2-3), 161-167. doi:10.1016/S0260-8774(02)00453-3
- Zong, Z., Qiu, J., Tinmanee, R., & Kirsch, L. E. (2012). Kinetic model for solid-state degradation of gabapentin. *Journal of Pharmaceutical Sciences*, 101(6), 2123-2133. doi:10.1002/jps.23115
- Zong, Z. X., Desai, S. D., Kaushal, A. M., Barich, D. H., Huang, H. S., Munson, E. J., . . . Kirsch, L. E. (2011). The Stabilizing Effect of Moisture on the Solid-State Degradation of Gabapentin. *AAPS PharmSciTech*, 12(3), 924-931. doi:10.1208/s12249-011-9652-8

## **Vita**

Nada Kittikunakorn graduated bachelor degree of science in Pharmaceutical Sciences (B.Sc.) from Chulalongkorn University, Thailand in 2012. After she graduated, she worked as a researcher in the Department of Research and Development Institute at the Government Pharmaceutical Organization, Thailand until 2016. Her responsibility included formulation development of solid oral dosage form, solid-state characterization, analytical testing, and preparation of regulatory documents for Thai FDA submission. In 2016, she received the scholarship from the Government Pharmaceutical Organization to pursue a doctoral degree in US. In August 2016, she came to the University of Texas at Austin and joined the research lab of Dr. Feng Zhang in Molecular Pharmaceutics and Drug Delivery department. Her research focused on the continuous twin-screw granulation to improve the tableability of poorly-compressible and thermal labile drug. During her time in graduate program, she has authored/co-authored 10 publications which have been submitted to or published in many leading journals.

Email: nada.k@utexas.edu

This dissertation was typed by the author.